JYVÄSKYLÄ STUDIES IN BIOLOGICAL AND ENVIRONMENTAL SCIENCE
205

Teemu Ihalainen

Intranuclear Dynamics in Parvovirus Infection

JYVÄSKYLÄN YLIOPISTO

JYVÄSKYLÄ STUDIES IN BIOLOGICAL AND ENVIRONMENTAL SCIENCE 205

Teemu Ihalainen

Intranuclear Dynamics in Parvovirus Infection

Esitetään Jyväskylän yliopiston matemaattis-luonnontieteellisen tiedekunnan suostumuksella
julkisesti tarkastettavaksi yliopiston Ambiotica-rakennuksen salissa YAA303
lokakuun 31. päivänä 2009 kello 12.

Academic dissertation to be publicly discussed, by permission of
the Faculty of Mathematics and Science of the University of Jyväskylä,
in the Building Ambiotica, YAA303, on October 31, 2009 at 12 o'clock noon.

UNIVERSITY OF JYVÄSKYLÄ

JYVÄSKYLÄ 2009

Intranuclear Dynamics in Parvovirus Infection

JYVÄSKYLÄ STUDIES IN BIOLOGICAL AND ENVIRONMENTAL SCIENCE 205

Teemu Ihalainen

Intranuclear Dynamics in Parvovirus Infection

UNIVERSITY OF JYVÄSKYLÄ

JYVÄSKYLÄ 2009

Editors
Varpu Marjomäki
Department of Biological and Environmental Science, University of Jyväskylä
Pekka Olsbo, Marja-Leena Tynkkynen
Publishing Unit, University Library of Jyväskylä

URN:ISBN:978-951-39-3697-6
ISBN 978-951-39-3697-6 (PDF)

ISBN 978-951-39-3671-6 (nid.)
ISSN 1456-9701

Jyväskylä University Printing House, Jyväskylä 2009

Science is a wonderful thing if one does not have to earn one's living at it.

Albert Einstein

A biophysicist talks physics to the biologists and biology to the physicists, but when he meets another biophysicist, they just discuss women

Unknown Author

ABSTRACT

Ihalainen, Teemu O.
Intranuclear Dynamics in Parvovirus Infection
Jyväskylä: University of Jyväskylä, 2009, 86 p.
(Jyväskylä Studies in Biological and Environmental Science
ISSN 1456-9701; 205)
ISBN 978-951-39-3697-6 (PDF), 978-951-39-3671-6 (nid.)
Yhteenveto: Tumansisäinen dynamiikka parvovirus infektiossa
Diss.

During the last decades DNA virus replication and transcription has been studied in different *in vitro* systems. These studies have yielded a myriad of information about DNA replication, gene regulation and messenger RNA (mRNA) processing. The recent advances in the confocal microscopy and in fluorescent protein technology have allowed the elucidation of these processes in living cells. In our studies we have used canine parvovirus as a model virus to study DNA replication, transcription and mRNA export dynamics. Two viral proteins were fused to fluorescent proteins, non-structural protein 1 (NS1) was fused to enhanced yellow fluorescent protein (EYFP) and virus protein 2 (VP2) to a photoactivable green fluorescent protein (PAGFP). Fluorescence photobleaching methods indicated that NS1-EYFP is able to shuttle between the cytoplasm and the nucleus. In the infected cells large viral replication compartment filled the whole nucleus, discarding the host cell chromatin to the nuclear periphery. In these cells, NS1-EYFP and proliferating cell nuclear antigen fused to EYFP (PCNA-EYFP), both of which are needed for the viral DNA replication, showed highly similar binding behaviour, yielding an estimate of the virus genome replication time. Fluorescence recovery after photobleaching, fluorescence correlation spectroscopy and Virtual Cell modelling indicated that the general protein mobility is increased in the virus infected nuclei. Photoactivation experiments showed that the majority of the virus capsids are able to diffuse inside the nucleus, but a large portion of the viral pariticles were almost immobile. Results of TATA binding protein EGFP fusion protein (TBP-EGFP) and transcription factor II B EGFP fusion protein (TFIIB-EGFP) studies support the overall consensus model of transcription initiation, where TFIID binds the promoter for a long time and TFIIB only helps the polymerase to attach to the promoter. Taken together, the results indicate that the host cell nucleus is highly reorganized in the infection.

Keywords: Canine parvovirus; diffusion; nuclear organelles; protein dynamics.

Teemu O. Ihalainen, University of Jyväskylä, Nanoscience Center, Department of Biological and Environmental Science, P.O. Box 35, FI-40014 University of Jyväskylä, Finland

Author's address Teemu Ihalainen
University of Jyväskylä, Dept. Biol. Env. Sci.
Survontie 9
FI-40500 Jyväskylä
Finland
teemu.o.ihalainen@jyu.fi

Supervisors Docent Maija Vihinen-Ranta
University of Jyväskylä, Dept. Biol. Env. Sci.
Survontie 9
FI-40500 Jyväskylä
Finland
mvihinen@jyu.fi

Professor Päivi Törmä
Helsinki University of Technology, Dept. Appl. Phys.
P.O.Box 5100,
FIN-02015 TKK
Finland
paivi.torma@hut.fi

Reviewers Docent Maria Vartiainen
University of Helsinki, Institute of Biotechnology
PO BOX 56
FI-00014 Helsinki
Finland

Docent Päivi Ojala
Biomedicum Helsinki, B530b2
PO Box 63 (Haartmaninkatu 8)
FI-00014 Helsinki
Finland

Opponent Professor Michael Kann
Laboratoire de Microbiologie Cellulaire et Moléculaire et Pathogénicité (UMR-CNRS 5234)
Université de Bordeaux II
Réplication et Expression Génétique des Génomes Eucaryotes, Bactériens et Viraux
146, rue Leo Saignat, Bat. 3A, 3ème étage
33076 BORDEAUX cedex
France

CONTENTS

LIST OF ORIGINAL PUBLICATIONS

This thesis is based on the following original papers, which will be referred in the text as following Roman numerals.

I Ihalainen, T.O., Niskanen, E.A., Jylhävä, J., Turpeinen T., Rinne J., Timonen J. & Vihinen-Ranta M. 2007 "Dynamics and interactions of parvoviral NS1 protein in the nucleus" Cellular Microbiology 9: 1946–1959

II Ihalainen, T.O., Niskanen, E.A., Jylhävä, J., Paloheimo O., Dross N., Smolander H., Langowski J., Timonen J. & Vihinen-Ranta M. 2009 "Parvovirus Induced Alterations in Nuclear Architecture and Dynamics" PLoS ONE, Acepted

III Ihalainen, T.O., Niskanen, E.A., Paloheimo O., Smolander H., Laurila J. & Vihinen-Ranta M. 2009 "Distribution and dynamics of transcription-associated proteins during parvovirus infection" Manuscript

RESPONSIBILITIES OF TEEMU IHALAINEN IN THE THESIS ARTICLES

Article I: I was responsible for planning the article together with Maija Vihinen-Ranta. Einari Niskanen constructed NS1-EYFP fusion protein. Tuomas Turpeinen and Jussi Timonen assisted in the FRAP data analysis. I was responsible for the confocal microscopy, FRAP, FLIP, data analysis and processing of article figures. I wrote the article together with Maija Vihinen-Ranta

Article II: I was responsible for planning the article and conducted the majority of the experiments. Einari Niskanen was responsible for the cloning, planned the FISH experiments and assisted in the BrdU experiments. Juulia Jylhävä assisted in the cloning PAGFP-VP2 and was responsible for the FISH experiments. Outi Paloheimo took part in PAGFP-VP2 characterization. Jussi Timonen assisted in the FRAP data analysis. Nicolas Dross assisted in the FFM and in the FFM data analysis. Hanna Smolander was responsible for the nuclear volume calculations. I was responsible for the remaining confocal microscopy, deconvolution, widefield microscopy, FRAP experiments and simulations, photoactivation experiments and simulations, FFM experiments, data analysis and article figures. I wrote the article together with Maija Vihinen-Ranta and Einari Niskanen took a part finalizing it.

Article III: I was responsible for planning the article and conducted the majority of the experiments. Hanna Smolander assisted in the TFIIB-EGFP FRAP experiments and Juha Laurila in the PML-EYFP FRAP experiments. I conducted the FRAP experiments, analyzed the data and prepared the article figures. I wrote the article together with Maija Vihinen-Ranta and Einari Niskanen took a part finalizing it.

Studies I, II and III were carried out under the supervision of Docent Maija Vihinen-Ranta. Study I was done in collaboration with Professor Jussi Tiomonen. Study II was conducted in collaboration with Professor Jussi Timonen and Professor Jörg Langowski

ABBREVIATIONS

AAV	Adenoassociated virus
AOTF	Acousto optical tunable filter
APC	Anaphase promoting factor
ATP	Adenosine-5'-triphosphate
CB	Cajal body
CDK	Cyclin dependent kinase
CPV	Canine parvovirus
CT	Chromatin territory
CTD	C-terminal domain
DMEM	Dulbecco's modified eagle medium
DNA	Deoxyribonucleic acid
ECFP	Enhanced cyan fluorescent protein
EGFP	Enhanced green fluorescent protein
EYFP	Enhanced yellow fluorescent protein
FCS	Fluorescence correlation spectroscopy
FFM	Fluorescence fluctuation microscopy
FLIP	Fluorescence loss in photobleaching
FPV	Feline parvovirus
FRAP	Fluorescence recovery after photobleaching
H2A	Histone 2A
H2B	Histone 2B
H3	Histone 3
H4	Histone 4
HP1	Heterochromatin protein 1
HSV1	Herpes simplex virus 1
IC	Interchromatin domain
INM	Inner nuclear membrane
LBR	Lamin B receptor
MOI	Multiplicity of infection
mRNA	Messenger RNA
mRNP	Messenger ribonucleoprotein
MSD	Mean square displacement
NE	Nuclear envelope
NES	Nuclear export signal
NLFK	Norderns laboratory feline kidney cells
NLS	Nuclear localization signal
NPC	Nuclear pore complex
NS1	Non-structural protein 1
NS2	Non-structural protein 2
NUP	Nuleoporin protein
ONM	Outer nuclear membrane
ORC	Origin of recognition complex

PABPN1	Poly-A-binding protein, nuclear 1
PAP	Poly-A polymerase
PFA	Paraformaldehyde
p.i.	post infection
PML	Promyeolytic leukemia
PAGFP	Photoactivable green fluorescent protein
PCNA	Proliferating cell nuclear antigen
PNS	Perinuclear space
SV40	Simian virus 40
TBP	TATA binding protein
TFIIA	Transcription factor II A
TFIIB	Transcription factor II B
TFIID	Transcription factor II D
TFIIE	Transcription factor II E
TFIIF	Transcription factor II F
TFIIH	Transcription factor II H
VP1	Virus protein 1
VP2	Virus protein 2
VP3	Virus protein 3

1 INTRODUCTION

Eukaryotic cell nucleus is highly organized and heterogenous cell organelle, containing the genetic material of the cell. In addition, it encloses extremely complex macromolecular machinery, which is used to maintain, repair, replicate and express the genome. The genetic material is packed into chromatin, which can be divided into more active euchromatin and more passive heterochromatin. The chromatin structure is highly dynamic and it can fluctuate between different states. The changes in the chromatin structure depend on the signals coming from outside of the cell, cell cycle phase, chromatin location inside the nucleus and on the chromatin content.

The diverse nuclear functions are localized into distinct, functionally different domains and nuclear organelles. These nuclear substructures show high complexity and can contain hundreds of different proteins. These structures are highly dynamic and their components are continuously exchanged with the nucleoplasm or with other nuclear structures. However, the nucleus is highly crowded environment where the protein diffusion can be hindered by other macromolecules. This crowded environment limits the reaction rates, affects the hybridization of the DNA and RNA strands and is suggested to be involved in the nuclear organelle assembly, thus it has an impact to almost every function of the nucleus.

Current knowledge about the fundamental nuclear functions, like DNA replication, repair and RNA transcription is based on studies conducted *in vitro*. However, during the last 10 years fluorescence microscopy has evolved from just a visualization technique to a complete toolbox, which can be used to achieve quantitative information about protein diffusion and interaction dynamics. Methods like fluorescence recovery after photobleaching, fluorescence loss in photobleaching, fluorophore photoactivation and fluorescence correlation spectroscopy can now be easily used to gain information about the biological processes as they take place, inside the living cells. Nevertheless, since these methods are relatively young, no universal quantitation methods have yet been discovered.

Viruses offer an interesting opportunity to study cellular processes. Since they are oblicate parasites, they rely on host cell metabolism in order to produce virus progeny. Especially small DNA viruses, which replicate inside the nucleus, provide a simple system for DNA replication and transcription studies. In this study we used canine parvovirus, a small DNA virus replicating inside the nucleus, to study the effect of virus infection to the nuclear organization, protein diffusion and binding dynamics, DNA replication and RNA transcription.

2 REVIEW OF THE LITERATURE

2.1 Overview of Eukaryotic Cell Nucleus

The most prominent structure of the eucaryotic cell is the nucleus. The nucleus contains the genetic material and a variety of different proteins involved in the genome replication; transcription activity control; RNA transcription, processing and export; and in maintenance of genomic stability. The nuclear envelope (NE) functions as a physical barrier, separating the nucleus from the cytoplasm (D'Angelo & Hetzer 2006). The NE is decorated with nuclear pore complexes (NPC) which allow molecules to move between the cytoplasm and the nucleus (Cook et al. 2007). The variety of different functions of the nucleus implies that the nuclear organization and dynamics are highly regulated.

2.1.1 Nuclear Envelope

The nuclear envelope is composed of uninterrupted inner and outer nuclear membranes (INM and ONM), from which the latter is continuous with the endoplasmic reticulum (ER) (D'Angelo & Hetzer 2006). The INM and ONM are separated by perinuclear space (PNS) (Stewart et al. 2007). Although the 3 membranes are continuous, they are biochemically distinct, each comprising a unique set of proteins (Schirmer & Gerace 2005, Schirmer & Foisner 2007). The INM is covered with nuclear lamin proteins, which form a fibrous nuclear lamina (D'Angelo & Hetzer 2006). The lamin proteins belong to the intermediate filament protein family and are divided into the B- or A/C-type lamins (Fisher et al. 1986, Gerace & Blobel 1980). The INM is connected to the lamina through several proteins, of which the lamin B receptor (LBR), emerin, and lamin-associated proteins (LAPs) are among the best characterized (Foisner & Gerace 1993, Worman et al. 1988, Zastrow et al. 2004). LBR has been also shown to bind to chromatinthrough heterochromatin protein 1 (HP1) (Ye & Worman 1996).

The otherwise intact nuclear envelope is interrupted by the NPCs, which form pores at the sites where INM and ONM are fused together. The pores in

the nuclear membrane were recognized already in 1950 (Callan & Tomlin 1950) but the 8-fold symmetry of the NPCs was discovered in the late 1960s (Gall 1967). A low-resolution three-dimensional model of the vertebrate membrane-bound NPC was achieved in early 1990s (Akey & Radermacher 1993), and the structure was refined 11 years later by studying intact nuclei (Beck et al. 2004). These models revealed the complex structure of the NPC. The center of the NPC, called the central pore or the transport channel, is occupied by a plug-like structure. At the cytoplasmic face, the 8 cytoplasmic filaments protrude from the cytoplasmic ring and point toward the center of the NPC. The cytoplasmic ring is attached to the luminal spoke ring, which is suggested to anchor the NPC to the nuclear membrane. Inside the nucleus, the nuclear ring precedes the nuclear basket. The nuclear basket is formed from 8 filaments, which project to the nucleoplasm and are connected by a distal ring.

Today, approximately 30 distinct nucleoporin proteins (NUPs) have been found from the NPC, in addition to several NPC-associated proteins (Cronshaw et al. 2002). The whole complex has a mass of 125 MDa (Reichelt et al. 1990) and a diameter and height of 125 nm and 110 nm, respectively (Beck et al. 2004). The NUPs containing multiple repeats of phenylalanine-glycine are suggested to line the central channel (Rout & Wente 1994) and are considered to be crucial for the nuclear transport of macromolecules (Terry et al. 2007). Molecules smaller than 40 kDa in size (diameter ~8 nm) can passively diffuse through the NPC but larger molecules have to be actively transported. It has been shown that the NPCs are able to pass nanoparticles up to 39 nm in size (Pante & Kann 2002), suggesting that the NPC central pore structure is highly elastic.

The active nuclear transport is mediated by transport receptors, which recognize the nuclear localization (import) signals (NLS) or the nuclear export signals (NES) in the cargo molecules (Terry et al. 2007). The NPCs can pass over 1000 molecules in a second, yielding a transported mass of about 100 MDa per second (Ribbeck & Gorlich 2001). Single-particle tracking studies have revealed that when the cargo molecules have entered the central channel, they show random walk behavior, diffusing back and forth in the channel, until they exit the pore (Yang & Musser 2006). The single cargo molecules interact for 10 ms with the pore, and the import efficiency (interaction events per successful imports) under physiological conditions is ~50 % (Yang & Musser 2006). In spite of the accumulating knowledge of NPCs, the detailed interactions between the NPC and the transported molecules have not been elucidated (Terry et al. 2007).

2.1.2 Chromatin Organization

The genome of an organism is packed into chromatin, where histone proteins bind to the DNA, forming nucleosomes and subsequently, densely packed DNA fibers. The nucleosomes are mainly composed of 4 different core histone proteins; histone H2A, H2B, H3, and H4. Four histone protein heterodimers (H2A-H2B and H3-H4) form an octameric assembly, and 147 nucleotides of DNA are wrapped around it (Chakravarthy et al. 2005). The histone proteins are subjected to a wide variety of different modifications, which include serine phosphorylation, lysine acetylation, lysine and arginine mono- or polymethylation, polyribosylation, sumoylation, and mono- or polyubiquitylation (Horn & Peterson 2006). In many cases, the effect of these modifications is still unknown, but some of the modifications associate with the packing state or the activity of the genomic region.

The chromatin has been traditionally divided into more condensed heterochromatin and to looser euchromatin. The heterochromatin is further divided into constitutive and facultative heterochromatin (Fedorova & Zink 2008). The constitutive heterochromatin, consisting of mainly highly repetitive DNA sequences such as the highly repetitive satellite DNA and transposons, is considered to be transcriptionally inactive (Grewal & Jia 2007). The general feature of the heterochromatin is histone hypoacetylation. In addition, in the constitutive heterochromatin, the histone H3 is usually trimethylated at lysine 9 (meH3K9) and 20 (meH3K20) (Peters et al. 2003) and monomethylated at lysine 27 (meH3K27) (Schotta et al. 2004). The histone H3 methylation meH3K9 also induces binding of heterochromatin protein 1 (HP1) (Lachner et al. 2001), which is involved in a wide variety of heterochromatin maintenance functions (Fanti & Pimpinelli 2008). The facultative heterochromatin is formed at specific gene-containing chromosomal regions that are potentially transcribed, and its formation is cell type- and developmental stage-dependent. In these regions, the histone H3s are often di- or trimethylated at lysine 9 and trimethylated at 27 (Lam et al. 2005a, Trojer & Reinberg 2007). In addition, histone H4 is usually deacetylated at lysine 16 (Carmen et al. 2002). The histone H3s are phosphorylated at serine 10 (pH3S10) when the chromatin is condensed in mitosis. Similar phosphorylation can also be detected in different apoptosis routes (Prigent & Dimitrov 2003).

The transcribed regions of the genome reside in the euchromatin area. This region needs to be accessible to a wide variety of proteins. The main features of the histone modifications are hyperacetylated histones H3 and H4 (Millar & Grunstein 2006). In the active gene region, histone H3 can be acetylated at lysines 9 and 14 and phosphorylated at serine 10 (Thomson et al. 2001). Other modifications include histone H3 methylation at lysine 4, 36, 72, and 79 (Horn & Peterson 2006, Shahbazian et al. 2005, Strahl et al. 1999, Xiao et al. 2003). Furthermore, different arginines in histones H3 and H4 (H3R2, H3R8, H3R17, H3R26, and H4R3) can be methylated in the euchromatin or heterochromatin regions (Ng et al. 2009).

Earlier studies indicated that the heterochromatin contains regions that are highly condensed and inactive. It was considered that the chromatin condensation was linked to the transcriptional inactivity. However, more recent studies have indicated that the heterochromatin is only 1.4 times more condensed than the euchromatin (Sadoni et al. 2001). AT-richness of the heterochromatin leads to more intense DNA labeling by DAPI and Hoechst. In addition, fixation and labeling procedures used in the conventional transmission electron microscopy can cause errors in the interpretation of the chromatin condensation. Therefore, it has been suggested that the previous reports about the chromatin condensation are biased by these labeling-related artifacts. Furthermore, heterochromatic repeats, like pericentromeric repeats, have been reported to be actively transcribed, from yeast to mammals (Fedorova & Zink 2008, Grewal & Jia 2007). In yeast, the actual formation of heterochromatin requires the processing of the transcribed heterochromatic repeats to small interfering RNAs that will then elict the RNA interference response (Grewal & Jia 2007, Kato et al. 2005). In line with this, it has been shown that the gene density, rather than the transcriptional activity, correlates with the chromatin condensation (Gilbert et al. 2004).

The different chromatin types also occupy different intranuclear locations. The heterochromatin surrounds the nucleolus and is typically also located close to the nuclear membrane. However, NPC regions are usually devoid of the heterochromatin (Manuelidis 1984). Fluorescence *in situ* hybridization with chromosome labeling has revealed distinct chromosome territories (CTs), in which chromosomes occupy defined locations (Pinkel et al. 1988, Tanabe et al. 2002). The gene-rich chromosomes are usually located in the nuclear interior, while the chromosomes containing fewer genes are situated close to the nuclear periphery (Cremer & Cremer 2001). The non-coding regions of the chromatin are often sequestered into the interior of the CT, as the actively transcribed regions are located at the surface (Scheuermann et al. 2004). The lacunae between the CTs form a 3-dimensional interchromatin domain compartment (IC), which forms channels throughout the nucleus and even tunnels through the CTs (Visser et al. 2000). The IC allows the rapid distribution of transcription and splicing factors throughout the nucleus (Misteli 2001).

2.1.3 Nuclear Substructures

In addition to chromatin, the nucleus contains many distinct domains, which are usually referred to as nuclear substructures or subnuclear organelles. The most prominent nuclear substructure is the nucleolus. In addition, the nuclear interior contains several substructures: Cajal bodies (CBs), promyelocytic leukaemia nuclear bodies (PML-NBs), transcription factories, splicing speckles, gems, and many others.

The nucleoli are large nuclear substructures, which take part in the ribosomal RNA transcription/modification and assembly of pre-ribosomes (Handwerger & Gall 2006). They contain approximately 700 different proteins, of which only 30 % is involved in the preceding functions (Lam et al. 2005b).

Today, it is relatively well established that nucleoli respond to various cellular stress situations, like UV irradiation, nucleotide depletion, heat shock, and hypoxia, leading to increased cellular p53 levels (Mayer & Grummt 2005, Rubbi & Milner 2003). In addition, enhanced ribosomal RNA (rRNA) synthesis is suggested to be important for tumorgenensis. Many viruses also target their proteins to the nucleolus (Sirri et al. 2008). The nucleoli are subcompartmentalized further to 3 parts: the innermost part of the nucleolus is the fibrillar center (FC); it is followed by dense fibrillar component (DFC), and the outermost part is the granular component (GC) (Raska et al. 2006). However, the exact location of RNA polymerase I transcription is not well established. It is suggested to take place in the DFC or in the border of the DFC and FC (McKeown & Shaw 2009).

Cajal bodies (formerly known as Coiled bodies) were discovered 100 years ago by Ramón y Cajal. CBs are involved in the biogenesis of different nuclear RNA molecules (Gall 2001) and especially in the assembly site for small nuclear ribonucleoparticles (snRNPs) (Morris 2008). The snRNP particles are involved in the spliceosome assembly and, therefore, in the pre-mRNA splicing. The markers for CBs are U7 small nuclear ribonucleoprotein, coilin, and survival motor neuron (SMN) proteins (Handwerger & Gall 2006). The coilin seems to be needed for the snRNP sequestration to the Cajal body (Bauer & Gall 1997). Energy depletion has been shown to increase the mobility of the Cajal bodies inside the nucleus, even though the movement is passive diffusion. Therefore, it was suggested that the Cajal bodies associate with chromatin, and this is perturbed under ATP depletion (Platani et al. 2002).

PML-NBs were named after the PML protein, which localizes to these nuclear bodies. PML-NBs are small, discrete intranuclear structures, with a diameter of 0.2–1.0 μm. The number of these structures, 5–30 per cell, depends on cell type, cell cycle phase, and cell differentiation stage (Ascoli & Maul 1991, Bernardi & Pandolfi 2007). The PML-NBs are dynamic structures, containing many proteins with variable residence times in the bodies (Weidtkamp-Peters et al. 2008). The bodies themselves have been shown to move in an ATP-dependent manner (Muratani et al. 2002), even though this study was criticized for using the wrong marker protein for PML-NBs (Wiesmeijer et al. 2002). The actual function of PML-NBs is not well established, but it is known that the protein-based core is partially surrounded by dense chromatin and possibly by newly synthesized mRNA (Boisvert et al. 2000). PML-NBs have been reported to be involved in various cellular functions, like transcriptional regulation (Zhong et al. 2000) and antiviral defense (Everett & Chelbi-Alix 2007), since many transcription factors and a wide variety of viral proteins localize to PML-NBs. In addition, it has been suggested that they are also involved in DNA damage response and apoptosis, considering that they colocalize with UV damage-induced ssDNA foci, contain DNA repair-related proteins (Boe et al. 2006, Dellaire & Bazett-Jones 2004), and activate p53 and inhibit its negative regulator MDM2 (Wang et al. 1998b).

The mRNA transcription takes place in discrete nuclear structures called transcription factories. The chromatin protrudes from the CT and forms loops

to the IC, where transcription factories are assembled. The local concentration of RNA polymerase II complexes in these regions is approximately 1000-fold higher than in the nucleoplasm (Carter et al. 2008). The interaction of different chromosomes has also been detected in the transcription factories (Branco & Pombo 2006). However, even though some active genes have been shown to locate close to each other, the distance between the genes indicates that they are located at different transcription factories (Brown et al. 2008).

The splicing speckles are irregularly shaped nuclear structures, including a large amount of mRNA splicing-related factors: small nuclear ribonucleoprotein particles, spliceosome subunits and other splicing related proteins (Lamond & Spector 2003). At the electron microscopy resolution level, the splicing speckles are composed of small granules, and therefore they are also called interchromatin granule clusters (Turner & Franchi 1987). The splicing speckles have been indicated to function as mRNA splicing factor storage sites, since the splicing factors have been observed to be recruited from the splicing speckles to the transcription site (Misteli et al. 1997). In addition, the splicing speckles have been shown to enlarge when the splicing is inhibited, suggesting that the splicing factors return to the splicing speckles when they are not actively used (O'Keefe et al. 1994). Some actively transcribed genes have been reported to be associated with splicing speckles, suggesting that the splicing factor reservoir is situated close to the transcription site (Brown et al. 2008).

Paraspeckles are nuclear organelles that closely associate with the splicing speckles (Lamond & Spector 2003). Their function is poorly characterized, but they seem to have a role in pre-mRNA splicing and nuclear retention of RNA. Their formation has been suggested to be nuclear noncoding RNA-dependent (Clemson et al. 2009). Gems are SMN protein-containing nuclear bodies that tightly associate with the Cajal bodies and show similar dynamic behavior (Liu & Dreyfuss 1996). However, in contrast to CBs, they do not contain snRNP particles (Matera 1998).

2.1.4 mRNA Transcription and Processing

In order to transform the genetic code into to a functional form, the cells transcribe the genetic information from the DNA into the RNA. Inside the nucleus, the mRNA is transcribed by the RNA polymerase II. The transcription process can be divided into three parts: promoter assembly and initiation, elongation, and finally termination (Wade & Struhl 2008). In the promoter assembly, the polymerase II enzyme is recruited to the promoter with the help of basal transcription factors (TFIIA, B, D, E, F, H) (Pokholok et al. 2002). TFIID harbors the TATA-binding protein (TBP) and several TBP-associated proteins (TAFs), which are recruited to the region near the TATA box sequence (Bell & Tora 1999). TFIID can also bind nucleosomes by associating with trimethylated histone H3 (Vermeulen et al. 2007). TFIIA stabilizes the binding of the TBP to the TATA box (Kraemer et al. 2001). TFIIF escorts the polymerase to the promoter (Flores et al. 1991) and TFIIB links the TFIID complex to the RNA

polymerase II holoenzyme (Buratowski et al. 1989, Ha et al. 1993). TFIIH functions as a helicase and helps the polymerase complex to melt the DNA duplex at the transcription start site (Spangler et al. 2001). TFIIE promotes TFIIH to phosphorylate the polymerase II C-terminus, which is a prerequisite for active transcription (Ohkuma et al. 1995). This preinitiation complex assembly is summarized in Figure 1.

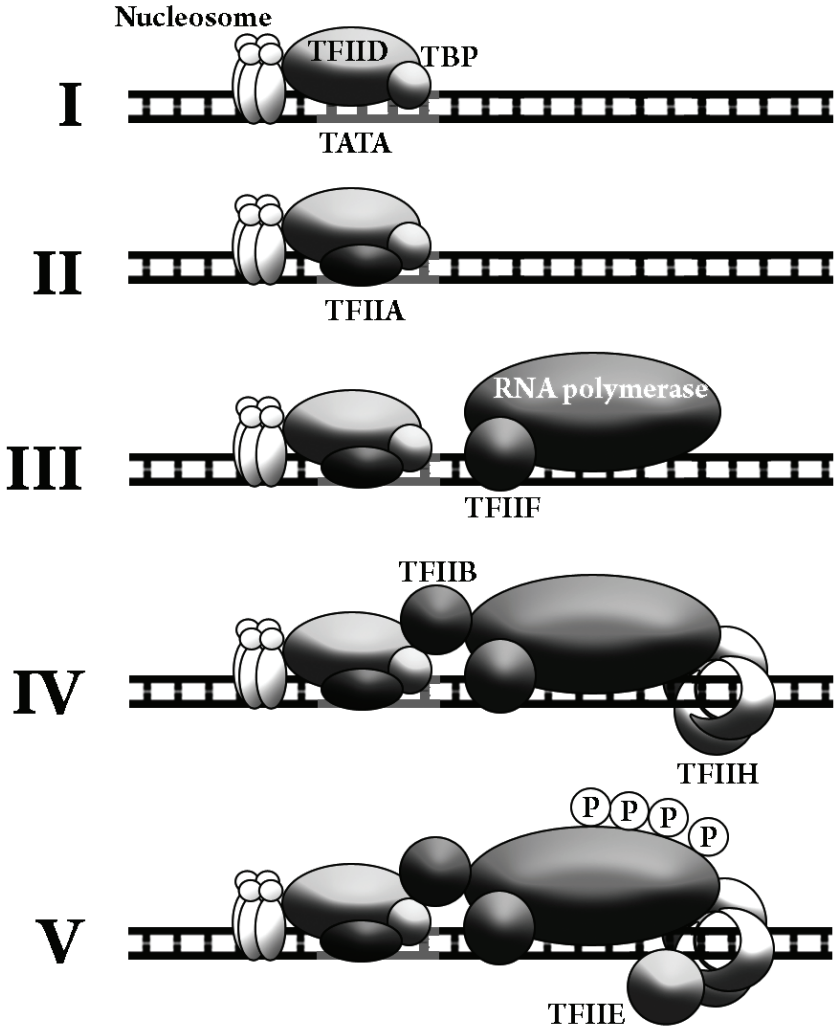

FIGURE 1 Schematic representation of the transcription initation. (I) TFIID containing TBP binds to the vicinity of TATA-box. (II) TFIIA stabilizes this binding and (III) TFIIF escorts the RNA polymerase to the promoter. (IV) TFIIB links the TFIID and polymerase and TFIIH, a helicase binds to the DNA. (V) TFIIH catalyzed phosphorylation (P) of RNA polymerase C-teminus is promoted by the TFIIE

The transcription is initiated when the first phosphodiester bond forms to the nascent RNA (Ohkuma et al. 1995). After the initiation step, the polymerase complexes escape the promoter, but a large portion of the polymerases are stalled at the proximal part of the promoter. This proximal pausing has been suggested to function in the transcription regulation: the polymerase complexes are assembled to the promoter but are stalled, waiting for other regulatory factors to allow transcription to proceed (Krumm et al. 1995). In addition, the transcription factors in the polymerase II are exchanged, from initiation factors to elongation factors, before the elongation can proceed (Pokholok et al. 2002). In a recent study, the RNA polymerase II dynamics were followed by live cell microscopy, fluorescence recovery after photobleaching, and photo activation experiments. The study revealed that only 1 of 90 RNA polymerases proceeded from promoter assembly to the elongation, and polymerases were often released from the template in every phase of the transcription. In addition, a small fraction of polymerases paused for several minutes during elongation, offering another possibility for transcription control (Darzacq et al. 2007). When the transcription is completed, the mRNA is further processed. These processing steps include 5′-end capping, splicing, and 3′-end polyadenylation (Sperling et al. 2008).

The 5′-end capping of the pre-mRNA is a necessary step for the following mRNA splicing, export, and translation steps. The reaction can be divided into 3 steps; (i) the triphosphate of the 5′-end is hydrolyzed to diphosphate, (ii) the guanosinemonophosphate is attached to this diphosphate, forming a 5′-5′ bond, and (iii) the guanosine is methylated (Gu & Lima 2005). The capping reaction is tightly coupled to the transcription, since the enzymes involved in the process - RNA triphosphatase, guanylyltransferase, and 7-methyltransferase - are recruited to the C-terminal domain (CTD) of the RNA polymerase II already in the early phase of the transcription (Bentley 2005).

The splicing of the pre-mRNA is accomplished by the spliceosome, which is composed of five small nuclear RNAs and hundreds of different proteins. The spliceosome is a large molecular structure resembling ribosomes in the size and complexity (Stanek & Neugebauer 2006). The splicing starts when the 5′-end of the intron forms a loop with itself by binding to an adenosine, about 100 nt from the exon-intron border. Then, a free OH-group of the released exon is attached to the following second exon (Proudfoot et al. 2002).

During the poly-adenylation step the nascent mRNA is first cleaved from the 3′-end, between the conserved AAUAAA and GU rich sequences. Then the poly-A-polymerase (PAP), with the help of several other proteins, catalyzes the synthesis of a poly-A tail of approximately 200 nt in length (Proudfoot 2004, Proudfoot et al. 2002). The length of the poly-A tail is controlled by poly-A-binding protein nuclear 1 (PABPN1, also known as PABP2). PABPN1 can bind to nascent poly-A tails about 11 nt in length and stimulate PAP activity in the synthesis reaction (Meyer et al. 2002). New PABPN1 molecules bind to the poly-A tail as it extends and forms a 21-nm particle, which is suggested to function as a "molecular ruler", leading to the formation of a 200-nt poly-A-tail (Keller et al. 2000).

Finally, the processed mRNA is exported to the cytoplasm, where protein translation takes place. The Poly-A tail seems to be important for the efficient export of the mRNA, and PABPN1 has been implicated to facilitate mRNA export (Chekanova & Belostotsky 2003). However, the mRNA is not exported as a naked RNA molecule where export factors bind but rather as a large complex, where different proteins, heterogenous nuclear ribonucleoproteins, splicing factors, and other mRNA processing factors are still bound. During the export of these messenger ribonucleoprotein particles (mRNPs), one of the most important proteins involved in the process is TAP (also known as NXF1) (Erkmann & Kutay 2004). TAP has been suggested to be involved in the export of 75 % of the mRNP particles (Herold et al. 2003). In a classical mRNP export process, the multiprotein TREX complex forms at the spliceosome and it interacts with the TAP. This leads to a process, where TAP binds directly to mRNA (Hautbergue et al. 2008). TAP has also affinity to bind nucleoporins at the NPC (Katahira et al. 1999). This affinity is decreased by heterodimerization of the TAP with p15 protein. Therefore, it has been suggested that p15 binding helps TAP (and mRNP particle) to diffuse through the nuclear pore. In this process, TAP first binds to the NPC, dimerizes with p15, and then diffuses through the pore (Katahira et al. 2002). In addition to splicing-coupled mRNP export, alternative export complexes can recruit TAP to mRNP. For example, a mRNA sequence coding for a leucine-rich ER sequestration signal can function in the TAP-mediated mRNP export, which is TREX-independent (Palazzo et al. 2007).

2.1.5 Viral Exploitation of Host Transcription Machinery

The viruses are obligate parasites, and therefore their DNA replication, transcription and mRNA translation processes depend on the host cell functions. Therefore, a virus infection offers a good experimental system to study these processes. Studies on viral and cellular transcription first identified several transcription factors, like Sp1, AP1 (Jun homodimer or Jun/Fos heterodimer), and oct-1 (Yaniv 2009). Papilloma, polyoma, and adenoviruses have had important roles in the transcription regulation studies.

The papilloma viruses contain a circular dsDNA genome of about 6500–8000 base pairs (bp) in length (Zheng & Baker 2006). Papilloma virus expresses its 3 non-structural proteins (E5, E6 and E7) from an early promoter. Late promoter presumably controls the expression of the remaining non-structural proteins (E1, E2, and E4) and the structural proteins (L1 and L2) (McCance 2005). The papilloma virus early promoter resembles the regular polymerase II promoter. It contains the TATA box element, for TFIID binding (Thierry 2009), a SP1 binding sequence close to the transcription initiation site (Hoppe-Seyler & Butz 1992), and two AP1 binding sites (Thierry et al. 1992). The papilloma promoter also contains also an oct-1 binding site to which nucleolin attaches in S-phase of the cell cycle and activates the transcription (Grinstein et al. 2002). This leads to temporal regulation of the transcription. The E2 protein can function as a transcription activator or repressor. In the latter case, it binds close

to the TATA box, restraining the TFIID binding to the TATA box by steric hindrance (Garcia-Carranca et al. 1988).

The polyomaviruses have a circular DNA genome, compromising a dsDNA minichromosome of about 5200 bp in length. It contains host-derived nucleosomes, and therefore it resembles the eukaryotic chromosomes (Fanning & Zhao 2009). One of the most-studied polyomaviruses has been the simian virus 40 (SV40). The importance of this virus has partially risen from the SV40-contaminated vaccines, which were administered to millions of people in the United States during 1955–1963 (Lee & Langhoff 2002). The SV40 early promoter controls the transcription of small and large t-antigen proteins. The late promoter directs the transcription of angoprotein and capsid proteins VP1, VP2, and VP3 (Eash et al. 2006). The SV40 transcription by polymerase II is regulated by several proteins, like NF-1, Sp1, and AP1 (Eash et al. 2006). Furthermore, SV40 large T-antigen protein has a pivotal role in the transcription activation, especially the late promoter. It can bind to TFIIA, TFIIB, TBP, Sp1, and RNA polymerase II, and it has been shown to stabilize the TBP-TFIIA complex (Damania & Alwine 1996, Damania et al. 1998, Johnston et al. 1996). The SV40 infection also increases the amount of Sp1 by 10-fold (Saffer et al. 1990). Since the Sp1 is a transcriptional regulator in approximately 30% of the mammalian genes, this upregulation also affects the cellular transcription (Cawley et al. 2004).

The adenoviruses have a large, linear dsDNA genome 36 kbp in length (Pombo et al. 1994). The genome contains early genes (E1A, E1B, E2A, E2B, E3, and E4), intermediate genes (IX and IVa2), and late genes (L1–L6) (Mei et al. 2003). The transcribed mRNAs are spliced, yielding tens of different proteins (Stone et al. 2003). The transcription is mainly performed by the RNA polymerase II, but a small region of the genome is transcribed by the RNA polymerase III. This produces a large pool of small, non-coding RNAs that antagonize the interferon-induced antiviral defense (Mathews & Shenk 1991). The immediate early proteins function as transcription regulators for several cellular and viral genes. The adenoviral promoters contain TATA box elements (TFIID binding site) and can have Sp1, AP1, NF1, and E2F binding sites, corresponding to the regular RNA polymerase II transcription (Hurst & Jones 1987, Leong et al. 1990, Mei et al. 2003, Stone et al. 2003, Yee et al. 1989).

2.1.6 DNA Replication

The genome of the mammalian cells is replicated in the S-phase of the cell cycle. The DNA replication is a complex process, involving a host of different proteins. This complex, a replisome, contains two DNA polymerases, primase, sliding clamps, clamp loader, helicase, and ssDNA-binding proteins (Figure 2).

DNA polymerases are the enzymatic complexes performing the actual replication. In mammalian cells the polymerases δ and ε are responsible for the leading and lagging strand synthesis (Langston & O'Donnell 2006). Ahead of the replication machinery, Mcm2-7 helicase opens the the DNA double helix.

The structural studies indicate that the Mcm2-7 forms double hexamers, with the ring-shaped hexamers in a head-to-head orientation (Gomez-Llorente et al. 2005). During the replication process, the heterotrimeric single-strand DNA-binding protein RPA protects the ssDNA and prevents a hairpin formation (Fanning et al. 2006). Before the synthesis of the new DNA strand, the tetrameric polymerase α-primase complex primes the DNA synthesis by forming a monomeric 8-12-nucleotide RNA primer, which can extended further to dimeric ~20-nt or trimeric ~30-nt lengths (Santocanale et al. 1993). Next, the 3′ OH-group is used as the start site for DNA replication (Santocanale et al. 1993). The polymerase α needs contacts with RPA protein to be stably associated to the primed site (Dornreiter et al. 1992).

The polymerase δ do not form stable contact with the DNA without accessory proteins. Proliferating cell nuclear antigen, PCNA, functions as a DNA sliding clamp in eukaryotic cells. It forms a circular homotrimer with possibly a pseudohexameric symmetry, which holds the polymerases δ and ε at the DNA strand (Moldovan et al. 2007). The sliding clamp is loaded to the DNA by the clamp loader complex RFC. In eukaryotic cells, the pentameric RFC binds ATP dependently to PCNA and forms the RFC:PCNA complex. The RFC:PCNA complex then associates with primed DNA and competes with polymerase α for RPA binding. When RFC:PCNA binds to the polymerase α, the polymerese is released from the primed sites and the sliding clamp is formed. The polymerase δ replaces the RFC by binding to the RPA and PCNA, and the DNA replication starts (Yuzhakov et al. 1999). At the double strand–single strand junction, this RFC replacement is further induced by the ATP hydrolysis leading to RFC dissociation (Bowman et al. 2004). In the bacteria, the clamp loader complex also links the leading and lagging strand polymerase complexes through the sliding clamps (Onrust et al. 1995, Stukenberg & O'Donnell 1995). The actual link between the polymerases in eukaryotic cells remains to be elucidated. However, an archeal homolog of the eukaryotic GINS complex can link the Mcm-helicase to the primase complex (Marinsek et al. 2006). There are several additional proteins involved in the DNA replication but their role in the actual replication process is poorly characterized (Langston & O'Donnell 2006). The suggested mammalian replication fork structure is shown in the Figure 2.

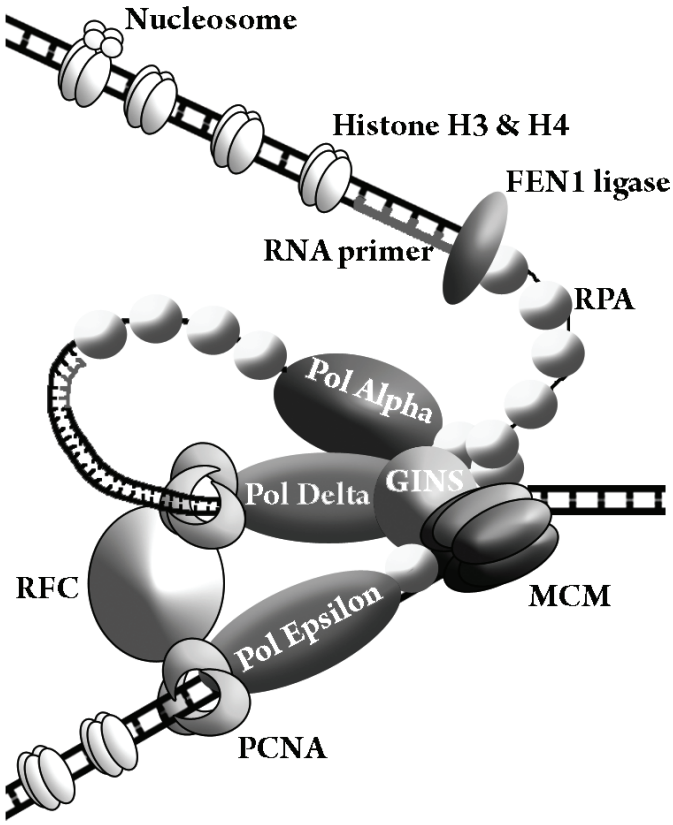

FIGURE 2 Suggested replication fork structure in mammalian cells.

2.1.7 Viral DNA replication

The viral genome replication strategies are extremely diverse; some viruses are almost completely dependent on the host replication machinery, whereas some code for their own replication proteins. The priming of the replication can proceed through normal RNA primer synthesis or by a hairpin structure formed by the viral genome. In some cases, a protein can also function as a primer and offer a free OH-group for DNA replication. Different cellular transcription factors can also be involved in the initiation of the replication.

Small DNA viruses have served as the model system for eukaryotic DNA replication for decades. The SV40 replication cycle resembles the host replication cycle, but the Mcm-helicase is replaced by the viral large T antigen. The large T antigen is a hexameric helicase, which also posseses dsDNA melting capability at the origin of replication, unlike the other helicases. However, similarly to MCM2-7 helicase, large T antigen can form a double hexameric structure at the origin of replication (Wessel et al. 1992). The polymerase α interacts with the large T antigen, binds to the DNA, and synthesizes the RNA primer (Smale & Tjian 1986).

Like the polyomaviruses, papillomaviruses need the host DNA replication machinery to replicate their genome. The human papilloma virus (HPV) produces two proteins, E1 and E2, which have fundamental roles in the DNA replication (Hebner & Laimins 2006). The E1 protein of bovine papilloma virus (BPV) has been shown to have ATPase activity, and it functions as a hexameric helicase (Sedman & Stenlund 1998). HPV E1 has also been shown to form double hexamers, identically to SV40 large T antigen and to the eukaryotic Mcm2-7 (Liu et al. 1998). E1 binds to the DNA also nonspecifically, and E2 protein aids E1 to find the specific origin of replication sequence (Hebner & Laimins 2006). Moreover, E1 also has RPA- and polymerase α-binding activity, thus enhancing the DNA replication. This, again, resembles the function of the SV40 large T antigen (Bonne-Andrea et al. 1995, Loo & Melendy 2004).

The adenoviruses code for three replication proteins: its own DNA polymerase, DNA binding protein (DBP), and precursor terminal protein (pTP). The origin of the replication sequence is GTAGTA in the inverted repeat regions in the genome. In addition, two cellular transcription factors, oct-1 and NF1, have been shown to enhance the adenovirus replication (de Jong & van der Vliet 1999). pTP protein is covalently attached to the 5′ end of the viral DNA. The DNA replication initiation is a protein-primed reaction, where viral DNA polymerase first attaches one cytidine to the pTP protein. This reaction is followed by attaching adenosine and thymidine nucleotides to the cytidine and forming a CAT trinucleotide. This tri-nucleotide is first hybridized to the second GTA sequence (from the template 3′-end) in the template strand and then jumps back for 3 nucleotides, to the first GTA sequence. Next, the elongation reaction is performed by the same viral DNA polymerase (King & van der Vliet 1994). This "jump-back" mechanism brings more accuracy to the priming reaction (de Jong & van der Vliet 1999). In the elongation phase, DBP unwinds the DNA without ATP hydrolysis. The multimerization and cooperative binding of DBP to the ssDNA is suggested to be the driving force behind the unwinding reaction (de Jong et al. 2003).

2.2 Diffusion Processes Inside Mammalian Cells

2.2.1 Translational Diffusion

When botanist Robert Brown observed the movements of the pollen grains in solution in the year 1828, he was puzzled by the apparent random movements of the grains. He concluded for the first time that this peculiar dance of the pollen grains had nothing to do with life or active movements of living matter. What Robert Brown was observing was the passive translational diffusion of pollen grains (i.e. Brownian motion). Almost a century later, in 1905, Albert Einstein was able to formulate an explanation for the phenomenon.

The translational diffusion is a process where solvent molecules bombard the particles in solution, leading to their random movements. Thus, the collisions convey the thermal energy of the solvent into kinetic energy of the

particles. Due to the random nature of the collisions, the particle has equal probability to move in any direction. Therefore the average velocity or the distance traveled by the particle approaches 0 as the observation time increases (Nelson 2004). Consequently, the diffusive motion is usually characterized by the mean square displacement (MSD). It is defined as the square distance between the positions, $s(t)$ and $s(t+\tau)$, which the particle occupies at time points t and $t+\tau$, averaged over all available steps. Hence, the MSD can be described as (Wachsmuth et al. 2008):

$$\left\langle d^2(\tau)\right\rangle = \left\langle [s(t+\tau)-s(t)]^2 \right\rangle = 2nD\tau \quad (1)$$

where d is the distance, $\langle ... \rangle$ denotes an average, n is the dimensionality of the diffusion, D is the diffusion coefficient of the particle, and τ the time interval between the measurement points. From the equation 1, we see that during the free diffusion, the MSD of the particle increases linearly as a function of the time. This kind of behavour has been reported for most of the mRNP particles inside the nucleus (Vargas et al. 2005).

According to the Stokes-Einstein relation, the diffusion coefficient D of the particle can be defined as:

$$D = \frac{k_b T}{6\pi\eta R_H} \quad (2)$$

In the equation, k_b is the Boltzman constant, T is the absolute temperature of the system, η is the viscosity of the solvent, and R_H is the hydrodynamic radius of the diffusing particle. Since the volume of a globular particle (assuming constant density) is relative to the cube of the radius, $V \propto r^3$, the changes in particle hydrodynamic radius are related to the cubic root of the particle mass, $R_H \propto \sqrt[3]{M}$. By combining this with the equation 1 and 2, we get a relation:

$$\left\langle d^2(\tau)\right\rangle \propto \frac{1}{\sqrt[3]{M}}\tau \quad (3)$$

The equation 3 shows that even small differences in the MSD (or in the diffusion coefficient of the particle) can indicate substantial differences in the mass of the particles.

2.2.2 Anomalous Subdiffusion

In the crowded environments the passive diffusion of the particles can be obstructed, leading to anomalous subdiffusion. In this case, the MSD is no longer linearly related to time, but the MSD can be described as (Guigas & Weiss 2008):

$$\left\langle d^2(\tau)\right\rangle \propto \tau^{\alpha},\ \alpha < 1 \quad (4)$$

The equation indicates slower diffusion in the case of a crowded environment. However, in the case of low crowding conditions or when the observation time increases, the equation collapses back to unobstructed diffusion (to equation 1), but in higher concentrations the subdiffusion duration increases (Saxton 2007). Computer simulations have indicated that in the cell cytoplasm, anomalous

subdiffusion can be observed on the time scale < 1 ms (Weiss et al. 2004). Anomalous subdiffusion has also been reported for Cajal bodies inside the nucleus (Platani et al. 2002), nascent ribosomes (Politz et al. 2003) and even for individual proteins (Kues et al. 2001).

2.2.3 Directed Movement

In the cellular environment, the active transport processes do not follow the simple rules of translational diffusion. In that case, the drift or transport velocity has to be included, and the MSD in 2 dimensions can be described by the following equation (Qian et al. 1991):

$$\left\langle d^2(\tau)\right\rangle = 4D\tau + v^2\tau^2 \quad (5)$$

where v is the velocity of the active transport. The equation 5 indicates that in the directed movement, the MSD grows faster than in pure diffusion, and this increase is related to the square of the observation time. In the case of pure active transport (D=0), the $\left\langle d^2(\tau)\right\rangle \propto \tau^2$, and if the $v = 0$ (pure diffusion), we again get the relation where $\left\langle d^2(\tau)\right\rangle \propto \tau$. If we assume that the actively transported complexes bind and unbind with the transport system (i.e., are partially freely diffusing and partially transported), we see that the MSD is related to:

$$\left\langle d^2(\tau)\right\rangle \propto \tau^{\beta},\ 1 \le \beta \le 2 \quad (6)$$

By comparing equations 1 and 6, we can easily distinguish the passive diffusion from the active transport of the particle. However, more detailed analysis of the active transport combined with translational diffusion includes also the binding-on, rate k_{on}, and -off rate, k_{off}, between the transport system and the transported cargo. In the equilibrium conditions, the average bound and unbound times are $t_{bound} = \frac{1}{k_{off}}$ and $t_{unbound} = \frac{1}{k_{on}}$, respectively. Thus, we can easily formulate the probability of the molecule to be bound (Saxton 1994):

$$P_{bound} = \frac{t_{bound}}{t_{bound} + t_{unbound}} \quad (7)$$

By combining this with the equation 5, we get formulation of the active transport combined with free translational diffusion, where binding and unbinding are taken into account (Saxton 1994):

$$\left\langle d^2(\tau)\right\rangle = 4(1 - P_{bound})D\tau + P_{bound}^2 v^2\tau^2 \quad (8)$$

However, in practice it is difficult to reliably measure simultaneously the on and off rates, the active transport velocity and the diffusion coefficient of the transported cargo.

2.2.4 Confined Diffusion

A more complex situation arises when the diffusing particle is confined to a closed corral. In the case of a stationary corral, the MSD in 2D can be calculated by (Gorisch et al. 2004):

$$\left\langle d^2(\tau)\right\rangle = \left\langle r_c^2\right\rangle \left(1 - e^{-\frac{4D\tau}{\left\langle r_c^2\right\rangle}}\right) \qquad (9)$$

In the equation, r_c^2 is the radius of gyration of the corral. PML bodies and Cajal bodies have been reported to show confined diffusion behavour, where they diffuse in and with a chromatin corral. Interestingly, an artificial nuclear body, formed by expressing Mx1-EYFP protein, showed identical behavour (Gorisch et al. 2004). The different diffusion bahaviour compared to the previous results (Platani et al. 2002), can be explained by the different imaging frame intervals, which were 10 s for (Gorisch et al. 2004) and 120-180 s for (Platani et al. 2002). The Figure 3 summarizes the MSD behaviors as a function of time in different situations.

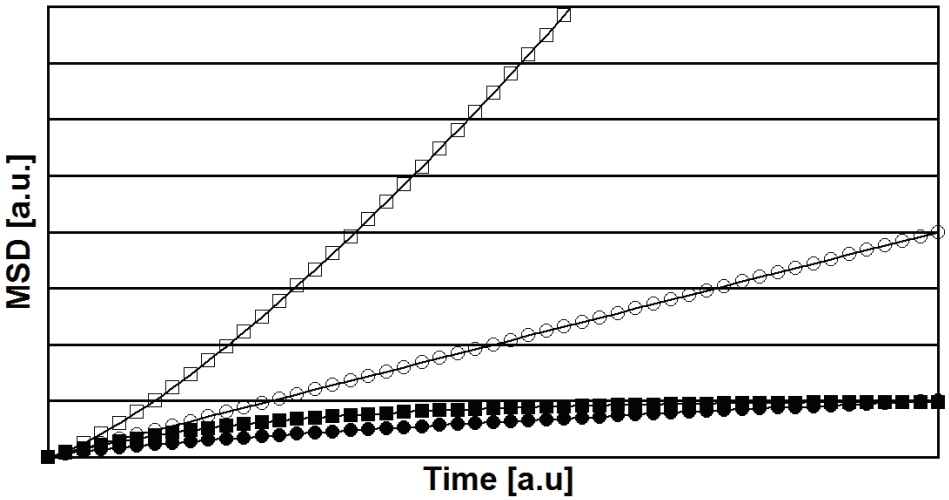

FIGURE 3 Mean square displacement behavior of diffusing particles. Diffusion with a flow (rectangle) leads to rapidly increasing MSD. In translational diffusion (circle), MSD grows linearly as a function of time. Diffusion within a corral (filled rectangle) leads first to linear MSD-time dependence, which slows down at later timepoints. In anomalous subdiffusion (filled circle), MSD has non-linear dependence to the time.

2.2.5 Facilitated Diffusion

In the biological systems, the simple translational diffusion would limit the reaction rates between the macromolecules to the Smoluchowski limit (von Hippel & Berg 1989):

$$k_{encounter} = 4\pi(D_A + D_B)(r_A + r_B)N_A 10^{-15} \quad (10)$$

In the equation, $k_{encounter}$ is the maximum encountering rate (units $M^{-1}s^{-1}$), D_A and D_B are the diffusion coefficients of the interacting molecules, r_A and r_B are the hydrodynamic radii of the molecules, and N_A is the Avogadro's number. Already in 1970, it was reported that the *lac* repressor found its target site on the DNA much faster than the Smoluchowski limit suggested (Riggs et al. 1970). Thus, it was shown that the inelastic nature of the collisions and non-specific interactions (van der Waals binding and charge-charge interactions) between the macromolecules allowed higher reaction on rates. In the case of protein-DNA interactions, these can lead to "hopping" and "sliding" of proteins along the DNA. In the hopping process, the protein collides with the DNA and then rolls and translocates along the DNA for 4-8 bases before unbinding. Additionally, in appropriate conditions, the proteins can also bind the DNA non-specifically for longer periods and diffuse or slide along the DNA strand (Berg et al. 1981). However, the protein sliding along the DNA corresponds to the 1D diffusion, and it is too slow to be the only translation process. However, the DNA concentration inside the nucleus is relatively high, and the proteins can be transferred easily between the closely located DNA strands. These processes increases the probability of specific binding and help the proteins to "sample" through the DNA (Gerland et al. 2002, von Hippel & Berg 1989).

2.3 Nucleus as a Dynamic Structure

The chromatin network is the major factor influencing intranuclear dynamics. The whole human genome is 2 x 3.1 billion base pairs (International Human Genome Sequencing Consortium 2004) in size. The haploid genome can be calculated to be 1 meter in length (0.34 nm per base pair), and if it would be as compact as physically possible, it would occupy a sphere of below 1 µm in radius. A more realistic volume of the genome can be approximated by calculating the radius of gyration of the DNA chain. When the DNA is assumed to behave as a self-avoiding ideal linear chain (Tegenfeldt et al. 2004), the radius of gyration of the whole genome can be calculated to be approximately 675 µm. The mammalian cell nucleus is usually oval-shaped, with axis radii of 10-15 µm, and therefore the genome needs to be highly packed. However, the genome packing needs to be dynamic, since during the cell cycle, different regions of the genome need to be exposed for transcription and replication. This is achieved by packing the DNA around the histone complexes.

The average nucle osome concentration has been indicated to be 140±28 µM in the nucleus of the interphase cells, but it can reach concentrations of 250 µM (Weidemann et al. 2003). In the vertebrate cells, the intranuclear

concentration of the DNA is reported to be 19 mg ml^{-1}, and the protein concentration can be high as 110 mg ml^{-1}. The histone proteins are the most abundant proteins in the nucleus, corresponding to over 6 % of the total protein content (Wachsmuth et al. 2008). In addition, the dense nuclear bodies are often located in the interchromosomal domains. In the *Xenopus* oocyte, the protein concentration inside the nuclear, bodies like nucleoli, Cajal bodies, and speckle domains can be even higher than in the nucleoplasm, reaching concentrations of 140-220 mg ml^{-1} (Handwerger et al. 2005). The average RNA concentration in the living mammalian cells has been measured to be 10-15 mg ml^{-1} (Zeskind et al. 2007). Accordingly, the macromolecule concentration in the nucleus can be summed to be approximately 150 mg ml^{-1}. This high concentration of macromolecules suggests that the diffusion processes inside the nucleus might be hindered.

The accessibility of the chromatin for macromolecules and nanoparticles has revealed chromatin networks with different "pore sizes." The studies showed that three different meshes can be found from the chromatin, with the pore sizes of 16-20 nm, 36-56 nm, and 60-100 nm. The 36-56-nm and 60-100-nm pore sizes correspond to perinuclear heterochromatin and euchromatin, respectively (Gorisch et al. 2003, Gorisch et al. 2005). Another study showed that even the condensed chromatin regions are accessible to macromolecules with a radius of gyration of 6 nm. Larger macromolecules, with a radius of gyration of 10 nm, showed limited access to perinuclear and perinucleolar chromatin regions, indicating a mesh pore size in the range of 20 nm (Verschure et al. 2003). This is in good agreement with the studies demonstrating rapid, simple diffusion of proteins through the chromatin mesh inside the nucleus (Kues et al. 2001). In line with this, a recent study indicated no correlation between the EGFP diffusion and chromatin concentration (Dross et al. 2009). Interestingly, in this study the EGFP diffusion coefficients had heterogeneous spatial distribution inside the nucleus, even though the chromatin content did not have an effect on the diffusion.

The diffusion of nanoparticles or larger nuclear bodies inside the nucleus depends on their size. The dextran nanoparticles, up to 580 kDa in size, diffuse relatively freely inside the nucleus, with a 75 % smaller diffusion coefficient, compared to water (Lukacs et al. 2000). The transcribed mRNP particles have been shown to diffuse passively through the nucleoplasm with a diffusion coefficient of 0.01–0.09 $\mu m^2 s^{-1}$. Part of the mRNP particles showed corralled diffusion, but directed movement was not observed (Shav-Tal et al. 2004).

In some cases, active movement has been suggested to be involved in the intranuclear movements. It was reported that adeno-associated virus (AAV) particles traveled inside the nucleus in linear trajectories (Seisenberger et al. 2001). Also, herpes simplex virus 1 (HSV1) has been shown to move in an energy and myosin-dependent manner inside the nucleus (Forest et al. 2005). The active movement is not limited to virus particles, since the activated gene loci can also be transported from the nuclear periphery to the inner parts of the nucleus. This movement was diminished by myosin mutants or by energy

depletion (Chuang et al. 2006). These results suggest the presence of still uncharacterized transport machinery inside the nucleus.

2.4 Methods to Study Diffusion in Living Cells

Light microscopy offers the possibility to follow dynamic processes inside the living cells. However, the spatial resolution in the light microscopy is usually limited by the diffraction, reducing the smallest resolvable distance between individual objects to ~200 nm. In addition, temporal resolution, light-detecting sensitivity of the photodetectors, and photostability of the fluorophores hinder the direct observation of the macromolecular diffusion (Pawley 2006). Even though the recent advances in the high-resolution light microscopy have shifted the resolution limit significantly below 100 nm (Betzig et al. 2006, Klar et al. 2000, Rust et al. 2006), the spatial resolution is still far from the molecular level. Nevertheless, indirect observation of diffusional processes is possible even with commercial imaging setups. Usually, the equilibrium of the system is disturbed, and the manner and the timescale by which the system reaches a new equilibrium give information about the diffusion and binding processes of the molecules.

The disturbance of the system can be achieved by irreversibly photobleaching the fluorescently labeled molecules under the study. In this case, the fluorescence recovery (i.e. the exchange of "dark" and "bright" molecules between the bleached area and surroundings) can be followed by timelapse imaging with the light microscope. The exchange rate yields information about the average molecular diffusion and binding in that area. This method is named fluorescence recovery after photobleaching (FRAP), and it has been widely used to study protein diffusion in living cells (Axelrod et al. 1976, Lippincott-Schwartz et al. 2001, Misteli 2001, Sprague & McNally 2005). In a similar experiment, the fluorescence loss from the areas surrounding the repeatedly bleached region can be measured. The fluorescence loss in photobleaching (FLIP), is related to the mobility of the fluorescent molecules between the bleached region and the region where the fluorescence loss is measured (Lippincott-Schwartz et al. 2003). However, accurate quantitation of the parameters related to the fluorescence recovery or loss processes is difficult, even though a wide variety of different mathematical models are available (Axelrod et al. 1976, Braga et al. 2004, Braga et al. 2007, Sprague et al. 2004, Sprague & McNally 2005). The initial conditions in these mathematical models usually assume a homogeneous, infinite pool of fluorophores, extremely fast bleaching process, Gaussian (or sharp) intensity profile after the bleach pulse, and no bleaching during the bleach phase. In addition, the fluorescence recovery data need to be normalized in order to calculate average recovery. The normalization processes also differ between the models.

An alternative approach to study diffusional processes is to use either photoactivable (Patterson & Lippincott-Schwartz 2002) or photoswitchable proteins (Chudakov et al. 2004). The former can be activated with near-UV light,

in which case they gain the ability to fluoresce at longer wavelengths. The latter changes its emission wavelength upon the excitation with near-UV light. In both cases, the activated or photoswitched molecules can be followed, and the fluorescence redistribution can yield information on the diffusion and the binding processes.

Almost-direct observation of the molecular diffusion is achieved by using fluorescence correlation spectroscopy (FCS). This method is based on the measurement and correlation of the average diffusion time of the molecules through the volume in which the excitation of the fluorophores takes place (Magde et al. 1974). Therefore, the local concentration of the fluorescent molecules must be low, in the range of 10–100 nM (Bacia et al. 2006, Kim et al. 2007).

In some cases, the diffusion of individual particles can be followed by single particle tracking (SPT). The method has been used to follow individual viral particles (Forest et al. 2005, Seisenberger et al. 2001), nanoparticles (Yum et al. 2009), nuclear bodies (Gorisch et al. 2004), and even individual proteins (Kues et al. 2001). In these cases, the MSD of the particle trajectories can be used to distinguish between different diffusion types (Gorisch et al. 2004, Yum et al. 2009).

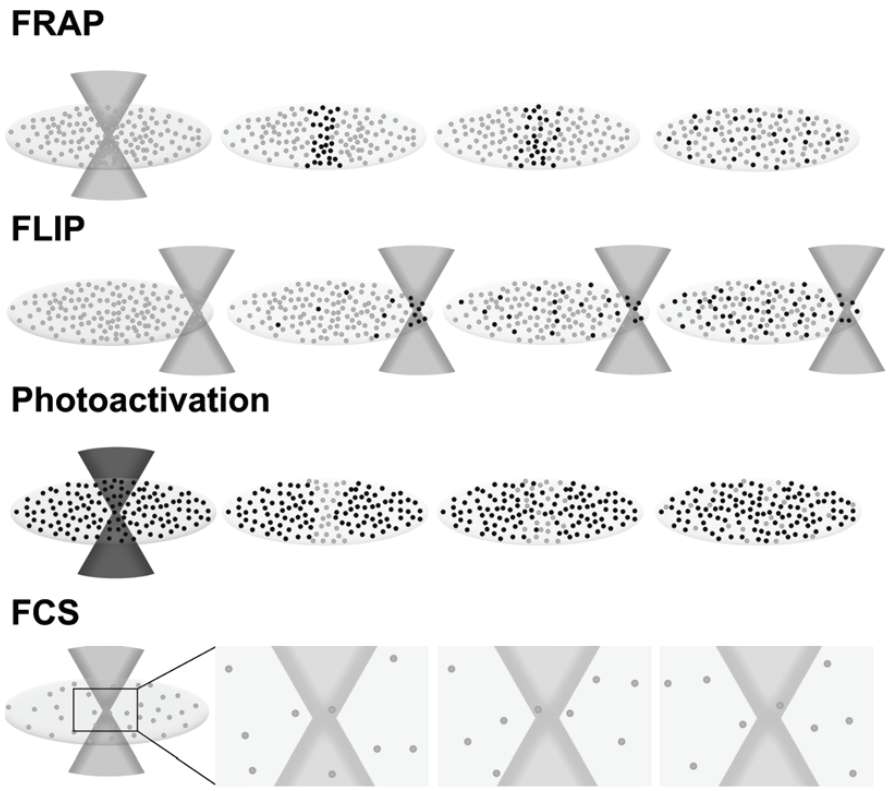

FIGURE 4 Schematic representation about FRAP, FLIP, photoactivation and FCS. In FRAP, fluorophores from a small region of the cell are irreversibly bleached with a high intensity laser and the recovery of the fluorescence is followed. In FLIP, laser light is used repeatedly to bleach the fluorescence and the fluorescence loss from a separate region is followed. In photoactivation experiments, fluorophores are activated, gaining the ability to fluoresce and the redistribution of the fluorescence is followed. FCS measures the time what the fluorophores spend in the confocal volume. This time is related to the mobility of the molecules.

2.5 Canine Parvovirus

Canine parvovirus (CPV), a member of the *Parvoviridae* family, is a small nonenveloped virus with a single-stranded negative sense linear DNA genome. The CPV infects young dogs, especically epithelial cells in lymphoids and intestine, leading to lymphopenia and severe diarrhea (Kerr et al. 2006). CPV emerged in the late 1960s or early 1970s, probably from feline panleukopenia virus or from wild carnivores (Shackelton et al. 2005, Truyen et al. 1998). The feline panleukopenia virus (FPV) and CPV have more than 99 % sequence homology in the genome, but their host ranges still differ (Parrish 1991).

The genome of the CPV contains two transcriptional units, one coding for the structural proteins VP1 and VP2 and the other for the non-structural

proteins NS1 and NS2. The structural protein VP1 contains a unique N-terminal sequence, which is spliced out from the otherwise identical VP2 mRNA (Reed et al. 1988). The nonstructural proteins NS1 and NS2 are also transcribed from the same gene, but messenger RNA splicing leads to a shift in the reading frame coding for the C-terminus of NS2 (Jongeneel et al. 1986, Wang et al. 1998a). The promoter sequence in the region of 4 mapping units (P4) functions as the promoter of the non-structural proteins NS1 and NS2. The second promoter at the location of 38 mapping units (P38) overlaps with the non-structural protein genes-coding sequences. This promoter activates the structural protein genes VP1 and VP2 (Reed et al. 1988).

2.5.1 Capsid Structure of Canine Parvovirus

The CPV capsids are composed of VP1, VP2, and VP3 proteins. VP2 is the major capsid protein; it is alternatively spliced from the gene also coding for VP1 protein. VP1 and VP2 proteins have identical C-terminal sequences, but VP1 harbors a 153-amino-acids longer N-terminus, which has been shown to contain the capsid nuclear localization sequence (Vihinen-Ranta et al. 1997), and it has phospholipase A 2 (PLA_2) enzymatic activity (Suikkanen et al. 2003b, Zadori et al. 2001). Usually, VP1 is present in the capsids at about 10-fold lower concentrations than VP2. VP3 is further processed from VP2 by proteolytical cleavage of 15-20 residues from the N-terminus (Kerr et al. 2006).

The icosahedral capsid structure of CPV was solved already in 1991 by Tsao et al. (Tsao et al. 1991). The structure contained VP2 protein, starting from the residue 22. Thus, the structure of the N-terminal region of the capsid proteins has not been solved. The structure indicated that all the capsid proteins had a typical eight-stranded beta-barrel ”jellyroll” fold (Tsao et al. 1991). However, the beta-barrel structure contains only a small portion of the structural protein, and the loops between the beta-strands represent ~85 % of the capsid protein (Kerr et al. 2006). The structural proteins form an icosahedron with a 2-fold, 3-fold, and 5-fold symmetry axes. The main features of the surface profile are the 3-fold spike, a higher region centered on the 3-fold axes, an elevated 5-fold ring surrounding the 5-fold axes, and 2-fold depression, located between neighboring 3-fold axes (Tsao et al. 1991). The subunit symmetry is represented in the Figure 5.

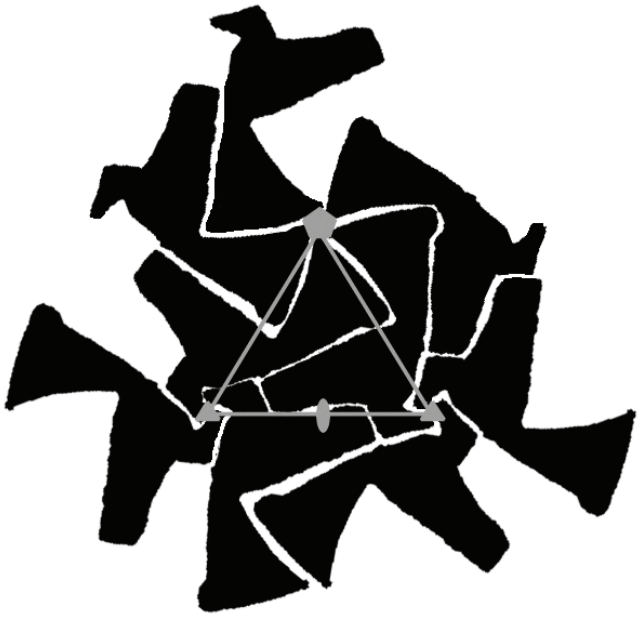

FIGURE 5 Organization of the structural proteins in the parvovirus capsids surface. Triangle represents one of the 20 facets of the icosahedron. Pentagon marks for the 5-fold symmetry axis, small triangles for 3-fold symmetry axes and oval for 2-fold symmetry axis. Adapted from Kerr et al. 2006

2.5.2 Non-Structural Proteins of Canine Parvovirus

Most of what we know about the autonomous parvoviral NS1 and its diverse functions comes from the studies of minute virus of mice (MVM), the rodent parvovirus LuIII, and aleutian mink disease parvovirus NS1 proteins. The NS1 is a 77-kDa, multifunctional protein whose functions are divided into different domains. The MVM NS1 contains an ATP-binding domain, which is needed for NS1 multimerization (Nuesch & Tattersall 1993). Multimeric NS1 has been shown to bind its DNA recognition sequence, $(ACCA)_{2\text{-}3}$, at the origin of replication (Cotmore et al. 1995), unwind the DNA with the help of NTP hydrolysis (Christensen et al. 1995b), and function as a 3′ to 5′ helicase (Christensen & Tattersall 2002, Pujol et al. 1997). NS1 is also able to nick the DNA and become covalently attached to the 5′-end of the DNA (Nuesch et al. 1995). These functions localize to the N-terminal (DNA binding) or central part (helicase) of the NS1 sequence (Kerr et al. 2006). NS1 also functions as a transcription regulator of the viral P38 promoter (Gavin & Ward 1990). The C-terminal part of the protein is vital for this function. However, the $(ACCA)_{2\text{-}3}$ binding sequence upstream of P38 seems to be important for the transcription regulation, suggesting that the N-terminal sequence is also important for this function (Gavin & Ward 1990, Legendre & Rommelaere 1994). It has been

suggested that the functions, including cytotoxic effects of NS1, are controlled by phosphorylation reactions (Corbau et al. 1999).

2.5.3 Canine Parvovirus Life Cycle in Cultured Cells

CPV entry starts at the cell surface by binding to the transferrin receptor (TfR). The virus enters the cells via dynamin-dependent endocytosis in clathrin-coated vesicles (Parker et al. 2001). Viruses are transported to the early endosomes and subsequently to the recycling endosomes. From the recycling endosomes, CPV particles traffic to the late endosomes and lysosomes (Suikkanen et al. 2002). The low pH in these structures induces conformational changes in the viral capsid, leading to the exposure of the unique N-terminus of the VP1 protein. (Parker & Parrish 2000, Vihinen-Ranta et al. 1998). It has been suggested that CPV is released from the lysosomes to the cytoplasm, and this release is dependent on the PLA_2 activity of the VP1 (Suikkanen et al. 2003a, Suikkanen et al. 2003b). After its release, CPV continues towards the nucleus by using microtubules and dynein (Suikkanen et al. 2003a). The microtubules have been reported to interact with cytoplasmic nucleoporin Nup358, thereby theoretically offering the virus a direct route to the nuclear envelope (Joseph & Dasso 2008). However, the significance of this link to the virus particle transport remains to be elucidated. The CPV capsids are able to enter the nucleus in seemingly intact form (Suikkanen et al. 2003a, Vihinen-Ranta et al. 2000). The capsids are too large to passively enter the nucleus; thus, the viruses are actively imported into the nucleus by using the NLS signal, located in the close proximity of the PLA_2 domain in the VP1 protein (Vihinen-Ranta et al. 1997).

Inside the nucleus, the viral genome is released from the capsid. The detailed release process is still uncharacterized. The transcription of the viral genes cannot take place before the single-stranded genome is converted into a double-stranded, transcription template. Subsequently, the genome replication processes are initiated from this so-called replicative form of the genome.

2.5.4 Canine Parvovirus Genome Replication and Transcription Regulation

The parvoviruses contain a linear, ssDNA genome with palindromic sequences at both ends. These sequences are capable to fold into hairpin duplexes (Kerr et al. 2006). Since the genome is of ssDNA, the transcription and genome replication of parvoviruses can start only after the complementary strand is synthesized. Therefore, the viruses depend on the activity of the host cell DNA replication machinery, and the complementary strand is synthesized only in the S-phase of the cell cycle. Onset of the viral genome synthesis has been shown to be dependent on Cyclin-A and Cyclin-A-associated kinase activity (Bashir et al. 2000). The 3'-end of the genome functions as the primer, and polymerase-α inhibition does not abolish the DNA synthesis *in vitro,* suggesting that primase activity is not needed in the replication reaction (Bashir et al. 2000). The genome replication of the parvoviruses proceeds through the rolling hairpin synthesis, where the palindromic sequences play a vital role (Figure 6) (Kerr et al. 2006).

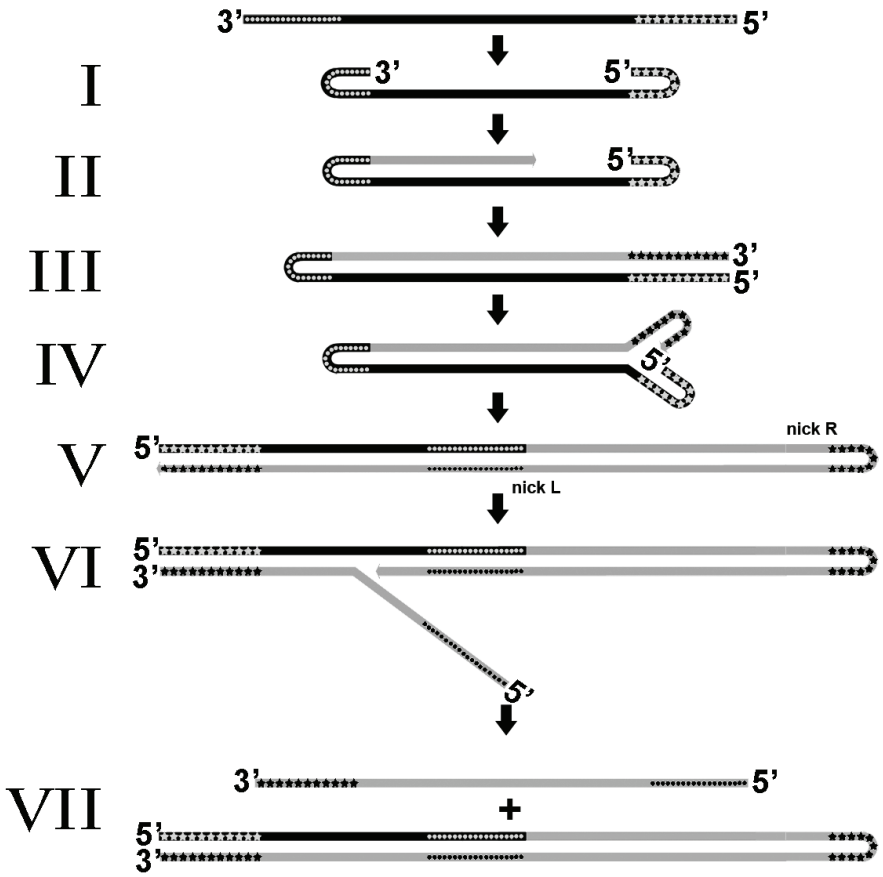

FIGURE 6 Schematic representation of the early phase of the parvovirus genome replication strategy. (I) Palindromic sequences (dots and stars) fold to hairpins and the (II) complementary strand is synthesized. (III - V) The hairpins are resolved and replicative form DNA is formed. (VI) DNA is nicked and (VII) first replicated genome forms. However, the replicated genome is in opposite polarity than the original genome. Adapted from Cotmore & Tattersall 2005

The parvoviral genome replication is dependent on NS1, RPA, PCNA, RFC, GMEB, HMG1/2 proteins, and polymerase-δ (Bashir et al. 2000, Christensen et al. 1997, Christensen & Tattersall 2002, Cotmore & Tattersall 1998). The replication starts by complementary strand synthesis, where the genome is converted to a dsDNA form. After the complementary sequence synthesis, transcription of viral genes leads to the production of NS1 protein. It has been shown that NS1 is needed to start the replication from the nick-R site (Fig. 6 III) *in vitro*. NS1 binds to a small non-hybridized "bubble" sequence and nicks the DNA with the help of HMG1/2 (Cotmore & Tattersall 1998). NS1 becomes covalently linked to the 5'-end of the DNA, and the replication can proceed.

The genome replication at the nick-L site (Fig. 6 VI) starts by NS1 binding to the $(ACCA)_{2\text{-}3}$ sequence at the origin of replication. NS1 multimeric assembly at this region is stimulated by cellular glucocorticoid modulatory element-binding (GMEB) protein (Christensen & Tattersall 2002). NS1 unwinds the DNA (Christensen et al. 1995b) and nicks the DNA with the help of GMEB (Christensen et al. 2001). During the process, NS1 becomes covalently attached to the formed 5′-end of the DNA (Nuesch et al. 1995). RPA binding stabilizes the formed ssDNA, and it has been suggested that RPA is recruited to the region by directly interacting with NS1 (Christensen & Tattersall 2002). The DNA synthesis is conducted by the polymerase-δ *in vitro* (Bashir et al. 2000), implying that it is the primary polymerase also *in vivo*. RFC protein is needed to load the PCNA complex to the DNA, which in turn holds the polymerase-δ at the DNA. NS1 functions as a helicase, which unwinds the DNA in the front of the polymerase complex (Christensen & Tattersall 2002, Pujol et al. 1997). The minimal parvoviral replication complex at the nick site L is summarized in Figure 7. At late stages of infection, the replication produces mostly single ssDNA genomes (Cotmore & Tattersall 2005), and the viral genome replication seems to be highly coupled to the virus assembly (Muller & Siegl 1983a).

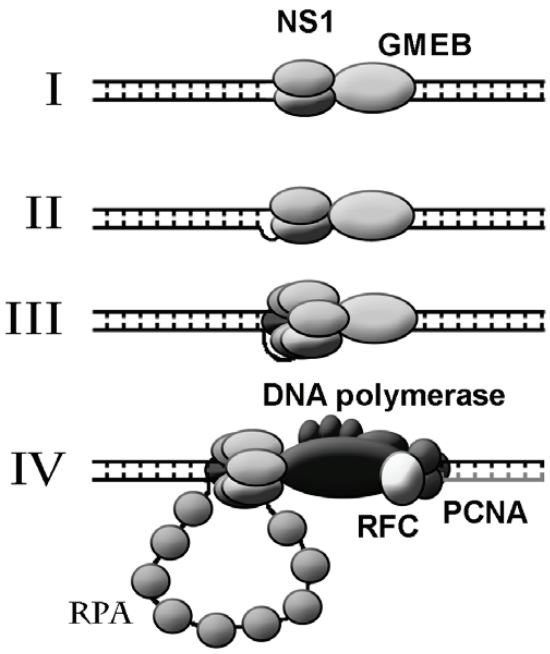

FIGURE 7 Schematic representation of the parvoviral replication fork structure at the nick L site (see figure 6). (I) NS1 binds to the origin of replication possibly in a dimeric form. Binding is induced by GMEB. (II) DNA is nicked by NS1 and covalent link forms between the NS1 and 5′-end of the DNA. (III) NS1 multimerizes and (IV) replication complex forms. RFC loads PCNA to the DNA, which in turn holds polymerase-δ in the DNA. RPA protein protects the ssDNA and prevents rehybridization.

The CPV transcription has not been studied as carefully as the MVM transcription but the genome organizations of the MVM and CPV are highly similar. The transcription of the parvovirus genome starts form the P4 promoter (Kerr et al. 2006). The MVM P4 activity is increased in the S-phase of the cell cycle and is strongly inhibited in the G1-arrested cells (Deleu et al. 1998). The P4 promoter contains common transcription activator bindings sites, like a GC-box, which binds the transcription factors SP1 (Pitluk & Ward 1991) and E2F (Deleu et al. 1999). The MVM P38 promoter also contains the GC-box, demonstrating the importance of SP1 for the transcription regulation of parvoviruses. It has been suggested that SP1 sequesters the basal transcription machinery to the promoters (Christensen et al. 1995a). The P38 promoter is activated over 1000-fold by the NS1 (Ahn et al. 1992). Near the P38, the NS1 binds to sequence termed transactivation region (tar) in an ATP-dependent manner (Christensen et al. 1995a). When the NS1 C-terminus was fused to the DNA-binding domain of the LexA transcription activator, the resulting chimera was able to activate LexA operator sites (Legendre & Rommelaere 1994). This suggests that the NS1 also interacts directly with the basal transcription machinery.

3 AIMS OF THE STUDY

The complex interplay between the viral and nuclear components has not been widely studied. In the present studies canine parvovirus was used as a model virus to illuminate these processes. In addition, viral protein diffusion and binding dynamics have not been elucidated in living, infected cells. In order to gain information about these processes, the objectives of the thesis were:

I. To study viral NS1 protein dynamics in living cells

II. To determine the changes in the location and dynamics of nuclear components caused by the viral infection

III. To elucidate the dynamics of key mRNA transcription and mRNA processing and transport proteins in the viral infection

4 SUMMARY OF THE MATERIALS AND METHODS

The materials and methods which were used in the studies can be found from the original publications. Tables below summarize the used materials and protocols.

TABLE 1 Fluorescent protein constructs used in the studies

Fluorescent Protein	Published	Publication
EGFP	-	I, II, III
EYFP	-	I, II
H2B-ECFP	(Weidemann et al. 2003)	II
H2B-EYFP	(Weidemann et al. 2003)	II
NS1-deYFP	-	II
NS1-EYFP	-	I
PCNA-EYFP	(Essers et al. 2005)	II
PABPN1-EGFP	(Calapez et al. 2002)	III
PML(IV)-ECFP	(Sourvinos & Everett 2002)	I
PML(IV)-EYFP	(Sourvinos & Everett 2002)	III
TAP-EGFP	(Calapez et al. 2002)	III
TBP-EGFP	(Chen et al. 2002)	III
TFIIB-EGFP	(Chen et al. 2002)	III
VP2-PAGFP	-	II

TABLE 2 Primary antibodies utilized in the studies

Antibodies (type)	Acquired	Publication
A3B10 (Mab)	Gift from C.R. Parrish, USA	II
BrdU (Mab)	Santa Cruz Biotech. USA	II
C#2 (Ab)	Gift from C.R. Parrish, USA	II
NS1 (Mab)	Gift from C. Astell, Canada	I, II
p80 (Ab)	Gift from A. Lammond, USA	I
PCNA (Ab)	Abcam, UK	I, II
SC-35 (Mab)	Abcam, UK	I

TABLE 3 Miscallenous fluorescent components used in the studies

Miscallenous Components	Acquired	Publication
anti-mouse & anti-rabbit IgG, Alexa Fluor-488	Invitrogen, USA	I, II
anti-mouse & anti-rabbit IgG, Alexa Fluor-555	Invitrogen, USA	II
anti-mouse & anti-rabbit IgG, Alexa Fluor-633	Invitrogen, USA	I, II
DAPI	Invitrogen, USA	II
DRAQ5	Biostatus Limited, UK	I
40 kDa FITC dextran	Invitrogen, USA	II
146 kDa TRICT dextran	Invitrogen, USA	II
500 kDa FITC dextran	Invitrogen, USA	II
5-Bromo-2-deoksyuridine	Sigma-Aldrich, USA	II

TABLE 4 Used protocols

Protocols	Equipment	Publication
Confocal Microscopy		
FLIP	Zeiss LSM510	I
FRAP	Zeiss LSM510	I, II, III
Imaging	Zeiss LSM510 & Olympus FV1000	I, II
Live Cell Imaging	Zeiss LSM510 & Olympus FV1000	I, II, III
Photoactivation	Olympus FV1000	II
Timelapse Imaging	Zeiss LSM510	I
Widefield Microscopy		
Fixed Cell Imaging	Zeiss CellObserver	II
Live Cell Imaging	Zeiss CellObserver	II
Miscallenous Protocols		
Antibody labelings	-	I, II
Transfections	-	I, II, III
DNase I treatments	-	II
Fluorescence Correlation Spectroscopy	(Weidemann et al. 2003)	II
Cloning	-	I, II
FISH	-	II
BrdU labeling	-	II
Microinjections	Eppendorf Transjector	II
Cell and Virus Culture	-	I, II, III

TABLE 5 Data analysis and processing

Data Analysis and Processing	Used Software(s)	Publication
Colocalization & Correlation	ImageJ & Excel	III
Deconvolution	SVI Huygens Essential	II
FCS fitting	Quickfit	II
FLIP quantitation	ImageJ & Excel	I
Fluorescence Intesity Measurements	ImageJ & Excel	II
FRAP quantitation	ImageJ & Excel	I, II, III
FRAP fitting	Matlab	I, II, III
FRAP experiment modelling	Virtual Cell	II
General Image Processing	ImageJ & Photoshop CS2	I, II, III

5 REVIEW OF THE RESULTS

5.1 NS1-EYFP Mimics Canine Parvovirus NS1 Behavior in NLFK Cells

Intranuclear accumulation of the canine parvovirus wild-type NS1 (wtNS1) protein in the virus infection was studied in highly synchronized NLFK cells. A punctuate nuclear pattern of wtNS1 emerged after 2 hours after the release of the cell synchronization block. The larger foci were detected as the infection proceeded, until the wtNS1-marked replication body filled the nucleus (I, Fig. 1.). The anti-NS1-labeled structures usually located in the close proximity of PML nuclear bodies and SC-35-marked nuclear speckles at 16 h post-infection (p.i.). Cajal bodies, highlighted with anti-p80 labeling, did not associate with the NS1 structures, unlike PCNA protein, which showed strong colocalization with the NS1 (I, Fig. 4).

In order to study NS1 dynamics in living cells, we constructed a fusion protein, where enhanced yellow fluorescent protein was fused to the C-terminus of NS1, yielding a 104-kDa fusion protein (I, Fig. 2). The successful cloning was confirmed by sequencing, and NS1-EYFP mRNA was detected by RT-PCR from the NLFK cells at 24 h post-transfection of the construct. NS1-EYFP protein localized strongly to the nucleus and showed mostly non-homogeneous distribution (I, Fig. 3). NS1-EYFP distribution was highly similar to wtNS1 in the infected cells, and immunolabeling of NS1 in these cells showed consistent fluorescence profiles (I, Fig. 2). In addition, structures marked with NS1-EYFP or wtNS1 had indistinguishable relations with PML bodies, splicing speckles, Cajal bodies, and PCNA (I, Fig. 4). NS1-EYFP allowed the study of how the replication bodies form as the infection proceeds. Live-cell confocal imaging revealed that durin infection NS1-EYFP first concentrated to the small foci, which enlarged and finally filled the whole nucleus. In non-infected control cells, the heterogeneous pattern of NS1-EYFP was detected, and it did not change during the observation time (I, Fig. 9)

.

5.2 NS1-EYFP Shows Dynamic Behavior in Absence of Infection

NS1-EYFP diffusion and binding dynamics were studied by fluorescence recovery after photobleaching (FRAP) and fluorescence loss in photobleaching (FLIP) experiments in the non-infected NFLK cells using laser scanning confocal microscopy. In the qualitative FRAP experiments, half of the nuclei of NS1-EYFP-expressing cells were photobleached with -ntensity laser, and the recovery of the fluorescence was followed by imaging a single confocal section. The recovery of the fluorescence was slow compared to the free EYFP, which showed full recovery after 10 seconds (I, Fig. 5). The NS1-EYFP-positive foci also recovered slowly, but the recovery indicated that the foci were dynamic and that NS1-EYFP was continuously exchanged between the foci and the nucleoplasm (I, Fig. 7). The nucleo-cytoplasmic shuttling of NS1-EYFP was studied by FLIP. NS1-EYFP diffusion from the nucleus to the cytoplasm was studied by repeatedly bleaching a small circular region in the cytoplasm. The data showed relatively fast fluorescence loss in the nucleus, indicating fast transport. The transport from the cytoplasm to the nucleus was studied by bleaching a small region inside the nucleus. The data indicated that the fluorescence was rapidly lost in the cytoplasm. However, also in this experiment, a small region of the cytoplasm, above and below the nucleus was bleached (I, Fig. 8).
Quantitative FRAP experiments were also conducted in the cells showing homogeneous NS1-EYFP fluorescence. In these studies, a small circular region of the cell was bleached, and the fluorescence recovery was followed with high frame rate confocal imaging. However, it was later discovered that the NS1-EYFP construct produced considerable amount of free EYFP. This was caused by the P38 promoter activity at the end of the gene coding for NS1, just prior to the EYFP gene. The production of free EYFP was abolished by modifying the TATA box of the P38 promoter and by removing the EYFP start codon. The production of free EYFP led to overestimation of the free pool of NS1-EYFP, and it masked a second, faster binding site. In the case of the NS1-EYFP FLIP experiments, it led to overestimated speed of the shuttling process. The subsequent studies were conducted with the modified version of the NS1-EYFP construct, named NS1-deYFP

5.3 The Canine Parvovirus Infection Leads to Profound Changes in Nuclear Architecture

The effect of canine parvovirus infection on the nuclear structures was studied by using immunofluorescence labeling, different fluorescent constructs, dextran microinjections (40 kDa radius of gyration, $r_g \approx 7$ nm, 146 kDa, $r_g \approx 13$ nm, and 500 kDa, $r_g \approx 24$ nm), confocal and widefield imaging and deconvolution.

5.3.1 Host Cell Chromatin Is Excluded from the Replication Body, Which Is Filled with Newly Synthesized Viral DNA

The formation of the replication body led to large changes in host cell chromatin. The chromatin was labeled with histone H2B-ECFP fusion protein or with 5-bromo-2-deoxy uridine (BrdU). The H2B-ECFP showed a dense ring of chromatin around the replication body (II, Fig. 1). Next, BrdU labeling was used to confirm that the host cell DNA also was packed to this region. Prior to infection, BrdU was incorporated into the host cell chromatin. The infection led to formation of a BrdU-labeled ring, which colocalized with the H2B-ECFP label (II, Fig. 3). The chromatin ring was highly packed, and even the free EYFP was unable to enter this region (II, Fig. S6). Dynamics of the chromatin condensation were also followed with timelapse imaging of infected, stably H2B-ECFP-expressing cells. The imaging showed that the chromatin condensation process is a relatively fast process, taking place in a few hours (II, Supplementary Movie M1). Even though the chromatin distribution was drastically different in infected cells, FRAP experiments indicated that H2B-EYFP binding dynamics were unaltered in infected cells (II, Fig. 3).

The fluorescence *in situ* hybridization experiments showed that the replication body is filled with viral DNA (II, Supplementary Fig. S3). BrdU labeling was used to study the formation of new DNA in the infected cells. Anti-BrdU antibody is able to label only ssDNA without denaturation steps. In the infected cells, the BrdU monoclonal antibody (MAb) labeled small foci inside the replication structures. When the cells were denatured, the labeling pattern was more homogeneous (II, Fig. 3). Surprisingly, the BrdU-positive foci, labeled without a denaturation step, were still visible 24 h after the chase. The DNA amount was measured with DAPI labeling and it showed an increase of over 2.5 times in infected cells at 24 h p.i. when compared to the G-phase cells. Lastly, the volume of the nucleus was measured from fixed cells, using confocal microscopy imaging and volume measurements. The volume of the nucleus showed an increase of about 3 times at 24 h p.i. (II, Fig. 4).

5.3.2 The Replication Body is a Homogeneous Structure

Fluorescently labeled dextrans were used to probe the nuclear organization and the parvoviral replication body substructures. In non-infected cells, the dextrans showed heterogeneous distribution, indicating that the nucleus is a compartmentalized structure with dense regions from which even the smallest dextrans are excluded. In the infected cells, the dextran distributions in the replication body area were homogeneous. However, the largest dextran was also partially excluded from the replication body and showed a concentrated ring around the replication structure (II, Fig. 1).

5.3.3 Protein Diffusion Dynamics Are Faster in Infected Cells

Protein diffusion dynamics were studied by fluorescence correlation spectroscopy (FCS) and FRAP in cells stably or transiently expressing free EYFP. In the FRAP experiments conducted in non-infected cells, the recovery of EYFP was fast, and the bleached region recovered in about 1 s (II, Fig. 5). The data were normalized, averaged, and fitted to the free diffusion model by Sprague et al. (Sprague et al. 2004). The fit was relatively good and gave a diffusion coefficient of D_{EYFP}=19 $\mu m^2 s^{-1}$. However, the fit showed a small inconsistency at the early recovery time points when compared to the measurements. Therefore, FCS was used to probe the EYFP diffusion. FCS measurements were conducted from transiently EYFP expressing cells, from several measurement points per cell. The FCS data indicated biphasic recovery, where 88 % of the EYFP diffused extremely fast, with a D_{EYFP}=50 $\mu m^2 s^{-1}$, and the rest had a diffusion coefficient D_{EYFP}=1 $\mu m^2 s^{-1}$. Consequently, the previous FRAP experiments were simulated using Virtual Cell software. Using the simulations, it was possible to take into account the fluorescence recovery during the bleach phase and use multiple EYFP populations with different diffusion coefficients. The FRAP recovery could be simulated with two EYFP populations; 96% had a diffusion coefficient D_{EYFP}=50 $\mu m^2 s^{-1}$ and the rest had D_{EYFP}=1 $\mu m^2 s^{-1}$ (II, Fig. 5).

In the infected cells, the fluorescence recovery was considerably faster, and the free diffusion model fit was clearly better, yielding a diffusion coefficient of D_{EYFP}=28 $\mu m^2 s^{-1}$. However, the fitting procedure does not take into account the diffusion during the bleach phase, and therefore Virtual Cell was used to simulate the recovery. Recovery could be reproduced with a single EYFP population, which diffused with a diffusion coefficient of D_{EYFP}=50 $\mu m^2 s^{-1}$. Together, these data indicate that the protein mobility is increased in the infected cells (II, Fig. 5).

5.3.4 Virus-Like Particles Diffuse Rapidly Inside the Nucleus

The dynamics of capsid protein VP2 was studied in cells expressing this protein fused to a photoactivable GFP (PAGFP). Western blot analysis confirmed that the PAGFP-VP2 construct had the predicted molecular weight (92 kDa) and was recognized by both the VP antibody and the EGFP antibody (II, Fig 2). In non-infected cells, the PAGFP-VP2 proteins were mostly concentrated in the nucleus, in addition to faint cytoplasmic fluorescence. The labeling pattern of VP Ab was similar to the distribution of PAGFP-VP2, while the capsid MAb labels were concentrated in to the nucleus (II, Fig. S2). This indicated that PAGFP-VP2 was able to form virus-like particles (VLPs), with a preferential location in the nucleus.

In photoactivation studies, the excitation of PAGFP at 488 nm was increased 10-20-fold by an activation laser pulse of 405-nm light. After photoactivation, PAGFP-VP2 diffused rapidly within the nucleus (II, Fig. 2). The loss of fluorescence on the photoactivation area was simulated by the Virtual Cell software. Such simulations indicated that in the activation region of

the non-infected cells, immediately after the activation pulse, about 81 % of activated PAGFP-VP2 had a diffusion coefficient of 5.0 $\mu m^2 s^{-1}$, while for about 19 % it was 0.02 $\mu m^2 s^{-1}$. For comparison, simulations of free PAGFP diffusion in non-infected cells showed a much higher diffusion coefficient of 18 $\mu m^2 s^{-1}$. In infected cells, the majority of PAGFP-VP2 fluorescence remained in the activation region, indicating that either the protein diffusion was slower or that this protein participated in some binding reactions (II, Fig. 2). The best fit for the data was achieved with Virtual Cell simulations with a two-component system. These simulations indicated that after the activation pulse, the faster population represented only 26 % of the activated PAGFP-VP2 in the activation region with a diffusion coefficient of D=5 $\mu m^2 s^{-1}$. The slower population (74 %) had a diffusion coefficient of D=0.001 $\mu m^2 s^{-1}$ (II, Fig. 2). In these experiments, the PAGFP-VP2 activation region was in the replication compartment, and the activated proteins diffused within the replication body.

5.3.5 NS1-EYFP and PCNA-EYFP Have Highly Similar Binding Dynamics

To elucidiate the dynamics of viral DNA replication, NS1-EYFP and PCNA-EYFP dynamics were studied in infected cells. FRAP experiments were conducted in the cells where replication body filled the whole nucleus, at 20–26 h p.i. NS1-EYFP recovery was extremely slow, indicating that the recovery was dominated by binding reactions. However, the binding-dominant recovery model gave a poor fit. Next, NS1-EYFP recovery was fitted to the full recovery model by Sprague et al. (Sprague et al. 2004), where the protein binding and the diffusion were taken into account. The fit was better but only with a NS1-EYFP diffusion coefficient of $D_{NS1\text{-}EYFP}$=1.78 $\mu m^2 s^{-1}$. If we assume that the previously free diffusion model fitting yielded a free EYPF diffusion coefficient of D_{EYFP}=28 $\mu m^2 s^{-1}$, mass scaling of $D_{NS1\text{-}EYFP}$=1.78 $\mu m^2 s^{-1}$ gives a protein size of 101 MDa, which is approximately 1000 times larger than the mass of NS1-EYFP fusion protein. Based on the poor fit and previously published reports that the NS1 is a multifunctional protein having multiple, different binding sites in the genome, we reused Virtual Cell software to simulate the recovery dynamics. In the models we first hypothesized that the NS1 binding site (i.e., the viral genome) can diffuse with an extremely small diffusion coefficient. The simulation represented the measured recovery really well with a pseudo on rate k^*_{on}=0.024±0.004 s^{-1} and off rate k_{off}=0.004±0.0007 s^{-1}, corresponding to a free diffusion time of 42 s and binding time of 250 s (II, Fig. 6). The NS1-EYFP diffusion coefficient was $D_{NS1\text{-}YFP}$=18 $\mu m^2 s^{-1}$ and the genome diffusion coefficient was D_{Genome}=0.01 $\mu m^2 s^{-1}$. However, it has been reported previously that the exogenous DNA is relatively immobile inside the nucleus (see Discussion section), and thus we proceeded to study the 2-binding site hypothesis, where NS1-EYFP is able to bind to two separate immobile binding sites, with different affinities. These simulations fit the data well. Now, the first binding site had $k^*_{on}=k_{off}$=0.1±0.02 s^{-1} and the second site had k^*_{on}=0.024±0.004 s^{-1} and off rate k_{off}=0.012±0.002 s^{-1}. The parameters yielded binding times of 10 s for the more transient binding and 83 s for the more stable binding site. In the

equilibrium conditions, 25 % of NS1-EYFP was bound to more transient sites, 50 % was bound to high-affinity sites, and 25 % was diffusing freely (II, Fig. 6).

BrdU and PCNA labeling experiments indicated that PCNA was spatially closely situated to the newly synthesized DNA. PCNA also strongly localized to the replication body as the infection proceeded. In the non-infected cells, the FRAP experiments showed fast recovery of PCNA-EYFP, with a recovery time comparable to free EYFP. The free diffusion coefficient of EYFP with these experimental parameters was D_{EYFP}=15±3 $\mu m^2 s^{-1}$. PCNA recovery was also fitted to the free diffusion model, yielding a $D_{PCNA\text{-}EYFP}$=9±2 $\mu m^2 s^{-1}$, suggesting that the trimeric form of PCNA-EYFP diffused freely inside the nucleus (II, Fig. 7). In the case of infection, the recovery of PCNA-EYFP was drastically slower, and fitting to the full model gave k^*_{on}=0.009±0.002 s^{-1} and off rate k_{off}=0.012±0.002 s^{-1}. They corresponded to the binding time of 83 s and free diffusion time of 111 s. The binding time of PCNA-EYFP was identical to the longer binding time of NS1-EYFP, even though the data analysis was technically completely different. NS1-EYFP parameters were obtained by Virtual Cell simulations and the PCNA-EYFP binding parameters were acquired by fitting of the data to the full recovery model (II, Fig. 7).

5.4 TBP-EGFP, TFIIB-EGFP, and PML-EYFP Are Different in Binding Behavior from Each Other

TBP is vital for the TATA box recognition, and together with TAF proteins, TBP forms the large multisubunit complex TFIID. The TBP-EGFP distribution and dynamics were studied in stably TBP-EGFP-expressing NFLK cells. Upon CPV infection, TBP-EGFP showed clear accumulation to the replication body region (III, Fig. 2). Next, the binding dynamics of TBP-EGFP were studied by FRAP. In the infected and non-infected cells, the TBP-EGFP recovery was slow compared to the free diffusion of EGFP (III, Fig. 2). The EGFP diffusion coefficient was D_{EGFP}=15±2 $\mu m^2 s^{-1}$. Since TBP is a component of the TFIID, a large 700-kDa (Burley & Roeder 1996) complex, simple mass scaling of the EGFP diffusion coefficient gives a theoretical diffusion of coefficient of TFIID D_{TFIID}=5.0±0.5 $\mu m^2 s^{-1}$. This was used in the TBP-EGFP recovery data-fitting. In the non-infected cells, the binding reaction pseudo on rate and the off rate of TBP-EGFP were k_{on}^*=0.0023±0.0003 s^{-1} and k_{off}=0.0060±0.0006 s^{-1} (III, Fig. 2), yielding a free diffusion time of 442 s and binding time of 167 s. In the case of CPV infection, the k_{on}^*=0.0068±0.0007 s^{-1} and k_{off}=0.017±0.0017 s^{-1} (III, Fig. 2), giving a free diffusion time of 147 s and binding time of 58.8 s for TBP-EGFP.

TFIIB is a protein that is needed in the mRNA transcription initiation. It has a homogeneous distribution within the nucleus, with a tendency to concentrate in the nucleolus. Markedly, in the infected cells the distribution was different, with the nucleolar localization nearly absent and with the pronounced accumulation to the replication body area (III, Fig. 3). FRAP was employed to study TFIIB-EGFP distribution in noninfected and infected cells stably expressing TFIIB-EGFP. In non-infected cells, free EGFP showed a diffusion

constant of D_{EGFP}=27±6 μm²s⁻¹. The diffusion constant for free TFIIB-EGFP, $D_{TFIIB\text{-}EGFP}$=20.4 μm²s⁻¹, was calculated by mass scaling of the EGFP diffusion coefficient by using equation 3 (TFIIB size of 33 kDa (Malik et al. 1991)). This diffusion constant was used in the fitting, which yielded the binding and unbinding rates for TFIIB-EGFP of k_{on}^*=0.22±0.05 s⁻¹ and k_{off}=1.8±0.4 s⁻¹. In the case of infection, FRAP indicated rate constants of k_{on}^*=0.33±0.07 s⁻¹ and k_{off}=1.6±0.4 s⁻¹ (III, Fig. 3). In control cells, 11 % of TFIIB-EGFP was bound and 89 % was freely diffusing. The free diffusion time was 4.5 s, and the binding time was 0.56 s. In the infected cells, 17 % of the protein was bound and 83 % was diffusing freely; in this situation, TFIIB-EGFP diffused only 3.0 s and stayed bound for 0.63 s. These results suggested that the virus infection mostly affected the binding of TFIIB-EGFP, but the release rate of TFIIB-EGFP stayed almost the same as in the control cells.

The PML body dynamics were studied by using PML-EYFP fusion protein, which was transiently transfected into the stably H2B-ECFP-expressing NLFK cells. In the infection, the PML bodies were often located to the nuclear periphery, avoiding the replication body area. When FRAP was used to study PML-EYFP dynamics, the slow recovery indicated long binding times. However, even though the infection changed the PML body location, it did not affect PML-EYFP binding (III, Fig. 6).

5.5 Diffusion Behavior of TAP-EGFP and PABPN1-EGFP Indicate Fast mRNA Dynamics in Infected Cells

Confocal microscopy of stably TAP-EGFP-expressing cells indicated that TAP-EGFP concentrated to the viral replication compartment (III, Fig. 4). In the non-infected cells, TAP-EGFP had homogeneous intranuclear distribution. Surprisingly, the fluorescence recovery in the FRAP experiments was identical in non-infected and infected cells (III, Fig. 4). The recovery was fitted to the free diffusion model, which yielded a diffusion coefficient of $D_{TAP\text{-}EGFP}$=2.2±0.3 μm²s⁻¹. The free diffusion coefficient of EGFP was D_{EGFP}=20±2 μm²s⁻¹. The molecular weight of TAP was 70 kDa (Liker et al. 2000), and the mass scaling of EGFP diffusion coefficient gave a diffusion coefficient of $D_{TAP\text{-}EGFP}$=13.0±1.3 μm²s⁻¹. This suggests that the TAP-EGFP shows effective diffusion behavior, with an effective diffusion coefficient of $D(eff)_{TAP\text{-}EGFP}$=2.2±0.3 μm²s⁻¹ (Sprague et al. 2004). Therefore, accurate k^*_{on} and k_{off} values and thus the binding and diffusion times can not be calculated. The fit yields only the relation k^*_{on}/k_{off}, which gives the ratio of bound/free molecules. The calculations indicated that in the equilibrium, 83 % of the TAP-EGFP was bound and the remaining population was diffusing freely.

The formation of the replication body also had a strong effect on the splicing speckle domains. In the non-infected cells transiently expressing PABPN1-EGFP, the speckle domains were randomly distributed in the nucleus, whereas in the case of CPV infection, the majority of the speckle domains was situated close to the nuclear membrane (III, FigS. 1). To investigate the possible

changes in PABPN1-EGFP dynamics in the CPV infection, we performed FRAP experiments in infected and in non-infected PABPN1-EGFP-expressing cells. The non-uniform distribution of PABPN1-EGFP prevented the use of conventional FRAP recovery models. Instead, a rectangular area in the middle of the nucleus was bleached, and recovery was followed every 0.5 s for a total time of 125 s (III, Fig. 5). When PABPN1-EGFP-expressing cells were infected with CPV, the recovery was slower, suggesting that either the diffusion of PABPN1-EGFP was slower or the binding of PABPN1-EGFP to mRNA poly-A tails was stronger and/or occurred more frequently. We modeled these situations by using Virtual Cell software, which allows the study of simultaneous binding to mobile binding sites and to the immobile speckle domains. We assumed that PABPN1-EGFP had a diffusion constant of $D=22\ \mu m^2 s^{-1}$, and its binding partner, mRNA, had diffusion constant $D=0.04\ \mu m^2 s^{-1}$ (Braga et al. 2007). The best fit to the data was achieved with mRNA binding rates of k*on=10±4 s-1 and koff=0.4±0.2 s-1 and speckle binding rates of k*on=0.025±0.008 s-1 and koff=0.020±0.007 s-1 (III, Fig. 5). The PABPN1-EGFP free diffusion time, mRNA binding time, and speckle binding time were 50 ms, and 2.5 s, and 50 s, respectively. PABPN1-EGFP was mostly bound to mRNA (91.7 % of the protein), but small fractions were diffusing freely (3.7 %) or in speckle domains (4.6 %). With infected cells we simulated the elevated pseudo on rate caused by the increased amount of mRNA. However, the best fit for the data was achieved when the speckle domain binding parameters were also modified. In this case, PABPN1-EGFP free diffusion time, mRNA binding time, and speckle binding time were 50 ms, and 2.5 s, and 1000 s, respectively (III, Fig. 5). Together, these models suggest that in CPV infection, PABPN1-EGFP is more frequently bound to mRNA, and the slower recovery can not be explained by hindered mRNA diffusion. In the infection, about 94.3 % of the protein was bound to mRNA, 5.3 % was inside the speckle domains, and 0.4 % was diffusing freely.

6 DISCUSSION

6.1 NS1-EYFP and wtNS1 Behave Similarly in CPV Infection

In order to study protein dynamics in living cells, we need to use agents that increase the contrast in the sample and somehow accentuate these proteins. In some cases, protein autofluorescence can be used (Reinert et al. 2007), but usually the proteins need to be labeled *in vivo* to achieve necessary contrast for microscopy. The easiest way to label proteins inside the living cells is to use genetically encoded tags that can be labeled using fluorophores (Griffin et al. 1998), which produce light photochemically (Boute et al. 2002) or which produce fluorescent light upon excitation by the appropriate wavelength of light; i.e., fluorescent proteins (Shaner et al. 2005).

With the purpose of studying NS1 dynamics in living cells, we constructed a fluorescent fusion protein, where NS1 was fused from its C-terminus to the yellow fluorescent protein, EYFP. EYFP is closely related to EGFP, which is 27 kDa in size (Yang et al. 1996), and has 2.4 x 4-nm beta-barrel structure (Giepmans et al. 2006). NS1 is a 77-kDa sized protein, thus it forms together with EYFP, a 104-kDa fusion protein. Simple mass scaling using eq. 3 gives only a 9 % decrease in the diffusion coefficient of NS1-EYFP compared to wtNS1, and therefore the diffusion behavior of the fusion protein is closely related to wtNS1.

NS1-EYFP was expressed in NLFK cells by transient transfection, but we failed to construct a stably NS1-EYFP-expressing cell line. This could be explained by the reported cytotoxic effects of NS1. They have been reported for parvovirus H-1 (Rayet et al. 1998) and MVM NS1 proteins (Legendre & Rommelaere 1992). In addition, MVM NS1 has been shown to induce cell cycle arrest (Op De Beeck et al. 2001). In the infected cells, NS1-EYFP and anti-NS1 antibody labeling had identical distributions, suggesting that NS1-EYFP mixes with wtNS1. In addition, the intranuclear localization of NS1-EYFP and wtNS1 in comparison to other nuclear organelles was similar, indicating that NS1-EYFP localized to the same structures inside the nucleus as wtNS1. Previous reports have identified a novel nuclear organelle formed during the parvovirus infection, named autonomous parvovirus-associated replication body (APAR-

body) (Cziepluch et al. 2000). CPV and H-1 NS1 foci contained similar components: PCNA, viral DNA, and newly synthesized DNA. These results indicate that APAR-bodies could be the sites for viral genome replication and possibly for progeny virus assembly, since those processes are highly coupled (Muller & Siegl 1983b). Correspondingly, the NS1 foci did not include PML, p80, or SC-35, and CPV NS1 was also excluded from nucleoli. In another report, several proteins were shown to localize to the replication bodies at late infection (Young et al. 2002). These proteins included cyclin-A, cyclin-E, PML, SMN, p80, and splicing factors.

6.2 NS1-EYFP Shuttling and NS1-EYFP Nuclear Accumulation During Infection Indicate Diverse NS1-EYFP Dynamics

Studies verifying the nuclear import and identical nuclear distribution between NS1-EYFP and wtNS1 suggest that NS1-EYFP functions as its wtNS1 counterpart. In addition, NS1-EYFP had the ability to induce the viral P38 promoter. Fluorescence loss in photobleaching experiments indicated that in the absence of infection, NS1-EYFP was able to shuttle between the cytoplasm and the nucleus, suggesting that the NLS and NES are functional in the fusion protein. NS1 has also been reported to have cytoplasmic functions, which would explain the movement between the cytoplasm and the nucleus (Nuesch et al. 1995).

When NS1-EYFP was expressed in non-infected cells, the NS1-EYFP-positive foci were spatially very stable and did not move or diffuse inside the nucleus. This suggests that the foci are attached to some nuclear structures. The foci can also be trapped by the chromatin corral, which has been reported to hinder the PML and Cajal body movement (Gorisch et al. 2004).

Nuclear body dynamics have also been studied by forming artificial nuclear bodies. Wild-type mouse Mx1 protein shows nuclear localization and nuclear body-like appearance (Dreiding et al. 1985). However, it has been reported that when inactive fusion protein Mx1-EYFP is expressed, it forms artificial nuclear bodies, and their diffusion is highly limited inside the nucleus by the chromatin (Gorisch et al. 2004). Therefore, it remains to be elucidated if NS1-EYFP-positive nuclear bodies are genuine nuclear organelles in the absence of the infection or just aggregations of NS1-EYFP protein.

Confocal timelapse imaging of the virus infection in NS1-EYFP-expressing cells showed the formation of the large viral replication compartment seen in the later time points of the infection. One can speculate that the viral genome replication, combined with the increased viral transcription and virus particle formation, leads to enlargement of this replication compartment. We did not observe any fusion events between the small NS1-EYFP foci during the infection; the larger foci fused only at later infection time points, when the replication compartment almost filled the whole nucleus.

6.3 Nuclear Size and its DNA Content Increases during the Infection and the Chromatin is Marginalized to Nuclear Periphery

Timelapse imaging of NS1-EYFP foci enlargement raised questions about the possible nuclear rearrangements during infection and especially about the intranuclear chromatin organization. The widefield timelapse imaging of H2B-ECFP-expressing cells indicated that the endogenous chromatin was discarded from the replication body area and that the nuclear volume increased during infection. Similar behavior has been shown for Herpex simplex virus-1 infection. The HSV-1 infection leads to a large increase in the interchromosomal space and compression of endogenous chromatin (Monier et al. 2000). DAPI labeling indicated that the amount of intranuclear DNA increased in a similar fashion to the nuclear volume as the infection proceeded. The non-infected cell nucleus contains high amounts of DNA and RNA (Wachsmuth et al. 2008). Higher amounts of DNA (endogenous + viral) could lead to slower movement of large protein complexes and especially viral capsids. The increased nuclear volume also keeps the DNA concentration approximately constant in the case of virus infection.

FISH and BrdU experiments showed that replication bodies contained newly synthesized viral DNA. BrdU labeling could also be permormed without the denaturation step. This suggests that in this case, only the synthesized ssDNA was labeled, since it is well established that a denaturation step is needed to expose the BrdU nucleotides from dsDNA. The results indicate that the infected cell nuclei contain accessible viral ssDNA, which is not packed into the capsid. This is surprising, since genome packing has been connected to the genome replication (Muller & Siegl 1983a). In addition, BrdU foci were still visible after 24 h after the BrdU chase, suggesting that a large portion of the newly synthesized ssDNA remained accessible to antibodies in the nucleus. BrdU label was not detected in the cytoplasm, even in the denatured cells, implying that virus capsids are not exported in large amounts from the nuclei of infected cells.

6.4 Intranuclear Protein Mobility Is Increased in Infected Nuclei

Previous timelapse imaging showed that the replication body is formed as the relatively small NS1-EYFP-positive foci enlarge and fill the nucleus. Therefore it was interesting to see what happened to dextrans of various sizes when they were microinjected into the nuclei before the infection. This way, we could probe the internal structure of the replication body and see if some dextrans were excluded from the replication body. Dextran microinjection indicated that the replication bodies were relatively homogeneous structures and accessible to virus-sized particles. Only the $r_g \approx 24$-nm particles were partially excluded from the replication body, as they showed a slight accumulation in the nuclear periphery.

EYFP was used as an indicator of free protein diffusion. The EYFP showed biphasic diffusion behavior, where part of EYFP was diffusing really slowly compared to the freely diffusing population. The EYFP diffusion coefficients in NLFK cell nuclei were in good agreement with those reported recently for EGFP inside the cell nuclei (Dross et al. 2009). In the infected cells, the EYFP distribution was relatively similar to non-infected cells, but the marginalized chromatin hindered EYFP diffusion to this region, leading to a formation of a darker nuclear rim close to the nuclear membrane. The FRAP experiments showed that the slow population of EYFP had disappeared, and the recovery was faster. Thus, the results indicate that protein can diffuse more freely in infected cells, increasing overall mobility of the proteins. The cause of the better mobility is still unknown. One can hypothesize that in the infected cells, the chromatin does not hinder the protein diffusion, since it is marginalized to the nuclear periphery. Surprisingly, it was recently reported that neither the diffusion coefficient, relative amount of slowly diffusing EGFP, nor their diffusion coefficients, was dependent on the chromatin density (Dross et al. 2009). However, it might still be possible that the chromatin density in non-infected cells is always above some certain threshold, which leads to biphasic diffusion behavior. Protein diffusion inside the nucleus has been previously studied only in non-infected cells (Dross et al. 2009, Kues et al. 2001, Pack et al. 2006), and to our knowledge, this is the first report on protein mobility inside the virus-infected nuclei.

According to the Smoluchowski relation, the maximum rate of binding between two interacting species is directly related to their diffusion (von Hippel & Berg 1989) and consequently to their encounter probability. With an increased mobility in the infected cells, the protein-binding reactions are expected to be faster. An enhanced kinetics of replication and assembly would be of obvious benefit to the virus. Higher molecular crowding has been shown to raise the DNA melting temperature and thereby enhance the rate of hybridization (Richter et al. 2008). Likewise, lower molecular crowding decreases the DNA hybridization affinity. This might help to maintain the replicated CPV in single-stranded form prior to assembly. Moreover, conditions of lower molecular crowding favor binding of the single-strand binding-protein RPA (Bashir et al. 2001) to ssDNA, thus preventing DNA hybridization.

6.5 Viral Capsids Show Rapid Diffusion Inside the Nucleus

Capsid protein dynamics were studied by photoactivation experiments of PAGFP-VP2 protein. Previously, it has been shown that EGFP-VP2 is able form intact VLP particles (Gilbert et al. 2006). Immunofluorescence labeling with an antibody that recognizes a region near the two-fold axes (Wikoff et al. 1994) suggests that the labeled intranuclear particles form at least trimeric units. In addition, it has been shown that MVM capsid proteins are imported to the nucleus in the trimeric form (Riolobos et al. 2006). Simulations of the photoactivation experiments suggested the existence of two separate PAGFP-

VP2 complexes in the activation region. Mass scaling of the PAGFP diffusion coefficient using eq. 3 gave theoretical diffusion coefficients of 11.9 $\mu m^2 s^{-1}$ for the PAGFP-VP2 monomer, 8.2 $\mu m^2 s^{-1}$ for the PAGFP-VP2 trimer, and 3.0 $\mu m^2 s^{-1}$ for the entire capsid. Previously, a diffusion coefficient of 17 $\mu m^2 s^{-1}$ had been measured with fluorescence correlation spectroscopy (FCS) for CPV VLPs in buffer (Gilbert et al. 2004). Based on the observation that the diffusion coefficients of virus-sized dextrans are ~25 % smaller in the nucleus than in water (Seksek et al. 1997), the nuclear diffusion coefficient of the CPV VLP can be estimated to be D=4.3 $\mu m^2 s^{-1}$. This, together with prior results on VLP assembly, trimer nuclear import, and our immunofluorescence data, suggests that the faster component corresponds to freely diffusing VLPs.

An adeno-associated virus, another parvovirus, has been shown to move along linear tracks in the nucleus (Seisenberger et al. 2001). Herpex Simplex virus 1 has also been shown to move in an actin- and energy-dependent manner (Forest et al. 2005). Our data suggest that the motion of CPV capsids within the nucleus occurs by passive diffusion. Moreover, in infected cells, the faster capsid population was shown to diffuse with the same diffusion coefficient as in the control cells. This allows for the capsids to travel a distance of 10 µm in 3.3 seconds. The photoactivation experiments indicated that the majority of the 74 % of PAGFP-VP2 redistributed extremely slowly from the activation region, with the activation spot still visible 10 minutes after activation. This fraction is likely to be bound to DNA, as shown previously for the LuIII parvovirus (Muller & Siegl 1983b). However, the proportions of rapidly and slowly diffusing populations are directly related to the photoactivation of these species and do not necessarily represent the steady state conditions in the nuclei. When analyzing the entire nucleus, 98% of the activated PAGFP-VP2 molecules were rapidly diffusing in the non-infected cells, in comparison with 80% in the infected cells.

6.6 PCNA and NS1 Show Similar Binding Durations in Infected Cells

The previous experiments showed that the expressed NS1-EYFP localized to the parvoviral replication bodies inside the nucleus. It showed identical distribution with the wild-type NS1 and shuttled between the cytoplasm and the nucleus. The replication bodies were shown to be homogeneous structures where protein mobility was increased and viral capsids could diffuse relatively freely. DNaseI treatments suggest that the NS1-EYFP sequestration to the nucleus is DNA-mediated. In addition, previously, it has been shown that NS1 is able to bind DNA non-specifically in low-salt conditions *in vitro* (Cotmore et al. 1995). Thus, we suggest that the NS1-binding substrate in the non-infected cell nuclei is DNA or some DNA-associated protein. Since NS1-EYFP fusion protein was able to induce the P38 promoter (Niskanen et al., manuscript), it was suggested that the C-terminal fusion does not block the transactivation

activity of NS1, which is also located at the C-terminal part of NS1 (Legendre & Rommelaere 1994).

The above experiments suggested that the parvoviral NS1 protein is able to bind non-specifically to DNA in vivo in the absence of virus infection. However, in the case of infection, our FRAP data, indicating long binding times of NS1 inside the replication body, were not well fitted by the recovery models of Spraque et al. (Sprague et al. 2004), which assumed the binding partner of fluorescent NS1 to be immobile. However, the FRAP recovery of NS1-deYFP could be reproduced with two different Virtual Cell models. In the first model, the binding partner of NS1-deYFP was assumed to be mobile and to diffuse slower than mRNA. We hypothesized that the mobile binding partner is the viral genome. Nevertheless, motility of the viral genome is improbable, as earlier studies have indicated that exogenous DNA in the cell nucleus is essentially immobile (Lukacs et al. 2000). The Minute virus of mice genome has been shown to contain multiple copies of two distinct binding sites for NS1 (Cotmore et al. 2007). Based on this and the improbable genome diffusion, a second model with two discrete binding sites was considered. This model gave an excellent fit to our data. The longer binding time of 83 s could reflect the time of viral genome synthesis, since NS1 functions as a helicase in the viral DNA replication. A similar binding time was measured for PCNA-EYFP, another component participating in the genome replication. The shortened binding time might reflect NS1 transcription activator behavior. NS1 is known to activate the parvoviral P38 promoter (Ahn et al. 1992).

PCNA has been shown to be needed for the parvoviral DNA replication in vitro (Christensen et al. 1997), and it has been found to accumulate in the parvoviral replication body (Cziepluch et al. 2000). Our FRAP experiments on PCNA-EYFP dynamics, performed in non-infected cells, indicated free diffusion with a diffusion coefficient of 9±2 $\mu m^2 s^{-1}$, which is compatible with the theoretical calculated diffusion coefficient for a PCNA-EYFP trimer. In line with this, cellular PCNA has been reported to form homotrimers and possibly loose double trimers (Naryzhny et al. 2005). However, the PCNA-EYFP diffusion coefficient is slightly smaller than the reported EGFP-PCNA effective diffusion coefficient of 15 $\mu m^2 s^{-1}$ (Essers et al. 2005). The small difference in the results may be explained by differences in the diffusion modeling, since Essers et al. used simulations to reconstruct the fluorescence recovery curve (Essers et al. 2005), and our results are based on the free diffusion model by (Sprague et al. 2004). It is well established that the used diffusion model yields too small diffusion coefficients (Braga et al. 2004). Nevertheless, the relative error can also be approximated to be the same in the EYFP FRAP experiments, suggesting that the mass scaling gives the correct approximation about the size of the diffusing PCNA.

In the S-phase of the cell cycle, PCNA associates strongly with the replication foci, with reported residence times ranging from ~25 s of half-life (Solomon et al. 2004) to a negligible turnover, indicative of a long half-life (Essers et al. 2005). Our data suggest that in the infected cells, PCNA-EYFP recovered slowly, with a binding time of 83 s, which was identical to the NS1

binding time. Similar binding times have been reported for many transcription-related or chromatin-binding proteins (binding times ~3–180 s), with the exception of H2B (binding time >3600 s) (Phair et al. 2004).

It is known that parvoviruses, which pack only + or – sense genomes, produce predominantly single viral ssDNA genomes (Cotmore & Tattersall 2005). PCNA and NS1 are both tightly involved in the parvoviral genome replication; PCNA is thought to remain bound to the DNA strand and hold the polymerase on the template, and NS1 is suggested to function as a helicase in the front of the polymerase. Therefore, we propose that the binding time of 83 s corresponds to the viral genome replication time. With a single-stranded viral genome of 5300 bases, this would lead to a synthesis rate of 64 bases/s, approximately twice that of cellular double-stranded DNA 33 base pairs/s (Jackson & Pombo 1998), but in the range of Epstein-Barr virus synthesis rate, 5-78 base pairs/s (Norio & Schildkraut 2004). Even faster DNA replication has been reported for adenovirus infection, with a seven-times-higher DNA replication activity than in non-infected cells (Yamashita et al. 1975).

6.7 TBP and TFIIB Bind Viral Promoter with Different Rates

TBP is involved in the TATA box recognition and binding in the promoter region. Previously, it has been shown that TBP interacts strongly with the chromatin, also staying bound during mitosis (Chen et al. 2002). The FRAP studies indicated that TBP-EGFP binds and is released more frequently in the infected cells. The difference in the binding times between the non-infected and infected cells may be caused by the lack of histone H3 in the viral genome. It has been reported that TFIID binds to H3 (Vermeulen et al. 2007), which can further increase the binding time to the promoter. Shorter free diffusion time (i.e. larger pseudo on rate) in the infection can be explained by the relative increase in the binding sites.

Transcription factor II B is one of the general transcription factors (GTFs) needed in RNA polymerase II-mediated transcription. In the classical model for the mRNA transcription initiation, TFIIB forms a link between TBP and the incoming RNA polymerase II (Deng & Roberts 2007). TFIIB has been reported to recover 100 times faster in the FRAP experiments than its functional partner, TBP (Chen et al. 2002). Overall, TFIIB-EGFP showed fast binding and unbinding in the cell nuclei. However, in the infected cells, the free diffusion time was 33 % shorter when compared to the non-infected cells. This shorter free diffusion time could be explained by the icreased concentration of binding sites (i.e. viral promoters) since the previous experiment indicated that the DNA content of the nucleus increases in infection.

It is relatively well established that in transcription, TFIIB dissociates from the pre-initiation complex PIC and does not travel along the DNA with polymerase II complex (Zawel et al. 1995). The RNA polymerase II has been shown to have 3 distinct kinetic fractions during transcription, corresponding to promoter binding, transcription initiation, and elongation, with mean residence

times at the template of 6 s, 54 s, and 517 s, respectively (Darzacq et al. 2007). Thus, our results on TBP-EGFP and TFIIB-EGFP binding dynamics suggest that the TBP stays bound to the promoter, and during this time several promoter binding events (~10) of polII can take place. TFIIB-EGFP functions perhaps only in the initial promoter recognition of the polII and is then rapidly released from the pre-initiation complex.

FRAP analysis of PML bodies, marginalized to the replication body periphery in infected cells, revealed slow recovery. The virus infection did not affect their recovery kinetics, described earlier (Weidtkamp-Peters et al. 2008). The results suggest that PML bodies might not participate in the late stages of CPV infection.

6.8 mRNA-Associated Proteins Show Fast Binding Dynamics

The poly-A-binding protein nuclear 1, PABPN1, is involved in various stages of mRNA lifecycle (Calado & Carmo-Fonseca 2000). Our data from non-infected cells confirmed previous observations that PABPN1 is localized to the splicing speckle domains and to the nucleoplasm (Calapez et al. 2002). In CPV-infected cells, PABPN1-EGFP distribution was similar to that of non-infected cells, although the speckle domains were usually situated close to the nuclear envelope. Even though both TAP and PABPN1 are mRNA-binding proteins, FRAP experiments indicated that their dynamics were completely different from each other.

FRAP experiments and virtual cell modeling suggested an increased amount of PABPN1-EGFP binding partners: i.e., mRNA in these cells. Possibly , a reduced mRNA diffusion rate could not alone explain the slower recovery of PABPN1-EGFP. Recent studies have demonstrated that a large proportion of PABPN1-EGFP is bound to mRNA, but the reported mRNA binding off rate was much higher than in our simulations (Braga et al. 2007). Differences in the results might arise from the different experimental set up. In our experiments, the frame rate was 2 frames/s, and the first image of the bleach ROI was taken about 100 ms after the bleach pulse, as these values were 12.8 frames/s and 39 ms in Braga et al., respectively. Moreover, in contrast to homogeneous nucleoplasm monitored by Braga et al. (Braga et al. 2007), we studied areas containing speckle domains. These differences made the accurate comparison of the results difficult. However, in both cases the binding of PABPN1-EGFP to mRNA was transient, and the free pool of PABPN1-EGFP was small.

TAP protein is involved in the mRNA export, and it has been shown to interact with nucleoporins and polyadenylated mRNA (Conti & Izaurralde 2001, Strawn et al. 2001). In non-infected cells, TAP had homogeneous intranuclear distribution. TAP also localized to the nuclear membrane in some cells. Even though TAP accumulated to the replication body area, the diffusion and binding dynamics did not change. The TAP recovery data were fitted with the free diffusion model, which gave a small diffusion coefficient of 2.2±0.3 $\mu m^2 s^{-1}$. Since TAP is a 70-kDa protein (Liker et al. 2000), this diffusion coefficient was

6.5-times too small, when compared to the theoretical diffusion coefficient of TAP, calculated from the free EYFP diffusion coefficient. However, the recovery data fitted well with the free diffusion model, and together they imply that the binding reaction processes are much faster than the free diffusion. In this case, reaction-diffusion equations reduce to a diffusion equation with a different diffusion coefficient, known as the effective diffusion coefficient (Sprague et al. 2004). This suggests that the TAP binding is very transient and shows rapid binding and unbinding events. Previously, it has been reported that inside the nucleus, TAP shows free diffusion behavior with a diffusion coefficient of $1.2\pm0.07\ \mu m^2 s^{-1}$ (Calapez et al. 2002). It was also reported that TAP-EGFP has 2 distinct populations inside the nucleus, which diffuse with different diffusion coefficients. However, our data fit well with the single population model. It has been published that the mRNA is transferred from the mRNA export adaptor proteins to TAP (Hautbergue et al. 2008). Yet, it is not known how the mRNA is released from the TAP. Our results suggest that the TAP binding to the mRNA is transient, and it might also be rapidly released from the mRNA in the cytoplasm. After its release, it could be then rapidly imported to the nucleus. In line with this, the cytoplasmic pool of TAP-EGFP was undetectable in our experiments.

6.9 Error Sources in FRAP experiments

The experimental error in the quantitative FRAP experiments is a sum of errors raised from the bleach area determination and the fluorescence intensity measurement errors. Second, perhaps even larger error sources are the normalization, fitting and simulation procedures used to quantitate the recoveries.

The major noise source in the confocal microscope is the statistical variation in the fluorescence signal. When a signal consists only of a limited number of photons, the variation of the signal follows the Poisson distribution. The standard deviation of the Poisson distribution is the square root of the number of detected photons, indicating that the variation between repeated measurements is larger in the case of low-intensity signals. This can be applied to the situation where we have homogeneous distribution of fluorescence, which is imaged with a confocal microscope. The resulting pixel intensities show variation according to the Poisson statistics.

It is well established that the confocal microscopy image or signal usually consists of less than 10 photons / pixel (Pawley 2006), and if we assume that the standard deviation of the Poisson distribution can be assumed to be the only error source, we have the following equation for the relative error:

$$\Delta = \frac{\sqrt{N}}{N}$$

where Δ is the error and N is the number of detected photons. The bleaching region used in the FRAP experiments is usually circular with a radius of approximately 10 pixels. Therefore, the average fluorescence intensity is

measured from ~314 pixels, which reduces the error. However, after the bleach pulse, at the early phase of the recovery, the intensity is extremely low, suggesting that the variation in the signal is also larger. If we oversimplify the situation and assume that the signal contains on average 6 photons per pixel, the relative error is 41 %. Next, we can also easily calculate the total relative error by combining the errors ((Taylor 1997)):

$$\delta = \frac{1}{p}\sqrt{(\Delta_1)^2 + (\Delta_2)^2 + \ldots + (\Delta_p)^2} = \frac{1}{p}\sqrt{p * \Delta^2} = \frac{\sqrt{\Delta^2}}{\sqrt{p}} = \frac{\Delta}{\sqrt{p}}$$

where δ is the sum of the error, p is the number of measured pixels, and Δ is the error of individual pixels. From the equation, we see that the sum of the error is directly proportional to the error in the individual pixel intensity measurements and inversely proportional to the square root of the number of measured pixels. If we assume that the bleach area radius is 10 pixels and that the signal contains on average 6 photons, total relative error is 2.3 %. The error can be over 5.5 % at the early phase of the recovery after a strong bleach pulse (average signal ~1 photon). In the case of live cell experiments and low expression levels, we can conclude that the error coming from the Poisson variation of the signal is large and needs to be acknowledged at the early time points of the recovery phase. Unfortunately, it can not be completely avoided, since the error rises from the small number of detected photons.

The second error source comes from the accuracy of the bleach area. The pixel size in the FRAP experiments is usually smaller than the point spread function (PSF) of the excitation laser. Thus, the selected bleach area is convoluted at the edges, according to the PSF. In addition, during the bleach process the confocal microscope scanner moves the laser spot over the bleach area. The actual bleaching is limited to the selected area by allowing the laser light to enter the sample. This is controlled by the acousto optical tunable filter (AOTF). The AOTF rise time (indicating the time needed to change the intensity from 10 % - 90 %) is in the range of 0.5 – 1.0 μs (Nitschke et al. 1997), and since the pixel dwell time in the confocal microscope is about 1 μs, this leads to uneven bleaching at the edges of the bleach area. Thus, when the radii are measured from the fixed cells, they usually show about 5-10 % deviation. Since a square of bleach area radius is needed to calculate the diffusion coefficient (Sprague et al. 2004), this error has the most prominent effect on the FRAP data quantitation. This leads to variations in the diffusion coefficients and binding rates.

The expression levels of the studied proteins also have a direct effect on the calculated binding reaction pseudo on rate. The pseudo on rate is defined $k^*_{on}=k_{on}[\text{Substrate}]$, where k_{on} is the reaction on rate and [Substrate] is the binding site concentration (Sprague et al. 2004). Therefore, a larger amount (i.e. higher expression levels of binding sites) leads to larger pseudo on rates and shorter diffusion times. In the case of virus infection, different cells might contain different copy numbers of the virus genome and, thus, possible binding sites.

Finally, since the invention of FRAP, several analytical models have been developed to quantitate the recovery of fluorescence and to assess the diffusion and the binding dynamics (Axelrod et al. 1976, Braga et al. 2004, Braga et al. 2007, Soumpasis 1983, Sprague et al. 2004). However, difficulties in implementing the boundary conditions and binding processes into an analytical evaluation lead to assumptions that do not reflect the experimental reality. The assumptions made in the established methods for FRAP evaluation include infinite, homogeneous fluorophore pools; fast bleaching compared to the time scales of the involved transport processes; and certain shapes of the bleach profiles. Recently, the recovery models have been adjusted to account for the diffusion during the bleach phase, which can lead to underestimated diffusion coefficients (Braga et al. 2004). However, even with these modifications, the assumptions of the geometrical constraints of the cell and its nucleus or the non-homogeneous fluorophore distribution inside the cell are oversimplified. Especially, diffusion coefficients of fast-diffusing proteins are difficult to measure using the conventional FRAP model (i.e., free EYFP, TFIIB-EGFP, and TAP-EGFP). Therefore, in many cases we used simulations to take these boundary conditions into account.

7 CONCLUSIONS

The main conclusions of this thesis are:

1. NS1-deYFP can be used as a marker for canine parvovirus replication structures. Its binding is DNA associated and it is able to shuttle between the cytoplasm and the nucleus in the absence of the infection. The viral replication structures contain large amounts of newly synthesized viral DNA.The structures are porous compartments, allowing the rapid diffusion of viruses and virus sized particles.

2. Parvovirus infection leads to profound changes in the nuclear organization. Many nuclear organelles are superseded by the viral replication compartment. Host cell chromatin condenses to the nuclear periphery and this condensation can also be used as an infection marker. In the infected cell nuclei, protein mobility is increased.

3. PCNA and NS1 binding dynamics are highly alike, yielding an estimate of the virus genome replication time. The virus infection changes the dynamics of transcription associated proteins.

The study demonstrates that CPV can be used as a model virus to study DNA replication and transcription. The benefits of this system are biosafety (CPV is unable to infect humans), versatility (CPV can infect wide variety of different cell lines) and simplicity (genome contains only 2 transcriptional units). Thus it offers a system, where host cell nucleus is filled with small DNA molecules, which are constantly transcribed and replicated.

Next key questions in the parvoviral infection induced nuclear reorganization are the causality of these changes and signaling routes. In addition, new cell culture methods like different 3D cell cultures or cocultures, allow studying infection processes in more "*in-vivo* like" environment. Moreover, it remains to be seen, if the protein mobility increase is typical only for CPV infection or also to other viruses.

Acknowledgements

This study was carried out at the University of Jyväskylä, at the Department of Biological and Environmental Science, Division of Molecular Biology.

I want to express my deepest gratitude to my supervisor Docent Maija Vihinen-Ranta for giving me the support and scientific freedom: under your supervision I had the opportunity to grow as a person and as a scientist. I also want to thank my second supervisor Professor Päivi Törmä for all the interesting projects, into which I had the possibility to participate in.

I am very grateful to my "unofficial supervisor" Professor Jussi Timonen for all the advices and excellent discussions during the years. In addition, I want to acknowledge Professor Jörg Lankowski for the collaboration.

I want to thank the official reviewers Päivi Ojala and Maria Vartiainen for their valuable comments and suggestions to improve the final version. I wish to express my deepest appreciation to Professor Michael Kann for kindly accepting the invitation to serve as the opponent in the public examination of the dissertation.

I sincerely want to thank all the co-authors of the original publications. Especially I wish to thank my good friends Einari and Johanna, without your friendship this thesis would not have been finished. I will definitely miss the endless brainstorming and discussions with a coffee mug in a hand. Acknowledgements go to Nicolas for all the help in the diffusion related studies, Tuomas for making Matlab slightly friendlier for the biologists and Milla for those countless labellings, cell culturing and laughs in the lab. In addition, I want to thank the former members of our group, Juulia and Mirka. Sincere appreciation goes also to my friend Jenni for all the scientific and non-scientific discussions about life, the universe and everything. Furthermore, I want to acknowledge Professor Markku Kulomaa and the people from the avidin related field: Vesa, Juha and Tiina.

Throughout the years I have had a privilege to supervise great master's thesis students, all my thanks to Juha, Jenni, Hanna, Outi, Sami and Anne for the great moments in the lab. Marjatta, Eila, Arja, Irene, Pirjo and Laura are acknowledged for their excellent technical support. Moreover, the whole staff of molecular recognition is thanked for the enjoyable working environment.

All my gratitude goes to my brothers and parents. You have believed in me and supported me throughout my studies. In a way, the beginning of this thesis took place a long ago, when I was only a child, during the years of play and imagination.

Finally, my deepest gratitude goes to my wife Anniina. You unconditionally supported and loved me during these years. You kept me sane when the times were dire. I want to dedicate my thesis to you.

The study was supported by the National Graduate School of Nanoscience and Academy of Finland. In addition, I want to thank FEBS, EMBO, Virustautien Tutkimussäätiö and Ellen & Artturi Nyyssönen Foundation for the financial support.

YHTEENVETO (RÉSUMÉ IN FINNISH)

Tumansisäinen dynamiikka parvovirus infektiossa

Virukset ovat loisten kaltaisia organismeja, jotka pystyvät monistumaan vain käyttämällä hyväksi isäntäsolun aineenvaihduntaa. Viruksen monistuminen voi johtaa isäntäsolun toiminan voimakkaaseen häiriintymiseen ja jopa kuolemaan. Virustaudit ovatkin maailmanlaajuisesti suuri uhka. Maailman terveysjärjestön mukaan infektiotauteihin kuoli vuonna 2002 noin 15 miljoonaa ihmistä. Kymmenen vaarallisimman taudin joukossa oli kaksi vain virusten aiheuttamaa sairautta (AIDS ja tuhkarokko), mutta näiden lisäksi kolmen muun sairausryhmän kohdalla viruksilla on merkittävä osa (alahengitysteiden infektiot, aivokalvon tulehdukset ja maha-suolitulehdukset). Virusten toiminnan selvittäminen onkin välttämätöntä uusien, spesifisten viruslääkkeiden kehittämiseksi. Tämänlisäksi virustutkimus on tuottanut suuren määrän yleistä tietoa solun perustoiminnoista, kuten DNA:n replikaatiosta, transkription säätelystä ja lähetti-RNA:n muokkaamisesta.

Virustutkimusmetodit ovat perinteisesti koostuneet molekyylibiologian ja biokemian eri tekniikoista. Viimeisen kahdenkymmenen vuoden aikana valomikroskopia on kehittynyt voimakkaasti, mikä nykyisin mahdollistaa elävien solujen valomikroskopian. Elävien solujen mikroskopia mahdollistaa solun prosessien tutkimisen aidossa ympäristössä, solun sisällä. Tutkimuksen kohteena olevat makromolekyylit täytyy kuitenkin erottaa solun muista rakenteista. Tarvittava kontrasti saadaan muodostettua käyttämällä esimerkiksi erilaisia fluorensoivia yhdisteitä. Fluoresenssi ilmiössä fluoresoiva molekyyli viritetään yleensä näkyvän alueen valolla. Viristystilanteessa valon perusyksikkö, fotoni, absorboituu ja sen energia siirtyy fluoresoivalle molekyylille. Molekyyli säilyy virittyneessä tilassa muutamia nanosekunteja, minkä jälkeen se palaa perustilalleen. Tämä johtaa fotonin emittoitumiseen. Kyseisen fotonin energia on kuitenkin pienempi kuin virityksessä absorboituneen fotonin ja siten emittoituneen valon aallonpituus on pidempi. Tämä aallonpituus ero viritys- ja emissio valon välillä mahdollistaa niiden erottamisen ja siten fluoresoivien molekyylien paikan ja määrän selvittämisen. Fluoresoivat molekyylit voidaan liittää kohteisiinsa vasta-aineiden välityksellä. Kyseisessä metodissa tiettyyn kohteeseen sitoutuva vasta-aine leimataan fluoresoivalla molekyylillä tai tämä vasta-aine tunnistetaan toisella, leimatulla vasta-aineella. Tämä, niin kutsuttu immunofluoresenssileimaus on laajasti käytetty tutkimusmetodi, niin solubiologisessa tutkumuksessa kuin myös diagnostiikassa. Metodina se on jo yli 60 vuotta vanha, ensimmäiset tutkimusjulkaisut, joissa ko. metodia oli käytetty ilmestyivät jo 1940-luvulla. Varsinkin elävien solujen kohdalla käytetään usein geneettisesti koodattavia leimoja. Nämä leimat mahdollistavat fluorensoivien molekyylien liittämisen tutkimksen kohteena oleviin molekyyleihin tai ovat itsessään fluorensoivia. Fluoresoivat proteiinit ovat esimerkki erittäin laajasti käytetyistä geneettisistä

leimoista. Niissä käytetään hyväksi meduusasta tai korallien proteiineja, jotka omaavat kyvyn fluorensoida tietyllä valolla suoritetun virityksen jälkeen. Tällaista proteiinia koodava geeni voidaan liittää tutkittavaa proteiinia koodaavaan geeniin, josta soluissa muodostuu fluoresoiva fuusioproteiini. Tämä tekniikka mahdollistaakin melkein kaikkien proteiinien toiminnan tutkimisen suoraan elävissä soluissa tai eliöissä. Vuoden 2008 kemian Nobel palkinto annettiinkin fluorensoiviin proteiineihin liittyvän teknologian kehittämisestä.

Väitöskirjassa tutkittiin solun toimintaa virusinfektiossa, keskittyen infektion aiheuttamien solun tuman rakenteiden ja dynamiikan muutoksiin. Tuman ja tumaproteiinien dynamiikka on toimintaa on tutkittu laajamittaisesti noin kymmenen vuotta ja siten se on suhteellisen nuori solubiologian ala. Tumasta on löydetty suuri määrä erilaisia organelleja, joiden tarkka toiminta on vielä karakterisoimatta. Useiden virusten on osoitettu vuorovaikutavan näiden rakenteiden kanssa, mutta näiden vuorovaikusten syy-seuraus suhteet ovat usein selvittämättä.

Tutkimuksessa käytettiin malliviruksena koiran parvovirusta, joka on pieni, yksijuosteisen DNA perimän omaava ikosahedraalinen virus. Sen genomi koostuu kahdesta traskriptionaalisesta yksiköstä, jotka tuottavat kahta viruksen kapsidi proteiinia, sekä kahta ei rakenteellsita proteiinia, jotka osallituvat viruksen genomen kopioimiseen. Virus infektoi nuoria koiria ja voi johtaa vakavaan ripuliin ja koiran kuolemaan. Soluun päästyään virus kulkeutuu tumaan, jossa se vapauttaa genominsa. Uusien viruspartikkelien muodostuminen tapahtuu myös tumassa. Tutkimuksissa halusimme selvittää virusproteiinien dynamiikkaa sekä tutkia miten solun omien proteiinien toiminta muuttuu. Viruksen tärkein ei-rakenteellinen proteiini (NS1) fuusioitiin keltaiseen fluoresoivaan proteiiniin ja merkittävin kapsidi proteiini (VP2) liitettiin valoaktivoitavaan vihreään fluoresoivaan proteiiniin. Näiden fuusioproteiinien toimintaa tutkittiin seuraamalla fluoresenssin palautumista, tai katoamista voimakkaan valopulssin jälkeen. Kyseisissä tutkimusmetodeissa käytetään nopeaa, voimakasta ja hyvin fokusoitua laservaloa, joka tuhoaa fluorensoivien molekyylien kyvyn fluorensoida. Mikäki kyseisen alueen pimennetyt fluoresoivat molekyylit pystyvät vaihtumaan ympäristön vielä fluorensoivien molekyylien kanssa, fluoresenssin palautuminen on suhteessa tähän vaihdantanopeuteen. Solujen eri osista voidaan myös mitata fluoresenssin katoamista, joka kertoo eri solujen osien välisestä vaihdannasta. Näiden metodien tuottaman informaation kvantitointi on kuitenkin hankalaa ja yleisiä matemaattisia malleja ei vielä ole kehitetty.

Kokeissa NS1 proteiini oli dynamiikaltaan monimuotoinen. Ilman infektiota sitä kuljetettiin jatkuvasti tuman ja sytoplasman välillä. Tumassa proteiini pystyi sitoutumaan DNA:han tai DNA:han sitoutuviin proteiineihin. Virusinfektiossa viruksen monistuminen tapahtuu replikaatiorakenteissa. Virusinfektion alkuvaiheessa nämä NS1 proteiinia sisältävät rakenteet ovat pieniä, mutta elävien solujen mikroskopia osoitti niiden nopean kasvun infektion edetessä. Tämän lisäksi mikroskopian avulla voitiin havaita voimakas isäntäsolun perimän pakkautuminen tuman reunoille. Tässä vaiheessa viruksen

replikaatiorakenne täytti koko tuman tilavuuden. Erikokoiset dekstraani nanopartikkelit pystyivät passiivisesti tunkeutumaan replikaatiorakenteiden sisään, osoittaen niiden olevan huokoisia rakenteita, joihin myös virus partikkelit pystyvät tunkeutumaan. Viruskapsidien liikettä tutkittiin valoaktivoitavan VP2 fuusioproteiinin avulla. Kokeet osoittivat että virus kapsidit pystyvät liikkumaan nopeasti tuman sisällä. Osa kapsideista oli kuitenkin voimakkaasti sitoutuneena tuman sisällä.

Fluoresenssin palautumiskokeet osoittivat että NS1 proteiini sitoutui ainakin kahteen erityyppiseen sitoutumispaikkaan. Sitoutumis aika oli identtinen DNA:n replikaatioon osallistuvan PCNA proteiinin kanssa. Aikaisemmin on voitu osoittaa että NS1 proteiini on mukana virus perimän monistumisessa, joten NS1 ja PCNA proteiinien samanlainen 83 sekunnin sitoutumisaika liittyy todennäköisesti virus genomin replikaatioaikaan. Lähetti-RNA:n transkriptioon liittyvien proteiinien dynamiikan tutkimukset vahvistivat nykyistä käsitystä transkription aloituksesta. Promoottoriin sitoutuvat proteiinit pysyivät promoottorissa pitkään kiinni, näihin verrattuna polymeraasi entsyymit aloittavat transkription nopeassa tahdissa. Lähetti-RNA:han sitoutuvien proteiinien liike oli samankaltaista sekä infektoiduissa että ei infektoiduissa soluissa. Kokeet viittasivat kuitenkin voimakkaaseen lähetti-RNA:n määrän kasvuun. Tuman sisäistä proteiinien diffuusiota tutkittiin fluoresenssi korrelaatio spektroskpialla ja fluoresenssin palautumiskokeilla, joita mallinnettiin Virtual Cell simulaatioilla. Simulaatioiden avulla pystyttiin toistamaan fluoresenssin palautumiskäyttäytyminen ja fluoresenssi korrelaatio spektroskopian tulokset olivat yhteneviä simulaatioiden kanssa. Kokeet ja simulaatiot osoittivat, että virusinfektiossa proteiinien mobiliteetti lisääntyy. Tämä johtaa nopeampiin sitoutumisreaktioihin ja pienentää DNA:n hybridisaation sulamislämpötilaa.

Tutkimus osoitti, että parvovirus infektio johtaa voimakkaaseen tuman uudelleen organisaatioon sekä isäntäsolun genomin marginalisaatioon. Samanaikaisesti viruksen replikaatio rakenteet kasvavat. Infektio johtaa myös proteiinien mobiliteetin kasvamiseen. Tulokset lisäksi osoittivat, että koiran parvovirusta voidaan käyttää malliviruksena tutkittaessa DNA:n replikaatiota ja transkriptiota.

REFERENCES

Ahn, J. K., Pitluk, Z. W. & Ward, D. C. 1992. The GC box and TATA transcription control elements in the P38 promoter of the minute virus of mice are necessary and sufficient for transactivation by the nonstructural protein NS1. J.Virol. 66(6): 3776-3783.

Akey, C. W. & Radermacher, M. 1993. Architecture of the Xenopus nuclear pore complex revealed by three-dimensional cryo-electron microscopy. J.Cell Biol. 122(1): 1-19.

Ascoli, C. A. & Maul, G. G. 1991. Identification of a novel nuclear domain. J.Cell Biol. 112(5): 785-795.

Axelrod, D., Koppel, D. E., Schlessinger, J., Elson, E. & Webb, W. W. 1976. Mobility measurement by analysis of fluorescence photobleaching recovery kinetics. Biophys.J. 16(9): 1055-1069.

Bacia, K., Kim, S. A. & Schwille, P. 2006. Fluorescence cross-correlation spectroscopy in living cells. Nat.Methods 3(2): 83-89.

Bashir, T., Horlein, R., Rommelaere, J. & Willwand, K. 2000. Cyclin A activates the DNA polymerase delta -dependent elongation machinery in vitro: A parvovirus DNA replication model. Proc.Natl.Acad.Sci.U.S.A. 97(10): 5522-5527.

Bashir, T., Rommelaere, J. & Cziepluch, C. 2001. In vivo accumulation of cyclin A and cellular replication factors in autonomous parvovirus minute virus of mice-associated replication bodies. J.Virol. 75(9): 4394-4398.

Bauer, D. W. & Gall, J. G. 1997. Coiled bodies without coilin. Mol.Biol.Cell 8(1): 73-82.

Beck, M., Forster, F., Ecke, M., Plitzko, J. M., Melchior, F., Gerisch, G., Baumeister, W. & Medalia, O. 2004. Nuclear pore complex structure and dynamics revealed by cryoelectron tomography. Science 306(5700): 1387-1390.

Bell, B. & Tora, L. 1999. Regulation of gene expression by multiple forms of TFIID and other novel TAFII-containing complexes. Exp.Cell Res. 246(1): 11-19.

Bentley, D. L. 2005. Rules of engagement: co-transcriptional recruitment of pre-mRNA processing factors. Curr.Opin.Cell Biol. 17(3): 251-256.

Berg, O. G., Winter, R. B. & von Hippel, P. H. 1981. Diffusion-driven mechanisms of protein translocation on nucleic acids. 1. Models and theory. Biochemistry 20(24): 6929-6948.

Bernardi, R. & Pandolfi, P. P. 2007. Structure, dynamics and functions of promyelocytic leukaemia nuclear bodies. Nat.Rev.Mol.Cell Biol. 8(12): 1006-1016.

Betzig, E., Patterson, G. H., Sougrat, R., Lindwasser, O. W., Olenych, S., Bonifacino, J. S., Davidson, M. W., Lippincott-Schwartz, J. & Hess, H. F. 2006. Imaging intracellular fluorescent proteins at nanometer resolution. Science 313(5793): 1642-1645.

Boe, S. O., Haave, M., Jul-Larsen, A., Grudic, A., Bjerkvig, R. & Lonning, P. E. 2006. Promyelocytic leukemia nuclear bodies are predetermined processing sites for damaged DNA. J.Cell.Sci. 119(Pt 16): 3284-3295.

Boisvert, F. M., Hendzel, M. J. & Bazett-Jones, D. P. 2000. Promyelocytic leukemia (PML) nuclear bodies are protein structures that do not accumulate RNA. J.Cell Biol. 148(2): 283-292.

Bonne-Andrea, C., Santucci, S., Clertant, P. & Tillier, F. 1995. Bovine papillomavirus E1 protein binds specifically DNA polymerase alpha but not replication protein A. J.Virol. 69(4): 2341-2350.

Boute, N., Jockers, R. & Issad, T. 2002. The use of resonance energy transfer in high-throughput screening: BRET versus FRET. Trends Pharmacol.Sci. 23(8): 351-354.

Bowman, G. D., O'Donnell, M. & Kuriyan, J. 2004. Structural analysis of a eukaryotic sliding DNA clamp-clamp loader complex. Nature 429(6993): 724-730.

Braga, J., Desterro, J. M. & Carmo-Fonseca, M. 2004. Intracellular macromolecular mobility measured by fluorescence recovery after photobleaching with confocal laser scanning microscopes. Mol.Biol.Cell 15(10): 4749-4760.

Braga, J., McNally, J. G. & Carmo-Fonseca, M. 2007. A reaction-diffusion model to study RNA motion by quantitative fluorescence recovery after photobleaching. Biophys.J. 92(8): 2694-2703.

Branco, M. R. & Pombo, A. 2006. Intermingling of chromosome territories in interphase suggests role in translocations and transcription-dependent associations. PLoS Biol. 4(5): e138.

Brown, J. M., Green, J., das Neves, R. P., Wallace, H. A., Smith, A. J., Hughes, J., Gray, N., Taylor, S., Wood, W. G., Higgs, D. R., Iborra, F. J. & Buckle, V. J. 2008. Association between active genes occurs at nuclear speckles and is modulated by chromatin environment. J.Cell Biol. 182(6): 1083-1097.

Buratowski, S., Hahn, S., Guarente, L. & Sharp, P. A. 1989. Five intermediate complexes in transcription initiation by RNA polymerase II. Cell 56(4): 549-561.

Burley, S. K. & Roeder, R. G. 1996. Biochemistry and structural biology of transcription factor IID (TFIID). Annu.Rev.Biochem. 65: 769-799.

Calado, A. & Carmo-Fonseca, M. 2000. Localization of poly(A)-binding protein 2 (PABP2) in nuclear speckles is independent of import into the nucleus and requires binding to poly(A) RNA. J.Cell.Sci. 113 (Pt 12)(Pt 12): 2309-2318.

Calapez, A., Pereira, H. M., Calado, A., Braga, J., Rino, J., Carvalho, C., Tavanez, J. P., Wahle, E., Rosa, A. C. & Carmo-Fonseca, M. 2002. The intranuclear mobility of messenger RNA binding proteins is ATP dependent and temperature sensitive. J.Cell Biol. 159(5): 795-805.

Callan, H. G. & Tomlin, S. G. 1950. Experimental Studies of on amphibian oocyte nuclei. I. Investigation of the structure of the nuclear membrane by electron microscope. Proc. Roy. Soc. (London) Ser. B. 137: 367.

Carmen, A. A., Milne, L. & Grunstein, M. 2002. Acetylation of the yeast histone H4 N terminus regulates its binding to heterochromatin protein SIR3. J.Biol.Chem. 277(7): 4778-4781.

Carter, D. R., Eskiw, C. & Cook, P. R. 2008. Transcription factories. Biochem.Soc.Trans. 36(Pt 4): 585-589.

Cawley, S., Bekiranov, S., Ng, H. H., Kapranov, P., Sekinger, E. A., Kampa, D., Piccolboni, A., Sementchenko, V., Cheng, J., Williams, A. J. *et al*. 2004. Unbiased mapping of transcription factor binding sites along human chromosomes 21 and 22 points to widespread regulation of noncoding RNAs. Cell 116(4): 499-509.

Chakravarthy, S., Park, Y. J., Chodaparambil, J., Edayathumangalam, R. S. & Luger, K. 2005. Structure and dynamic properties of nucleosome core particles. FEBS Lett. 579(4): 895-898.

Chekanova, J. A. & Belostotsky, D. A. 2003. Evidence that poly(A) binding protein has an evolutionarily conserved function in facilitating mRNA biogenesis and export. RNA 9(12): 1476-1490.

Chen, D., Hinkley, C. S., Henry, R. W. & Huang, S. 2002. TBP dynamics in living human cells: constitutive association of TBP with mitotic chromosomes. Mol.Biol.Cell 13(1): 276-284.

Christensen, J., Cotmore, S. F. & Tattersall, P. 2001. Minute virus of mice initiator protein NS1 and a host KDWK family transcription factor must form a precise ternary complex with origin DNA for nicking to occur. J.Virol. 75(15): 7009-7017.

Christensen, J., Cotmore, S. F. & Tattersall, P. 1997. A novel cellular site-specific DNA-binding protein cooperates with the viral NS1 polypeptide to initiate parvovirus DNA replication. J.Virol. 71(2): 1405-1416.

Christensen, J., Cotmore, S. F. & Tattersall, P. 1995a. Minute virus of mice transcriptional activator protein NS1 binds directly to the transactivation region of the viral P38 promoter in a strictly ATP-dependent manner. J.Virol. 69(9): 5422-5430.

Christensen, J., Pedersen, M., Aasted, B. & Alexandersen, S. 1995b. Purification and characterization of the major nonstructural protein (NS-1) of Aleutian mink disease parvovirus. J.Virol. 69(3): 1802-1809.

Christensen, J. & Tattersall, P. 2002. Parvovirus initiator protein NS1 and RPA coordinate replication fork progression in a reconstituted DNA replication system. J.Virol. 76(13): 6518-6531.

Chuang, C. H., Carpenter, A. E., Fuchsova, B., Johnson, T., de Lanerolle, P. & Belmont, A. S. 2006. Long-range directional movement of an interphase chromosome site. Curr.Biol. 16(8): 825-831.

Chudakov, D. M., Verkhusha, V. V., Staroverov, D. B., Souslova, E. A., Lukyanov, S. & Lukyanov, K. A. 2004. Photoswitchable cyan fluorescent protein for protein tracking. Nat.Biotechnol. 22(11): 1435-1439.

Clemson, C. M., Hutchinson, J. N., Sara, S. A., Ensminger, A. W., Fox, A. H., Chess, A. & Lawrence, J. B. 2009. An architectural role for a nuclear noncoding RNA: NEAT1 RNA is essential for the structure of paraspeckles. Mol.Cell 33(6): 717-726.

Conti, E. & Izaurralde, E. 2001. Nucleocytoplasmic transport enters the atomic age. Curr.Opin.Cell Biol. 13(3): 310-319.
Cook, A., Bono, F., Jinek, M. & Conti, E. 2007. Structural biology of nucleocytoplasmic transport. Annu.Rev.Biochem. 76: 647-671.
Corbau, R., Salom, N., Rommelaere, J. & Nuesch, J. P. 1999. Phosphorylation of the viral nonstructural protein NS1 during MVMp infection of A9 cells. Virology 259(2): 402-415.
Cotmore, S. F., Christensen, J., Nuesch, J. P. & Tattersall, P. 1995. The NS1 polypeptide of the murine parvovirus minute virus of mice binds to DNA sequences containing the motif [ACCA]2-3. J.Virol. 69(3): 1652-1660.
Cotmore, S. F., Gottlieb, R. L. & Tattersall, P. 2007. Replication initiator protein NS1 of the parvovirus minute virus of mice binds to modular divergent sites distributed throughout duplex viral DNA. J.Virol. 81(23): 13015-13027.
Cotmore, S. F. & Tattersall, P. 2005. Genome packaging sense is controlled by the efficiency of the nick site in the right-end replication origin of parvoviruses minute virus of mice and LuIII. J.Virol. 79(4): 2287-2300.
Cotmore, S. F. & Tattersall, P. 1998. High-mobility group 1/2 proteins are essential for initiating rolling-circle-type DNA replication at a parvovirus hairpin origin. J.Virol. 72(11): 8477-8484.
Cremer, T. & Cremer, C. 2001. Chromosome territories, nuclear architecture and gene regulation in mammalian cells. Nat.Rev.Genet. 2(4): 292-301.
Cronshaw, J. M., Krutchinsky, A. N., Zhang, W., Chait, B. T. & Matunis, M. J. 2002. Proteomic analysis of the mammalian nuclear pore complex. J.Cell Biol. 158(5): 915-927.
Cziepluch, C., Lampel, S., Grewenig, A., Grund, C., Lichter, P. & Rommelaere, J. 2000. H-1 parvovirus-associated replication bodies: a distinct virus-induced nuclear structure. J.Virol. 74(10): 4807-4815.
Damania, B. & Alwine, J. C. 1996. TAF-like function of SV40 large T antigen. Genes Dev. 10(11): 1369-1381.
Damania, B., Lieberman, P. & Alwine, J. C. 1998. Simian virus 40 large T antigen stabilizes the TATA-binding protein-TFIIA complex on the TATA element. Mol.Cell.Biol. 18(7): 3926-3935.
D'Angelo, M. A. & Hetzer, M. W. 2006. The role of the nuclear envelope in cellular organization. Cell Mol.Life Sci. 63(3): 316-332.
Darzacq, X., Shav-Tal, Y., de Turris, V., Brody, Y., Shenoy, S. M., Phair, R. D. & Singer, R. H. 2007. In vivo dynamics of RNA polymerase II transcription. Nat.Struct.Mol.Biol. 14(9): 796-806.
de Jong, R. N. & van der Vliet, P. C. 1999. Mechanism of DNA replication in eukaryotic cells: cellular host factors stimulating adenovirus DNA replication. Gene 236(1): 1-12.
de Jong, R. N., van der Vliet, P. C. & Brenkman, A. B. 2003. Adenovirus DNA replication: protein priming, jumping back and the role of the DNA binding protein DBP. Curr.Top.Microbiol.Immunol. 272: 187-211.
Deleu, L., Fuks, F., Spitkovsky, D., Horlein, R., Faisst, S. & Rommelaere, J. 1998. Opposite transcriptional effects of cyclic AMP-responsive elements in

confluent or p27KIP-overexpressing cells versus serum-starved or growing cells. Mol.Cell.Biol. 18(1): 409-419.
Deleu, L., Pujol, A., Faisst, S. & Rommelaere, J. 1999. Activation of promoter P4 of the autonomous parvovirus minute virus of mice at early S phase is required for productive infection. J.Virol. 73(5): 3877-3885.
Dellaire, G. & Bazett-Jones, D. P. 2004. PML nuclear bodies: dynamic sensors of DNA damage and cellular stress. Bioessays 26(9): 963-977.
Deng, W. & Roberts, S. G. 2007. TFIIB and the regulation of transcription by RNA polymerase II. Chromosoma 116(5): 417-429.
Dornreiter, I., Erdile, L. F., Gilbert, I. U., von Winkler, D., Kelly, T. J. & Fanning, E. 1992. Interaction of DNA polymerase alpha-primase with cellular replication protein A and SV40 T antigen. EMBO J. 11(2): 769-776.
Dreiding, P., Staeheli, P. & Haller, O. 1985. Interferon-induced protein Mx accumulates in nuclei of mouse cells expressing resistance to influenza viruses. Virology 140(1): 192-196.
Dross, N., Spriet, C., Zwerger, M., Muller, G., Waldeck, W. & Langowski, J. 2009. Mapping eGFP oligomer mobility in living cell nuclei. PLoS ONE 4(4): e5041.
Eash, S., Manley, K., Gasparovic, M., Querbes, W. & Atwood, W. J. 2006. The human polyomaviruses. Cell Mol.Life Sci. 63(7-8): 865-876.
Erkmann, J. A. & Kutay, U. 2004. Nuclear export of mRNA: from the site of transcription to the cytoplasm. Exp.Cell Res. 296(1): 12-20.
Essers, J., Theil, A. F., Baldeyron, C., van Cappellen, W. A., Houtsmuller, A. B., Kanaar, R. & Vermeulen, W. 2005. Nuclear dynamics of PCNA in DNA replication and repair. Mol.Cell.Biol. 25(21): 9350-9359.
Everett, R. D. & Chelbi-Alix, M. K. 2007. PML and PML nuclear bodies: implications in antiviral defence. Biochimie 89(6-7): 819-830.
Fanning, E., Klimovich, V. & Nager, A. R. 2006. A dynamic model for replication protein A (RPA) function in DNA processing pathways. Nucleic Acids Res. 34(15): 4126-4137.
Fanning, E. & Zhao, K. 2009. SV40 DNA replication: from the A gene to a nanomachine. Virology 384(2): 352-359.
Fanti, L. & Pimpinelli, S. 2008. HP1: a functionally multifaceted protein. Curr.Opin.Genet.Dev. 18(2): 169-174.
Fedorova, E. & Zink, D. 2008. Nuclear architecture and gene regulation. Biochim.Biophys.Acta 1783(11): 2174-2184.
Fisher, D. Z., Chaudhary, N. & Blobel, G. 1986. cDNA sequencing of nuclear lamins A and C reveals primary and secondary structural homology to intermediate filament proteins. Proc.Natl.Acad.Sci.U.S.A. 83(17): 6450-6454.
Flores, O., Lu, H., Killeen, M., Greenblatt, J., Burton, Z. F. & Reinberg, D. 1991. The small subunit of transcription factor IIF recruits RNA polymerase II into the preinitiation complex. Proc.Natl.Acad.Sci.U.S.A. 88(22): 9999-10003.
Foisner, R. & Gerace, L. 1993. Integral membrane proteins of the nuclear envelope interact with lamins and chromosomes, and binding is modulated by mitotic phosphorylation. Cell 73(7): 1267-1279.

Forest, T., Barnard, S. & Baines, J. D. 2005. Active intranuclear movement of herpesvirus capsids. Nat.Cell Biol. 7(4): 429-431.
Gall, J. G. 2001. A role for Cajal bodies in assembly of the nuclear transcription machinery. FEBS Lett. 498(2-3): 164-167.
Gall, J. G. 1967. Octagonal nuclear pores. J.Cell Biol. 32(2): 391-399.
Garcia-Carranca, A., Thierry, F. & Yaniv, M. 1988. Interplay of viral and cellular proteins along the long control region of human papillomavirus type 18. J.Virol. 62(11): 4321-4330.
Gavin, B. J. & Ward, D. C. 1990. Positive and negative regulation of the minute virus of mice P38 promoter. J.Virol. 64(5): 2057-2063.
Gerace, L. & Blobel, G. 1980. The nuclear envelope lamina is reversibly depolymerized during mitosis. Cell 19(1): 277-287.
Gerland, U., Moroz, J. D. & Hwa, T. 2002. Physical constraints and functional characteristics of transcription factor-DNA interaction. Proc.Natl.Acad.Sci.U.S.A. 99(19): 12015-12020.
Giepmans, B. N., Adams, S. R., Ellisman, M. H. & Tsien, R. Y. 2006. The fluorescent toolbox for assessing protein location and function. Science 312(5771): 217-224.
Gilbert, L., Toivola, J., Lehtomaki, E., Donaldson, L., Kapyla, P., Vuento, M. & Oker-Blom, C. 2004. Assembly of fluorescent chimeric virus-like particles of canine parvovirus in insect cells. Biochem.Biophys.Res.Commun. 313(4): 878-887.
Gilbert, L., Toivola, J., Valilehto, O., Saloniemi, T., Cunningham, C., White, D., Makela, A. R., Korhonen, E., Vuento, M. & Oker-Blom, C. 2006. Truncated forms of viral VP2 proteins fused to EGFP assemble into fluorescent parvovirus-like particles. J.Nanobiotechnology 4: 13.
Gilbert, N., Boyle, S., Fiegler, H., Woodfine, K., Carter, N. P. & Bickmore, W. A. 2004. Chromatin architecture of the human genome: gene-rich domains are enriched in open chromatin fibers. Cell 118(5): 555-566.
Gomez-Llorente, Y., Fletcher, R. J., Chen, X. S., Carazo, J. M. & San Martin, C. 2005. Polymorphism and double hexamer structure in the archaeal minichromosome maintenance (MCM) helicase from Methanobacterium thermoautotrophicum. J.Biol.Chem. 280(49): 40909-40915.
Gorisch, S. M., Richter, K., Scheuermann, M. O., Herrmann, H. & Lichter, P. 2003. Diffusion-limited compartmentalization of mammalian cell nuclei assessed by microinjected macromolecules. Exp.Cell Res. 289(2): 282-294.
Gorisch, S. M., Wachsmuth, M., Ittrich, C., Bacher, C. P., Rippe, K. & Lichter, P. 2004. Nuclear body movement is determined by chromatin accessibility and dynamics. Proc.Natl.Acad.Sci.U.S.A. 101(36): 13221-13226.
Gorisch, S. M., Wachsmuth, M., Toth, K. F., Lichter, P. & Rippe, K. 2005. Histone acetylation increases chromatin accessibility. J.Cell.Sci. 118(Pt 24): 5825-5834.
Grewal, S. I. & Jia, S. 2007. Heterochromatin revisited. Nat.Rev.Genet. 8(1): 35-46.
Griffin, B. A., Adams, S. R. & Tsien, R. Y. 1998. Specific covalent labeling of recombinant protein molecules inside live cells. Science 281(5374): 269-272.

Grinstein, E., Wernet, P., Snijders, P. J., Rosl, F., Weinert, I., Jia, W., Kraft, R., Schewe, C., Schwabe, M., Hauptmann, S. *et al*. 2002. Nucleolin as activator of human papillomavirus type 18 oncogene transcription in cervical cancer. J.Exp.Med. 196(8): 1067-1078.

Gu, M. & Lima, C. D. 2005. Processing the message: structural insights into capping and decapping mRNA. Curr.Opin.Struct.Biol. 15(1): 99-106.

Guigas, G. & Weiss, M. 2008. Sampling the cell with anomalous diffusion - the discovery of slowness. Biophys.J. 94(1): 90-94.

Ha, I., Roberts, S., Maldonado, E., Sun, X., Kim, L. U., Green, M. & Reinberg, D. 1993. Multiple functional domains of human transcription factor IIB: distinct interactions with two general transcription factors and RNA polymerase II. Genes Dev. 7(6): 1021-1032.

Handwerger, K. E., Cordero, J. A. & Gall, J. G. 2005. Cajal bodies, nucleoli, and speckles in the Xenopus oocyte nucleus have a low-density, sponge-like structure. Mol.Biol.Cell 16(1): 202-211.

Handwerger, K. E. & Gall, J. G. 2006. Subnuclear organelles: new insights into form and function. Trends Cell Biol. 16(1): 19-26.

Hautbergue, G. M., Hung, M. L., Golovanov, A. P., Lian, L. Y. & Wilson, S. A. 2008. Mutually exclusive interactions drive handover of mRNA from export adaptors to TAP. Proc.Natl.Acad.Sci.U.S.A. 105(13): 5154-5159.

Hebner, C. M. & Laimins, L. A. 2006. Human papillomaviruses: basic mechanisms of pathogenesis and oncogenicity. Rev.Med.Virol. 16(2): 83-97.

Herold, A., Teixeira, L. & Izaurralde, E. 2003. Genome-wide analysis of nuclear mRNA export pathways in Drosophila. EMBO J. 22(10): 2472-2483.

Hoppe-Seyler, F. & Butz, K. 1992. Activation of human papillomavirus type 18 E6-E7 oncogene expression by transcription factor Sp1. Nucleic Acids Res. 20(24): 6701-6706.

Horn, P. J. & Peterson, C. L. 2006. Heterochromatin assembly: a new twist on an old model. Chromosome Res. 14(1): 83-94.

Hurst, H. C. & Jones, N. C. 1987. Identification of factors that interact with the E1A-inducible adenovirus E3 promoter. Genes Dev. 1(10): 1132-1146.

International Human Genome Sequencing Consortium. 2004. Finishing the euchromatic sequence of the human genome. Nature 431(7011): 931-945.

Jackson, D. A. & Pombo, A. 1998. Replicon clusters are stable units of chromosome structure: evidence that nuclear organization contributes to the efficient activation and propagation of S phase in human cells. J.Cell Biol. 140(6): 1285-1295.

Johnston, S. D., Yu, X. M. & Mertz, J. E. 1996. The major transcriptional transactivation domain of simian virus 40 large T antigen associates nonconcurrently with multiple components of the transcriptional preinitiation complex. J.Virol. 70(2): 1191-1202.

Jongeneel, C. V., Sahli, R., McMaster, G. K. & Hirt, B. 1986. A precise map of splice junctions in the mRNAs of minute virus of mice, an autonomous parvovirus. J.Virol. 59(3): 564-573.

Joseph, J. & Dasso, M. 2008. The nucleoporin Nup358 associates with and regulates interphase microtubules. FEBS Lett. 582(2): 190-196.

Katahira, J., Straesser, K., Saiwaki, T., Yoneda, Y. & Hurt, E. 2002. Complex formation between Tap and p15 affects binding to FG-repeat nucleoporins and nucleocytoplasmic shuttling. J.Biol.Chem. 277(11): 9242-9246.

Katahira, J., Strasser, K., Podtelejnikov, A., Mann, M., Jung, J. U. & Hurt, E. 1999. The Mex67p-mediated nuclear mRNA export pathway is conserved from yeast to human. EMBO J. 18(9): 2593-2609.

Kato, H., Goto, D. B., Martienssen, R. A., Urano, T., Furukawa, K. & Murakami, Y. 2005. RNA polymerase II is required for RNAi-dependent heterochromatin assembly. Science 309(5733): 467-469.

Keller, R. W., Kuhn, U., Aragon, M., Bornikova, L., Wahle, E. & Bear, D. G. 2000. The nuclear poly(A) binding protein, PABP2, forms an oligomeric particle covering the length of the poly(A) tail. J.Mol.Biol. 297(3): 569-583.

Kerr, J. R., Cotmore, S. F., Bloom, M. E., Linden, M. R. & Parrish, C. P. 2006. Parvoviruses. Oxford University Press Inc., New York, USA.

Kim, S. A., Heinze, K. G. & Schwille, P. 2007. Fluorescence correlation spectroscopy in living cells. Nat.Methods 4(11): 963-973.

King, A. J. & van der Vliet, P. C. 1994. A precursor terminal protein-trinucleotide intermediate during initiation of adenovirus DNA replication: regeneration of molecular ends in vitro by a jumping back mechanism. EMBO J. 13(23): 5786-5792.

Klar, T. A., Jakobs, S., Dyba, M., Egner, A. & Hell, S. W. 2000. Fluorescence microscopy with diffraction resolution barrier broken by stimulated emission. Proc.Natl.Acad.Sci.U.S.A. 97(15): 8206-8210.

Kraemer, S. M., Ranallo, R. T., Ogg, R. C. & Stargell, L. A. 2001. TFIIA interacts with TFIID via association with TATA-binding protein and TAF40. Mol.Cell.Biol. 21(5): 1737-1746.

Krumm, A., Hickey, L. B. & Groudine, M. 1995. Promoter-proximal pausing of RNA polymerase II defines a general rate-limiting step after transcription initiation. Genes Dev. 9(5): 559-572.

Kues, T., Peters, R. & Kubitscheck, U. 2001. Visualization and tracking of single protein molecules in the cell nucleus. Biophys.J. 80(6): 2954-2967.

Lachner, M., O'Carroll, D., Rea, S., Mechtler, K. & Jenuwein, T. 2001. Methylation of histone H3 lysine 9 creates a binding site for HP1 proteins. Nature 410(6824): 116-120.

Lam, A. L., Pazin, D. E. & Sullivan, B. A. 2005a. Control of gene expression and assembly of chromosomal subdomains by chromatin regulators with antagonistic functions. Chromosoma 114(4): 242-251.

Lam, Y. W., Trinkle-Mulcahy, L. & Lamond, A. I. 2005b. The nucleolus. J.Cell.Sci. 118(Pt 7): 1335-1337.

Lamond, A. I. & Spector, D. L. 2003. Nuclear speckles: a model for nuclear organelles. Nat.Rev.Mol.Cell Biol. 4(8): 605-612.

Langston, L. D. & O'Donnell, M. 2006. DNA replication: keep moving and don't mind the gap. Mol.Cell 23(2): 155-160.

Lee, W. & Langhoff, E. 2002. Polyomavirus and Human Cancer. Graft 5: S73-8.

Legendre, D. & Rommelaere, J. 1994. Targeting of promoters for trans activation by a carboxy-terminal domain of the NS-1 protein of the parvovirus minute virus of mice. J.Virol. 68(12): 7974-7985.

Legendre, D. & Rommelaere, J. 1992. Terminal regions of the NS-1 protein of the parvovirus minute virus of mice are involved in cytotoxicity and promoter trans inhibition. J.Virol. 66(10): 5705-5713.

Leong, K., Lee, W. & Berk, A. J. 1990. High-level transcription from the adenovirus major late promoter requires downstream binding sites for late-phase-specific factors. J.Virol. 64(1): 51-60.

Liker, E., Fernandez, E., Izaurralde, E. & Conti, E. 2000. The structure of the mRNA export factor TAP reveals a cis arrangement of a non-canonical RNP domain and an LRR domain. EMBO J. 19(21): 5587-5598.

Lippincott-Schwartz, J., Altan-Bonnet, N. & Patterson, G. H. 2003. Photobleaching and photoactivation: following protein dynamics in living cells. Nat.Cell Biol. Suppl: S7-14.

Lippincott-Schwartz, J., Snapp, E. & Kenworthy, A. 2001. Studying protein dynamics in living cells. Nat.Rev.Mol.Cell Biol. 2(6): 444-456.

Liu, J. S., Kuo, S. R., Makhov, A. M., Cyr, D. M., Griffith, J. D., Broker, T. R. & Chow, L. T. 1998. Human Hsp70 and Hsp40 chaperone proteins facilitate human papillomavirus-11 E1 protein binding to the origin and stimulate cell-free DNA replication. J.Biol.Chem. 273(46): 30704-30712.

Liu, Q. & Dreyfuss, G. 1996. A novel nuclear structure containing the survival of motor neurons protein. EMBO J. 15(14): 3555-3565.

Loo, Y. M. & Melendy, T. 2004. Recruitment of replication protein A by the papillomavirus E1 protein and modulation by single-stranded DNA. J.Virol. 78(4): 1605-1615.

Lukacs, G. L., Haggie, P., Seksek, O., Lechardeur, D., Freedman, N. & Verkman, A. S. 2000. Size-dependent DNA mobility in cytoplasm and nucleus. J.Biol.Chem. 275(3): 1625-1629.

Magde, D., Elson, E. L. & Webb, W. W. 1974. Fluorescence correlation spectroscopy. II. An experimental realization. Biopolymers 13(1): 29-61.

Malik, S., Hisatake, K., Sumimoto, H., Horikoshi, M. & Roeder, R. G. 1991. Sequence of general transcription factor TFIIB and relationships to other initiation factors. Proc.Natl.Acad.Sci.U.S.A. 88(21): 9553-9557.

Manuelidis, L. 1984. Different central nervous system cell types display distinct and nonrandom arrangements of satellite DNA sequences. Proc.Natl.Acad.Sci.U.S.A. 81(10): 3123-3127.

Marinsek, N., Barry, E. R., Makarova, K. S., Dionne, I., Koonin, E. V. & Bell, S. D. 2006. GINS, a central nexus in the archaeal DNA replication fork. EMBO Rep. 7(5): 539-545.

Matera, A. G. 1998. Of coiled bodies, gems, and salmon. J.Cell.Biochem. 70(2): 181-192.

Mathews, M. B. & Shenk, T. 1991. Adenovirus virus-associated RNA and translation control. J.Virol. 65(11): 5657-5662.

Mayer, C. & Grummt, I. 2005. Cellular stress and nucleolar function. Cell.Cycle 4(8): 1036-1038.

McCance, D. J. 2005. Transcriptional regulation by human papillomaviruses. Curr.Opin.Genet.Dev. 15(5): 515-519.
McKeown, P. C. & Shaw, P. J. 2009. Chromatin: linking structure and function in the nucleolus. Chromosoma 118(1): 11-23.
Mei, Y. F., Skog, J., Lindman, K. & Wadell, G. 2003. Comparative analysis of the genome organization of human adenovirus 11, a member of the human adenovirus species B, and the commonly used human adenovirus 5 vector, a member of species C. J.Gen.Virol. 84(Pt 8): 2061-2071.
Meyer, S., Urbanke, C. & Wahle, E. 2002. Equilibrium studies on the association of the nuclear poly(A) binding protein with poly(A) of different lengths. Biochemistry 41(19): 6082-6089.
Millar, C. B. & Grunstein, M. 2006. Genome-wide patterns of histone modifications in yeast. Nat.Rev.Mol.Cell Biol. 7(9): 657-666.
Misteli, T. 2001. Protein dynamics: implications for nuclear architecture and gene expression. Science 291(5505): 843-847.
Misteli, T., Caceres, J. F. & Spector, D. L. 1997. The dynamics of a pre-mRNA splicing factor in living cells. Nature 387(6632): 523-527.
Moldovan, G. L., Pfander, B. & Jentsch, S. 2007. PCNA, the maestro of the replication fork. Cell 129(4): 665-679.
Monier, K., Armas, J. C., Etteldorf, S., Ghazal, P. & Sullivan, K. F. 2000. Annexation of the interchromosomal space during viral infection. Nat.Cell Biol. 2(9): 661-665.
Morris, G. E. 2008. The Cajal body. Biochim.Biophys.Acta 1783(11): 2108-2115.
Muller, D. E. & Siegl, G. 1983a. Maturation of parvovirus LuIII in a subcellular system. I. Optimal conditions for in vitro synthesis and encapsidation of viral DNA. J.Gen.Virol. 64(Pt 5): 1043-1054.
Muller, D. E. & Siegl, G. 1983b. Maturation of parvovirus LuIII in a subcellular system. II. Isolation and characterization of nucleoprotein intermediates. J.Gen.Virol. 64(Pt 5): 1055-1067.
Muratani, M., Gerlich, D., Janicki, S. M., Gebhard, M., Eils, R. & Spector, D. L. 2002. Metabolic-energy-dependent movement of PML bodies within the mammalian cell nucleus. Nat.Cell Biol. 4(2): 106-110.
Naryzhny, S. N., Zhao, H. & Lee, H. 2005. Proliferating cell nuclear antigen (PCNA) may function as a double homotrimer complex in the mammalian cell. J.Biol.Chem. 280(14): 13888-13894.
Nelson, P. (2004). Biological Physics (2004: W.H. Freeman and Company).
Ng, S. S., Yue, W. W., Oppermann, U. & Klose, R. J. 2009. Dynamic protein methylation in chromatin biology. Cell Mol.Life Sci. 66(3): 407-422.
Nitschke, R., Wilhelm, S., Borlinghaus, R., Leipziger, J., Bindels, R. & Greger, R. 1997. A modified confocal laser scanning microscope allows fast ultraviolet ratio imaging of intracellular Ca2+ activity using Fura-2. Pflugers Arch. 433(5): 653-663.
Norio, P. & Schildkraut, C. L. 2004. Plasticity of DNA replication initiation in Epstein-Barr virus episomes. PLoS Biol. 2(6): e152.
Nuesch, J. P., Cotmore, S. F. & Tattersall, P. 1995. Sequence motifs in the replicator protein of parvovirus MVM essential for nicking and covalent

attachment to the viral origin: identification of the linking tyrosine. Virology 209(1): 122-135.
Nuesch, J. P. & Tattersall, P. 1993. Nuclear targeting of the parvoviral replicator molecule NS1: evidence for self-association prior to nuclear transport. Virology 196(2): 637-651.
Ohkuma, Y., Hashimoto, S., Wang, C. K., Horikoshi, M. & Roeder, R. G. 1995. Analysis of the role of TFIIE in basal transcription and TFIIH-mediated carboxy-terminal domain phosphorylation through structure-function studies of TFIIE-alpha. Mol.Cell.Biol. 15(9): 4856-4866.
O'Keefe, R. T., Mayeda, A., Sadowski, C. L., Krainer, A. R. & Spector, D. L. 1994. Disruption of pre-mRNA splicing in vivo results in reorganization of splicing factors. J.Cell Biol. 124(3): 249-260.
Onrust, R., Finkelstein, J., Naktinis, V., Turner, J., Fang, L. & O'Donnell, M. 1995. Assembly of a chromosomal replication machine: two DNA polymerases, a clamp loader, and sliding clamps in one holoenzyme particle. I. Organization of the clamp loader. J.Biol.Chem. 270(22): 13348-13357.
Op De Beeck, A., Sobczak-Thepot, J., Sirma, H., Bourgain, F., Brechot, C. & Caillet-Fauquet, P. 2001. NS1- and minute virus of mice-induced cell cycle arrest: involvement of p53 and p21(cip1). J.Virol. 75(22): 11071-11078.
Pack, C., Saito, K., Tamura, M. & Kinjo, M. 2006. Microenvironment and effect of energy depletion in the nucleus analyzed by mobility of multiple oligomeric EGFPs. Biophys.J. 91(10): 3921-3936.
Palazzo, A. F., Springer, M., Shibata, Y., Lee, C. S., Dias, A. P. & Rapoport, T. A. 2007. The signal sequence coding region promotes nuclear export of mRNA. PLoS Biol. 5(12): e322.
Pante, N. & Kann, M. 2002. Nuclear pore complex is able to transport macromolecules with diameters of about 39 nm. Mol.Biol.Cell 13(2): 425-434.
Parker, J. S., Murphy, W. J., Wang, D., O'Brien, S. J. & Parrish, C. R. 2001. Canine and feline parvoviruses can use human or feline transferrin receptors to bind, enter, and infect cells. J.Virol. 75(8): 3896-3902.
Parker, J. S. & Parrish, C. R. 2000. Cellular uptake and infection by canine parvovirus involves rapid dynamin-regulated clathrin-mediated endocytosis, followed by slower intracellular trafficking. J.Virol. 74(4): 1919-1930.
Parrish, C. R. 1991. Mapping specific functions in the capsid structure of canine parvovirus and feline panleukopenia virus using infectious plasmid clones. Virology 183(1): 195-205.
Patterson, G. H. & Lippincott-Schwartz, J. 2002. A photoactivatable GFP for selective photolabeling of proteins and cells. Science 297(5588): 1873-1877.
Pawley, J. B. 2006. Handbook of biological confocal microscopy. 985 p., Springer Science+Business Media, New York, USA.
Peters, A. H., Kubicek, S., Mechtler, K., O'Sullivan, R. J., Derijck, A. A., Perez-Burgos, L., Kohlmaier, A., Opravil, S., Tachibana, M., Shinkai, Y., Martens,

J. H. & Jenuwein, T. 2003. Partitioning and plasticity of repressive histone methylation states in mammalian chromatin. Mol.Cell 12(6): 1577-1589.

Phair, R. D., Scaffidi, P., Elbi, C., Vecerova, J., Dey, A., Ozato, K., Brown, D. T., Hager, G., Bustin, M. & Misteli, T. 2004. Global nature of dynamic protein-chromatin interactions in vivo: three-dimensional genome scanning and dynamic interaction networks of chromatin proteins. Mol.Cell.Biol. 24(14): 6393-6402.

Pinkel, D., Landegent, J., Collins, C., Fuscoe, J., Segraves, R., Lucas, J. & Gray, J. 1988. Fluorescence in situ hybridization with human chromosome-specific libraries: detection of trisomy 21 and translocations of chromosome 4. Proc.Natl.Acad.Sci.U.S.A. 85(23): 9138-9142.

Pitluk, Z. W. & Ward, D. C. 1991. Unusual Sp1-GC box interaction in a parvovirus promoter. J.Virol. 65(12): 6661-6670.

Platani, M., Goldberg, I., Lamond, A. I. & Swedlow, J. R. 2002. Cajal body dynamics and association with chromatin are ATP-dependent. Nat.Cell Biol. 4(7): 502-508.

Pokholok, D. K., Hannett, N. M. & Young, R. A. 2002. Exchange of RNA polymerase II initiation and elongation factors during gene expression in vivo. Mol.Cell 9(4): 799-809.

Politz, J. C., Tuft, R. A. & Pederson, T. 2003. Diffusion-based transport of nascent ribosomes in the nucleus. Mol.Biol.Cell 14(12): 4805-4812.

Pombo, A., Ferreira, J., Bridge, E. & Carmo-Fonseca, M. 1994. Adenovirus replication and transcription sites are spatially separated in the nucleus of infected cells. EMBO J. 13(21): 5075-5085.

Prigent, C. & Dimitrov, S. 2003. Phosphorylation of serine 10 in histone H3, what for? J.Cell.Sci. 116(Pt 18): 3677-3685.

Proudfoot, N. 2004. New perspectives on connecting messenger RNA 3' end formation to transcription. Curr.Opin.Cell Biol. 16(3): 272-278.

Proudfoot, N. J., Furger, A. & Dye, M. J. 2002. Integrating mRNA processing with transcription. Cell 108(4): 501-512.

Pujol, A., Deleu, L., Nuesch, J. P., Cziepluch, C., Jauniaux, J. C. & Rommelaere, J. 1997. Inhibition of parvovirus minute virus of mice replication by a peptide involved in the oligomerization of nonstructural protein NS1. J.Virol. 71(10): 7393-7403.

Qian, H., Sheetz, M. P. & Elson, E. L. 1991. Single particle tracking. Analysis of diffusion and flow in two-dimensional systems. Biophys.J. 60(4): 910-921.

Raska, I., Shaw, P. J. & Cmarko, D. 2006. Structure and function of the nucleolus in the spotlight. Curr.Opin.Cell Biol. 18(3): 325-334.

Rayet, B., Lopez-Guerrero, J. A., Rommelaere, J. & Dinsart, C. 1998. Induction of programmed cell death by parvovirus H-1 in U937 cells: connection with the tumor necrosis factor alpha signalling pathway. J.Virol. 72(11): 8893-8903.

Reed, A. P., Jones, E. V. & Miller, T. J. 1988. Nucleotide sequence and genome organization of canine parvovirus. J.Virol. 62(1): 266-276.

Reichelt, R., Holzenburg, A., Buhle, E. L.,Jr, Jarnik, M., Engel, A. & Aebi, U. 1990. Correlation between structure and mass distribution of the nuclear

pore complex and of distinct pore complex components. J.Cell Biol. 110(4): 883-894.
Reinert, K. C., Gao, W., Chen, G. & Ebner, T. J. 2007. Flavoprotein autofluorescence imaging in the cerebellar cortex in vivo. J.Neurosci.Res. 85(15): 3221-3232.
Ribbeck, K. & Gorlich, D. 2001. Kinetic analysis of translocation through nuclear pore complexes. EMBO J. 20(6): 1320-1330.
Richter, K., Nessling, M. & Lichter, P. 2008. Macromolecular crowding and its potential impact on nuclear function. Biochim.Biophys.Acta 1783(11): 2100-2107.
Riggs, A. D., Bourgeois, S. & Cohn, M. 1970. The lac repressor-operator interaction. 3. Kinetic studies. J.Mol.Biol. 53(3): 401-417.
Riolobos, L., Reguera, J., Mateu, M. G. & Almendral, J. M. 2006. Nuclear transport of trimeric assembly intermediates exerts a morphogenetic control on the icosahedral parvovirus capsid. J.Mol.Biol. 357(3): 1026-1038.
Rout, M. P. & Wente, S. R. 1994. Pores for thought: nuclear pore complex proteins. Trends Cell Biol. 4(10): 357-365.
Rubbi, C. P. & Milner, J. 2003. Disruption of the nucleolus mediates stabilization of p53 in response to DNA damage and other stresses. EMBO J. 22(22): 6068-6077.
Rust, M. J., Bates, M. & Zhuang, X. 2006. Sub-diffraction-limit imaging by stochastic optical reconstruction microscopy (STORM). Nat.Methods 3(10): 793-795.
Sadoni, N., Sullivan, K. F., Weinzierl, P., Stelzer, E. H. & Zink, D. 2001. Large-scale chromatin fibers of living cells display a discontinuous functional organization. Chromosoma 110(1): 39-51.
Saffer, J. D., Jackson, S. P. & Thurston, S. J. 1990. SV40 stimulates expression of the transacting factor Sp1 at the mRNA level. Genes Dev. 4(4): 659-666.
Santocanale, C., Foiani, M., Lucchini, G. & Plevani, P. 1993. The isolated 48,000-dalton subunit of yeast DNA primase is sufficient for RNA primer synthesis. J.Biol.Chem. 268(2): 1343-1348.
Saxton, M. J. 2007. A biological interpretation of transient anomalous subdiffusion. I. Qualitative model. Biophys.J. 92(4): 1178-1191.
Saxton, M. J. 1994. Single-particle tracking: models of directed transport. Biophys.J. 67(5): 2110-2119.
Scheuermann, M. O., Tajbakhsh, J., Kurz, A., Saracoglu, K., Eils, R. & Lichter, P. 2004. Topology of genes and nontranscribed sequences in human interphase nuclei. Exp.Cell Res. 301(2): 266-279.
Schirmer, E. C. & Foisner, R. 2007. Proteins that associate with lamins: many faces, many functions. Exp.Cell Res. 313(10): 2167-2179.
Schirmer, E. C. & Gerace, L. 2005. The nuclear membrane proteome: extending the envelope. Trends Biochem.Sci. 30(10): 551-558.
Schotta, G., Lachner, M., Sarma, K., Ebert, A., Sengupta, R., Reuter, G., Reinberg, D. & Jenuwein, T. 2004. A silencing pathway to induce H3-K9 and H4-K20 trimethylation at constitutive heterochromatin. Genes Dev. 18(11): 1251-1262.

Sedman, J. & Stenlund, A. 1998. The papillomavirus E1 protein forms a DNA-dependent hexameric complex with ATPase and DNA helicase activities. J.Virol. 72(8): 6893-6897.

Seisenberger, G., Ried, M. U., Endress, T., Buning, H., Hallek, M. & Brauchle, C. 2001. Real-time single-molecule imaging of the infection pathway of an adeno-associated virus. Science 294(5548): 1929-1932.

Seksek, O., Biwersi, J. & Verkman, A. S. 1997. Translational diffusion of macromolecule-sized solutes in cytoplasm and nucleus. J.Cell Biol. 138(1): 131-142.

Shackelton, L. A., Parrish, C. R., Truyen, U. & Holmes, E. C. 2005. High rate of viral evolution associated with the emergence of carnivore parvovirus. Proc.Natl.Acad.Sci.U.S.A. 102(2): 379-384.

Shahbazian, M. D., Zhang, K. & Grunstein, M. 2005. Histone H2B ubiquitylation controls processive methylation but not monomethylation by Dot1 and Set1. Mol.Cell 19(2): 271-277.

Shaner, N. C., Steinbach, P. A. & Tsien, R. Y. 2005. A guide to choosing fluorescent proteins. Nat.Methods 2(12): 905-909.

Shav-Tal, Y., Darzacq, X., Shenoy, S. M., Fusco, D., Janicki, S. M., Spector, D. L. & Singer, R. H. 2004. Dynamics of single mRNPs in nuclei of living cells. Science 304(5678): 1797-1800.

Sirri, V., Urcuqui-Inchima, S., Roussel, P. & Hernandez-Verdun, D. 2008. Nucleolus: the fascinating nuclear body. Histochem.Cell Biol. 129(1): 13-31.

Smale, S. T. & Tjian, R. 1986. T-antigen-DNA polymerase alpha complex implicated in simian virus 40 DNA replication. Mol.Cell.Biol. 6(11): 4077-4087.

Solomon, D. A., Cardoso, M. C. & Knudsen, E. S. 2004. Dynamic targeting of the replication machinery to sites of DNA damage. J.Cell Biol. 166(4): 455-463.

Soumpasis, D. M. 1983. Theoretical analysis of fluorescence photobleaching recovery experiments. Biophys.J. 41(1): 95-97.

Sourvinos, G. & Everett, R. D. 2002. Visualization of parental HSV-1 genomes and replication compartments in association with ND10 in live infected cells. EMBO J. 21(18): 4989-4997.

Spangler, L., Wang, X., Conaway, J. W., Conaway, R. C. & Dvir, A. 2001. TFIIH action in transcription initiation and promoter escape requires distinct regions of downstream promoter DNA. Proc.Natl.Acad.Sci.U.S.A. 98(10): 5544-5549.

Sperling, J., Azubel, M. & Sperling, R. 2008. Structure and function of the Pre-mRNA splicing machine. Structure 16(11): 1605-1615.

Sprague, B. L. & McNally, J. G. 2005. FRAP analysis of binding: proper and fitting. Trends Cell Biol. 15(2): 84-91.

Sprague, B. L., Pego, R. L., Stavreva, D. A. & McNally, J. G. 2004. Analysis of binding reactions by fluorescence recovery after photobleaching. Biophys.J. 86(6): 3473-3495.

Stanek, D. & Neugebauer, K. M. 2006. The Cajal body: a meeting place for spliceosomal snRNPs in the nuclear maze. Chromosoma 115(5): 343-354.

Stewart, C. L., Roux, K. J. & Burke, B. 2007. Blurring the boundary: the nuclear envelope extends its reach. Science 318(5855): 1408-1412.

Stone, D., Furthmann, A., Sandig, V. & Lieber, A. 2003. The complete nucleotide sequence, genome organization, and origin of human adenovirus type 11. Virology 309(1): 152-165.

Strahl, B. D., Ohba, R., Cook, R. G. & Allis, C. D. 1999. Methylation of histone H3 at lysine 4 is highly conserved and correlates with transcriptionally active nuclei in Tetrahymena. Proc.Natl.Acad.Sci.U.S.A. 96(26): 14967-14972.

Strawn, L. A., Shen, T. & Wente, S. R. 2001. The GLFG regions of Nup116p and Nup100p serve as binding sites for both Kap95p and Mex67p at the nuclear pore complex. J.Biol.Chem. 276(9): 6445-6452.

Stukenberg, P. T. & O'Donnell, M. 1995. Assembly of a chromosomal replication machine: two DNA polymerases, a clamp loader, and sliding clamps in one holoenzyme particle. V. Four different polymerase-clamp complexes on DNA. J.Biol.Chem. 270(22): 13384-13391.

Suikkanen, S., Aaltonen, T., Nevalainen, M., Valilehto, O., Lindholm, L., Vuento, M. & Vihinen-Ranta, M. 2003a. Exploitation of microtubule cytoskeleton and dynein during parvoviral traffic toward the nucleus. J.Virol. 77(19): 10270-10279.

Suikkanen, S., Antila, M., Jaatinen, A., Vihinen-Ranta, M. & Vuento, M. 2003b. Release of canine parvovirus from endocytic vesicles. Virology 316(2): 267-280.

Suikkanen, S., Saajarvi, K., Hirsimaki, J., Valilehto, O., Reunanen, H., Vihinen-Ranta, M. & Vuento, M. 2002. Role of recycling endosomes and lysosomes in dynein-dependent entry of canine parvovirus. J.Virol. 76(9): 4401-4411.

Tanabe, H., Muller, S., Neusser, M., von Hase, J., Calcagno, E., Cremer, M., Solovei, I., Cremer, C. & Cremer, T. 2002. Evolutionary conservation of chromosome territory arrangements in cell nuclei from higher primates. Proc.Natl.Acad.Sci.U.S.A. 99(7): 4424-4429.

Taylor, J.R. (1997). An introduction to error analysis

Tegenfeldt, J. O., Prinz, C., Cao, H., Chou, S., Reisner, W. W., Riehn, R., Wang, Y. M., Cox, E. C., Sturm, J. C., Silberzan, P. & Austin, R. H. 2004. From the Cover: The dynamics of genomic-length DNA molecules in 100-nm channels. Proc.Natl.Acad.Sci.U.S.A. 101(30): 10979-10983.

Terry, L. J., Shows, E. B. & Wente, S. R. 2007. Crossing the nuclear envelope: hierarchical regulation of nucleocytoplasmic transport. Science 318(5855): 1412-1416.

Thierry, F. 2009. Transcriptional regulation of the papillomavirus oncogenes by cellular and viral transcription factors in cervical carcinoma. Virology 384(2): 375-379.

Thierry, F., Spyrou, G., Yaniv, M. & Howley, P. 1992. Two AP1 sites binding JunB are essential for human papillomavirus type 18 transcription in keratinocytes. J.Virol. 66(6): 3740-3748.

Thomson, S., Clayton, A. L. & Mahadevan, L. C. 2001. Independent dynamic regulation of histone phosphorylation and acetylation during immediate-early gene induction. Mol.Cell 8(6): 1231-1241.

Trojer, P. & Reinberg, D. 2007. Facultative heterochromatin: is there a distinctive molecular signature? Mol.Cell 28(1): 1-13.

Truyen, U., Geissler, K., Parrish, C. R., Hermanns, W. & Siegl, G. 1998. No evidence for a role of modified live virus vaccines in the emergence of canine parvovirus. J.Gen.Virol. 79 (Pt 5)(Pt 5): 1153-1158.

Tsao, J., Chapman, M. S., Agbandje, M., Keller, W., Smith, K., Wu, H., Luo, M., Smith, T. J., Rossmann, M. G. & Compans, R. W. 1991. The three-dimensional structure of canine parvovirus and its functional implications. Science 251(5000): 1456-1464.

Turner, B. M. & Franchi, L. 1987. Identification of protein antigens associated with the nuclear matrix and with clusters of interchromatin granules in both interphase and mitotic cells. J.Cell.Sci. 87 (Pt 2)(Pt 2): 269-282.

Vargas, D. Y., Raj, A., Marras, S. A., Kramer, F. R. & Tyagi, S. 2005. Mechanism of mRNA transport in the nucleus. Proc.Natl.Acad.Sci.U.S.A. 102(47): 17008-17013.

Vermeulen, M., Mulder, K. W., Denissov, S., Pijnappel, W. W., van Schaik, F. M., Varier, R. A., Baltissen, M. P., Stunnenberg, H. G., Mann, M. & Timmers, H. T. 2007. Selective anchoring of TFIID to nucleosomes by trimethylation of histone H3 lysine 4. Cell 131(1): 58-69.

Verschure, P. J., van der Kraan, I., Manders, E. M., Hoogstraten, D., Houtsmuller, A. B. & van Driel, R. 2003. Condensed chromatin domains in the mammalian nucleus are accessible to large macromolecules. EMBO Rep. 4(9): 861-866.

Vihinen-Ranta, M., Kakkola, L., Kalela, A., Vilja, P. & Vuento, M. 1997. Characterization of a nuclear localization signal of canine parvovirus capsid proteins. Eur.J.Biochem. 250(2): 389-394.

Vihinen-Ranta, M., Kalela, A., Makinen, P., Kakkola, L., Marjomaki, V. & Vuento, M. 1998. Intracellular route of canine parvovirus entry. J.Virol. 72(1): 802-806.

Vihinen-Ranta, M., Yuan, W. & Parrish, C. R. 2000. Cytoplasmic trafficking of the canine parvovirus capsid and its role in infection and nuclear transport. J.Virol. 74(10): 4853-4859.

Visser, A. E., Jaunin, F., Fakan, S. & Aten, J. A. 2000. High resolution analysis of interphase chromosome domains. J.Cell.Sci. 113 (Pt 14)(Pt 14): 2585-2593.

von Hippel, P. H. & Berg, O. G. 1989. Facilitated target location in biological systems. J.Biol.Chem. 264(2): 675-678.

Wachsmuth, M., Caudron-Herger, M. & Rippe, K. 2008. Genome organization: balancing stability and plasticity. Biochim.Biophys.Acta 1783(11): 2061-2079.

Wade, J. T. & Struhl, K. 2008. The transition from transcriptional initiation to elongation. Curr.Opin.Genet.Dev. 18(2): 130-136.

Wang, D., Yuan, W., Davis, I. & Parrish, C. R. 1998a. Nonstructural protein-2 and the replication of canine parvovirus. Virology 240(2): 273-281.

Wang, Z. G., Ruggero, D., Ronchetti, S., Zhong, S., Gaboli, M., Rivi, R. & Pandolfi, P. P. 1998b. PML is essential for multiple apoptotic pathways. Nat.Genet. 20(3): 266-272.

Weidemann, T., Wachsmuth, M., Knoch, T. A., Muller, G., Waldeck, W. & Langowski, J. 2003. Counting nucleosomes in living cells with a combination of fluorescence correlation spectroscopy and confocal imaging. J.Mol.Biol. 334(2): 229-240.

Weidtkamp-Peters, S., Lenser, T., Negorev, D., Gerstner, N., Hofmann, T. G., Schwanitz, G., Hoischen, C., Maul, G., Dittrich, P. & Hemmerich, P. 2008. Dynamics of component exchange at PML nuclear bodies. J.Cell.Sci. 121(Pt 16): 2731-2743.

Weiss, M., Elsner, M., Kartberg, F. & Nilsson, T. 2004. Anomalous subdiffusion is a measure for cytoplasmic crowding in living cells. Biophys.J. 87(5): 3518-3524.

Wessel, R., Schweizer, J. & Stahl, H. 1992. Simian virus 40 T-antigen DNA helicase is a hexamer which forms a binary complex during bidirectional unwinding from the viral origin of DNA replication. J.Virol. 66(2): 804-815.

Wiesmeijer, K., Molenaar, C., Bekeer, I. M., Tanke, H. J. & Dirks, R. W. 2002. Mobile foci of Sp100 do not contain PML: PML bodies are immobile but PML and Sp100 proteins are not. J.Struct.Biol. 140(1-3): 180-188.

Wikoff, W. R., Wang, G., Parrish, C. R., Cheng, R. H., Strassheim, M. L., Baker, T. S. & Rossmann, M. G. 1994. The structure of a neutralized virus: canine parvovirus complexed with neutralizing antibody fragment. Structure 2(7): 595-607.

Worman, H. J., Yuan, J., Blobel, G. & Georgatos, S. D. 1988. A lamin B receptor in the nuclear envelope. Proc.Natl.Acad.Sci.U.S.A. 85(22): 8531-8534.

Xiao, T., Hall, H., Kizer, K. O., Shibata, Y., Hall, M. C., Borchers, C. H. & Strahl, B. D. 2003. Phosphorylation of RNA polymerase II CTD regulates H3 methylation in yeast. Genes Dev. 17(5): 654-663.

Yamashita, T., Arens, M. & Green, M. 1975. Adenovirus deoxyribonucleic acid replication. II. Synthesis of viral deoxyribonucleic acid in vitro by a nuclear membrane fraction from infected KB cells. J.Biol.Chem. 250(9): 3273-3279.

Yang, F., Moss, L. G. & Phillips, G. N.,Jr. 1996. The molecular structure of green fluorescent protein. Nat.Biotechnol. 14(10): 1246-1251.

Yang, W. & Musser, S. M. 2006. Nuclear import time and transport efficiency depend on importin beta concentration. J.Cell Biol. 174(7): 951-961.

Yaniv, M. 2009. Small DNA tumour viruses and their contributions to our understanding of transcription control. Virology 384(2): 369-374.

Ye, Q. & Worman, H. J. 1996. Interaction between an integral protein of the nuclear envelope inner membrane and human chromodomain proteins homologous to Drosophila HP1. J.Biol.Chem. 271(25): 14653-14656.

Yee, A. S., Raychaudhuri, P., Jakoi, L. & Nevins, J. R. 1989. The adenovirus-inducible factor E2F stimulates transcription after specific DNA binding. Mol.Cell.Biol. 9(2): 578-585.

Young, P. J., Jensen, K. T., Burger, L. R., Pintel, D. J. & Lorson, C. L. 2002. Minute virus of mice NS1 interacts with the SMN protein, and they

colocalize in novel nuclear bodies induced by parvovirus infection. J.Virol. 76(8): 3892-3904.
Yum, K., Na, S., Xiang, Y., Wang, N. & Yu, M. F. 2009. Mechanochemical delivery and dynamic tracking of fluorescent quantum dots in the cytoplasm and nucleus of living cells. Nano Lett. 9(5): 2193-2198.
Yuzhakov, A., Kelman, Z., Hurwitz, J. & O'Donnell, M. 1999. Multiple competition reactions for RPA order the assembly of the DNA polymerase delta holoenzyme. EMBO J. 18(21): 6189-6199.
Zadori, Z., Szelei, J., Lacoste, M. C., Li, Y., Gariepy, S., Raymond, P., Allaire, M., Nabi, I. R. & Tijssen, P. 2001. A viral phospholipase A2 is required for parvovirus infectivity. Dev.Cell. 1(2): 291-302.
Zastrow, M. S., Vlcek, S. & Wilson, K. L. 2004. Proteins that bind A-type lamins: integrating isolated clues. J.Cell.Sci. 117(Pt 7): 979-987.
Zawel, L., Kumar, K. P. & Reinberg, D. 1995. Recycling of the general transcription factors during RNA polymerase II transcription. Genes Dev. 9(12): 1479-1490.
Zeskind, B. J., Jordan, C. D., Timp, W., Trapani, L., Waller, G., Horodincu, V., Ehrlich, D. J. & Matsudaira, P. 2007. Nucleic acid and protein mass mapping by live-cell deep-ultraviolet microscopy. Nat.Methods 4(7): 567-569.
Zheng, Z. M. & Baker, C. C. 2006. Papillomavirus genome structure, expression, and post-transcriptional regulation. Front.Biosci. 11: 2286-2302.
Zhong, S., Salomoni, P. & Pandolfi, P. P. 2000. The transcriptional role of PML and the nuclear body. Nat.Cell Biol. 2(5): E85-90.